



**UNIVERSITÀ  
DEGLI STUDI  
DI TRIESTE**

**UNIVERSITÀ DEGLI STUDI DI TRIESTE**  
**XXXVIII CICLO DEL DOTTORATO DI RICERCA IN**  
**INGEGNERIA INDUSTRIALE E DELL'INFORMAZIONE**

Finanziato dall'Unione europea - NextGenerationEU

**INNOVATIVE METHODOLOGY FOR THE  
PRELIMINARY DESIGN OF PASSENGER VESSELS  
FOR SUSTAINABLE COASTAL NAVIGATION**

Settore scientifico-disciplinare: IIND - 01 / B

DOTTORANDO

**DONATO PADOLECCHIA**

COORDINATORE

**PROF. FULVIO BABICH**

SUPERVISORE DI TESI

**PROF. VITTORIO BUCCI**

CO-SUPERVISORE DI TESI

**PROF. SERENA BERTAGNA**

**ANNO ACCADEMICO 2024/2025**



Finanziato  
dall'Unione europea  
NextGenerationEU



Ministero  
dell'Università  
e della Ricerca



Italiadomani  
PIANO NAZIONALE  
DI RIPRESA E RESILIENZA



UNIVERSITÀ  
DEGLI STUDI  
DI TRIESTE



## **Abstract**

In recent years, the preliminary design of passenger vessels for coastal navigation has experienced a significant increase in complexity, driven by the interaction between stringent regulatory requirements, environmental sustainability objectives, operational constraints, and growing expectations in terms of comfort and accessibility. In this context, decisions taken during the early stages of the design process are crucial to the overall performance of vessels throughout their entire life cycle, highlighting the need for a critical rethinking of traditional design paradigms.

This research proposes an innovative methodology for the concept design of passenger vessels intended for coastal transport, based on the integration of parametric design, Systems Engineering, and Concurrent Engineering. A critical analysis of the classical design spiral model has revealed the limitations of sequential processes in managing the high level of interdependence between hull and systems, particularly in contexts characterised by stringent operational constraints.

The distinctive contribution of the present study lies in the development of an integrated computational pipeline for preliminary design, implemented within a parametric environment, which enables the automatic and systematic generation of complete and technically coherent vessel configurations. The methodology combines parametric hull models, the algorithmic definition of general arrangements, propulsion system layouts, preliminary structural assessments, and regulatory and performance feasibility checks. Exploration of the design space is carried out using Design of Experiments techniques, ensuring a homogeneous coverage of the multidimensional domain of design variables.

Particular attention is devoted to technological solutions consistent with sustainability objectives, such as the adoption of series hybrid propulsion architectures and the use of aluminium alloys as the reference structural material, also assessed from a life-cycle perspective. The methodology is validated through a case study related to passenger transport in the Gulf of Trieste, demonstrating the capability of the tool to generate admissible design variants, analyse key design trade-offs, and support informed decision-making in the early stages of the design process.

The results confirm that the proposed approach overcomes the main limitations of traditional processes by enabling a more effective management of interdependencies among design variables, increasing the speed and transparency of the decision-making process, and improving the overall quality of design decisions, in support of a more sustainable and flexible naval design for contemporary coastal mobility.

---

**Contents**

Introduction .....	1
Chapter 1 .....	9
Parametric Design as a Paradigm for Ship Exploration .....	9
1.1. Process Logic and Parametric Design Thinking .....	10
1.2. Parametric Methodology Applied to Ship Design .....	12
1.2.1. General Characterization of Parametric Techniques: FPA vs. FFD.....	12
1.2.2. The Mathematical Formalism of Non-Uniform Rational B-Splines .....	15
1.2.3. Critique of Commercial Computer-Aided Preliminary Ship Design Systems and Methodological Justification.....	16
1.3. Grasshopper: A Methodological Environment for Parametric Prototyping .....	16
Chapter 2 .....	19
Methodological Constraints and Technological Choices .....	19
2.1. Methodology for the Selection of the Propulsion System .....	20
2.1.1. Technical Analysis and Critical Review of Propulsion Architectures .....	20
2.1.2. Series Hybrid: Architectural Principles and Controlled Power Flow .....	21
2.1.3. Parallel Hybrid: Architectural Principles and Combined Mechanical-Electrical Power Flow.....	23
2.1.4. Comparative Synthesis and Final Rationale for the Solution.....	26
2.2. Hull Form Selection.....	26
2.2.1. Operational Framework.....	28
2.3. Structural Material Selection: Condition of the National Fleet and Prospects .....	30
2.3.1. Glass-Reinforced Plastic: technological maturity and end-of-life criticalities.. .....	31
2.3.2. Marine aluminium alloys: recyclability and durability .....	34
2.3.3. HDPE: thermoplastic potential and current regulatory constraints .....	35

---

2.3.4. Critical synthesis .....	38
Chapter 3 .....	40
Methodological Workflow and Process Overview .....	40
3.1. 3D Parametric Hull .....	46
3.1.1. Generating Curves and Their Role within the Integrated Pipeline.....	46
Parametric Definition of the Centre Line .....	50
Parametric Definition of the Sheer Line.....	53
Parametric Definition of the Chine Line .....	55
3.1.2. Identification of the Design Variables.....	59
3.1.3. Output .....	61
3.2. Resistance, Propulsive selection and System Integration.....	66
3.2.1. Identification of the Design Variables.....	73
3.2.2. Output .....	75
3.3. 3D General Arrangement Plan and Structures.....	77
3.3.1. Identification of the Design Variables.....	81
3.3.2. Output .....	83
3.4. Parametric Sampling Techniques: Design of Experiments .....	87
3.5. Feasibility Analysis.....	89
Chapter 4 .....	92
Case study–based validation of the proposed methodology.....	92
4.1. Case-study framework and definition of the parametric design domain .....	93
4.1.1. Operational requirements for passenger transport services in the Gulf of Trieste .....	94
4.1.2. Translation of operational requirements into parametric variables .....	98
4.2. Resistance, Propulsive selection and System Integration.....	100
4.3. 3D General Arrangement Plan and Structures.....	105

---

---

4.3.1.	Integration of the Primary Structure and Dimensional Constraints .....	106
4.3.2.	Parametric Determination of Passenger Capacity .....	107
4.3.3.	Parametric Definition of the Main-Deck General Arrangement .....	109
4.4.	Configuration of the base model and description of the outputs .....	113
4.5.	Generation of design variants through Design of Experiments .....	126
4.6.	Feasibility Checks and Regulatory Compliance .....	127
Chapter 5	.....	129
Results and Discussion	.....	129
5.1.	Analysis of infeasibility causes and constraint violations .....	132
5.2.	Key Outputs and Statistical Distributions.....	134
5.3.	Relationships and Trade-offs among the Outputs.....	137
5.4.	Sensitivity Analysis of Input Variables .....	139
5.5.	Design implications and discussion.....	142
5.6.	State-of-the-art benchmarking .....	143
Conclusions	.....	147
Appendix I	.....	153
Nomenclature	.....	153
Appendix II	.....	157
modeFrontier report	.....	157
Bibliography	.....	162
List of Figures	.....	168
List of Tables	.....	172
List of Publications	.....	174

## Introduction

The design of vessels intended for passenger transport within coastal and intermodal mobility has increasingly become a complex engineering and socio-economic challenge. Contemporary requirements impose the need to combine traditional criteria—such as safety, stability, and reliability, with emerging objectives including energy efficiency, reduced environmental impact, minimisation of Operating Expenditure (OPEX), ease of integration with land-based transport systems, and guaranteed accessibility for users with reduced mobility. Within this context, concept design plays a strategic role: decisions made in the early design phases decisively influence the overall performance and operational costs of a vessel throughout its entire life cycle [1]. Such decisions must therefore result from an informed balance among numerous conflicting objectives [2].

The paradigm that has dominated both academic training and professional practice in marine engineering is the so-called “design spiral”, whose fundamental structure was formalised by J. H. Evans in the mid-twentieth century in a series of contributions published in the *Transactions of the Society of Naval Architects and Marine Engineers* (Figure 1) [3]. The spiral conceives design as an iterative sequence in which the definition of requirements leads to an initial estimate of dimensions, which in turn guides hull modelling and the development of the general arrangement. Stability assessments and performance evaluations feed back into the design parameters in a cycle repeated until convergence. The strength of this framework lies in its conceptual clarity: it explicitly reveals the interdependencies among heterogeneous disciplinary domains and provides a structure for the progressive refinement of initial assumptions [3].

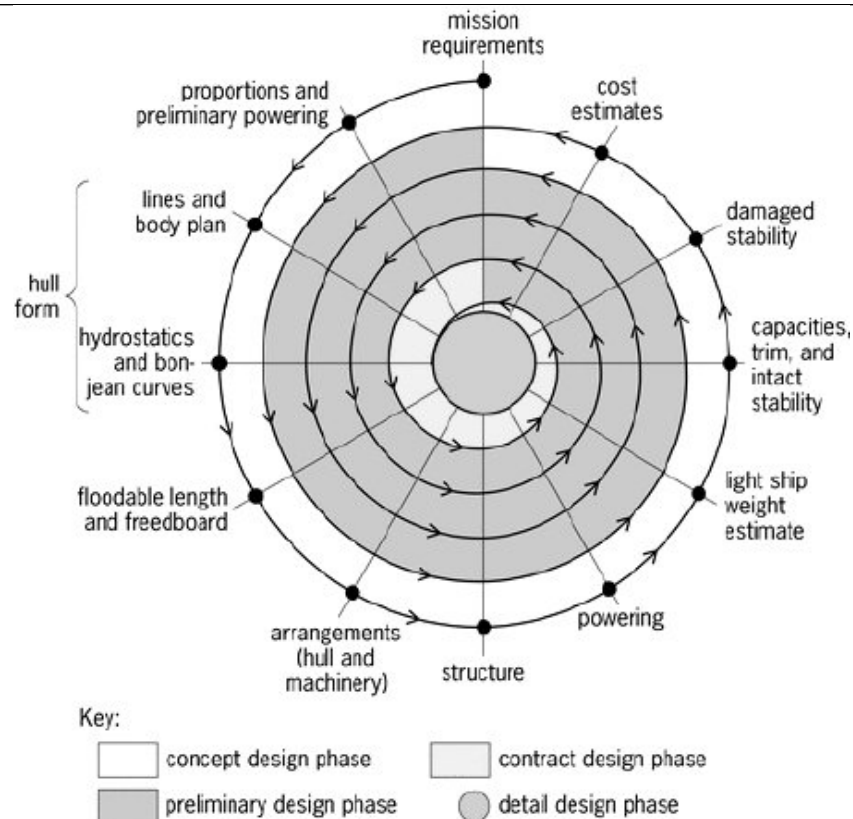


Figure 1 The traditional Evans' spiral illustrating the iterative nature of early-stage ship design (Evans, 1959) [4]

Numerous design manuals, including the foundational text by Apostolos Papanikolaou [1], reproduce the spiral model in its entirety, underlining its centrality in industrial practice. Although subject to variants and adaptations, its methodological structure remains substantially unchanged: the ship “comes into being” gradually, through successive approximations, and the project evolves as more accurate information becomes available.

However, when the spiral model is applied to the design of passenger vessels for daily commuting, significant practical limitations emerge. Maritime commuting contexts are characterised by stringent operational constraints, high service frequency, service continuity, integration with land-based modes, and strong time and cost pressures, which require a high degree of design flexibility [5]. Under such conditions, the classical model exhibits noteworthy limitations in its ability to explore alternatives, in the speed of iteration, and in the integrated management of interdependencies across design domains.

Within this framework, the General Arrangement (GA) plays a central role as the primary interface between operational requirements, passenger experience, regulatory compliance, and the allocation of technical volumes. For commuter vessels, GA decisions influence

---

passenger flow efficiency during peak-hour embarkation and disembarkation, accessibility and safety standards, evacuation performance, and the overall functional integration of propulsion, energy storage, and service systems. GA therefore operates not as a secondary architectural product, but as a multidisciplinary integrator, linking hydrodynamics, stability, structural layout, human-factors considerations, and port-side operational constraints [6]. Its early and accurate definition is essential to minimise downstream redesign and ensure that the vessel can meet demanding service patterns without compromising comfort, safety, or maintainability.

In traditional processes, still largely reliant on manual or semi-manual tools, especially for internal layout definition, the development of the GA is often treated as a strictly consequential activity following hull-form determination. GA is frequently developed using two-dimensional CAD tools and experience-based heuristics, yet it embodies critical decisions regarding space distribution, passenger flow paths, and accessibility requirements. This separation between hull form and internal arrangement creates a “decoupling” of processes that translates into increased complexity and higher costs whenever structural, stability, or operational constraints emerge in later stages of the design. The resulting need to manually redraw 2D layouts or revise previously approved plans leads to frequent rework phases, substantially affecting the time-to-market of the design solution [7].

This rigidity is particularly detrimental in the design of vessels that must maximise operational efficiency and accessibility while minimising costs and complying with strict regulations. A concrete risk is the so-called “early fixation”: early decisions, based on precedents or limited assumptions, anchor the project and hinder the exploration of innovative solutions that could provide improved trade-offs among comfort, capacity, stability, and energy consumption. Recent literature highlights that, despite advances in hull modelling, internal arrangement remains one of the least digitalised and most experience-dependent domains [8]. The trial-and-error methods typical of traditional approaches fail to adequately explore the design space [9]. Moreover, the slow pace at which alternative design configurations can be generated and assessed further exacerbates these limitations. In conventional workflows, each new variant, whether involving a modification of the hull geometry, the repositioning of major technical volumes, or a reallocation of passenger spaces, requires a sequence of manual adjustments across multiple drawings and calculation sheets. This leads to evaluation cycles that may span days or weeks, restricting the number

of alternatives that can be realistically explored during early-stage design. As a consequence, the design space is sampled sparsely and often in a non-systematic manner, with many potentially valuable configurations left unexplored simply because the cost, time, or personnel effort required to develop them is prohibitive. This inherently low iteration speed stands in stark contrast with the needs of commuter vessel design, where small variations in layout, weight distribution, or system arrangement can significantly affect operability, safety, and energy performance, and where rapid comparative assessments are essential to achieve meaningful optimisation.

To address these challenges, the scientific community and the shipbuilding industry have promoted a methodological evolution shifting from the sole spiral-based approach toward Systems Engineering and Concurrent Engineering practices, in which disciplines work in parallel and requirements are managed and traced systematically from the earliest stages. Concurrent Engineering in the ship sector aims to reduce feedback times, improve interdisciplinary coordination, and integrate regulatory and performance assessments within a co-design workflow [10].

A comparison is therefore proposed between conventional, linearly organised design and a design paradigm based on concurrent engineering (Figure 2).

#### “Normal” Engineering

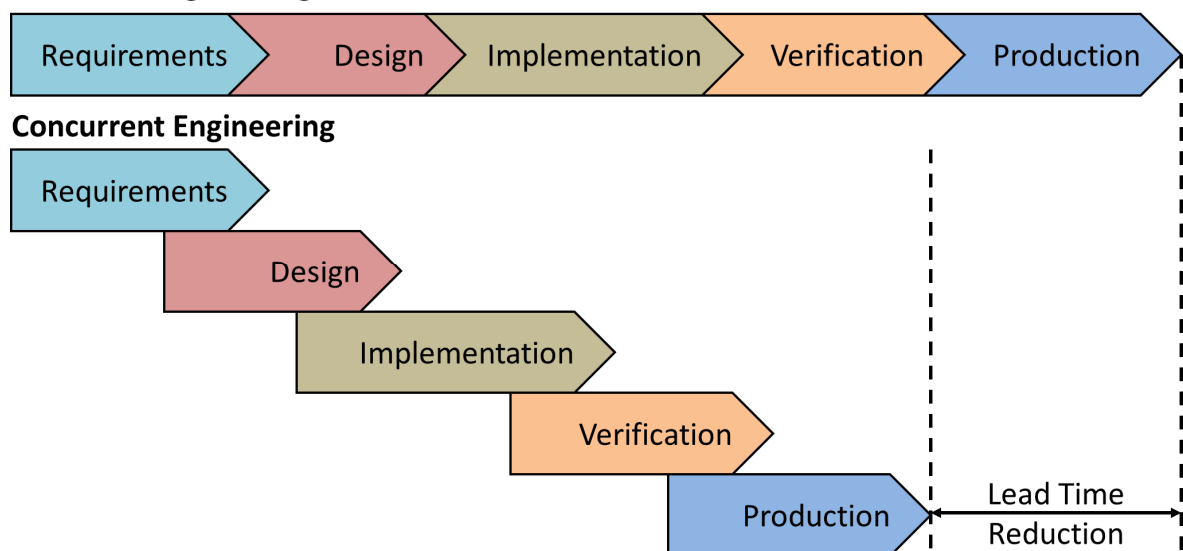


Figure 2 Comparison between conventional, linearly organised design and a concurrent-engineering-based design paradigm [11]

---

Alongside these organisational changes, the technological tools available for ship design have undergone a radical evolution. Innovations can be grouped into three main categories: parametric modelling, design-optimisation techniques, and data-driven approaches.

Parametric hull modelling is now a well-established field: using tools such as B-splines, NURBS, or Free Form Deformation (FFD), hull geometry can be expressed through a set of high-level parameters that control the shape consistently and reproducibly [12], [13]. Parametrisation not only accelerates the design process: it transforms the hull into a family of forms that can be queried and compared, enabling design-space exploration, multi-objective optimisation, and integration with reduced-order or surrogate models that allow performance evaluation at sustainable computational cost [14].

Examples of hybrid systems combining parametric, generative and interactive strategies—such as GenYacht [9]—demonstrate the potential of Generative Design Techniques (GDT) to efficiently explore the design space while maintaining user control. In parallel, data-driven approaches, including generative adversarial networks and diffusion-based models, have shown the ability to generate geometrically plausible and hydrodynamically competitive hull forms when appropriate constraints are applied [15], [16]. These contributions consistently highlight that automatic generation is powerful, but that practical effectiveness depends on the early integration of engineering and regulatory constraints.

These developments fundamentally reshape the role of the designer, shifting the focus from the production of individual solutions toward the definition of meaningful design spaces, feasibility rules and evaluation metrics. Parametric approaches combined with Design of Experiments (DoE) and multi-objective optimisation enable systematic exploration of the design space; however, empirical evidence shows that without early constraint integration, large-scale generation results in a high percentage of infeasible solutions, with feasibility rates often on the order of 5–10% [7], [7], [14], [15], [15].

Generative tools alone are therefore insufficient: the design process must be conceived as an integrated pipeline in which variant generation, performance assessment and regulatory verification interact from the earliest iterations [17]. In this sense, the dialogue between Systems Engineering and Naval Architecture becomes essential. Systems Engineering orients the project toward the functions the system must perform, establishing measurable and traceable requirements; Concurrent Engineering promotes the parallel action of

---

disciplines, reducing feedback times between layout, structure, systems, and operational performance. When integrated, these approaches do not replace Evans' spiral but transform it: the spiral retains its value as an iterative verification scheme, but is fuelled by much faster and more comprehensive exploration and filtering mechanisms [17], [18].

Within this integrated perspective, environmental sustainability and emission minimisation emerge as dominant design constraints for contemporary passenger vessels, particularly in the context of coastal and commuter transport [19]. The reduction of atmospheric emissions—both local pollutants and greenhouse gases ( $CO_2$ ,  $NO_x$ ,  $SO_x$ , particulate) [20]—is no longer a secondary optimisation objective, but a binding requirement imposed by international regulations and decarbonisation strategies [21]. Recent literature clearly shows that effective emission reduction relies on integrated measures: resistance minimisation through optimised hull forms [22], adoption of hybrid or fully electric propulsion architectures [23], efficient propulsors tailored to operational profiles, complementary Energy Efficiency Technologies (EETs) [24], and optimised structural and material solutions aimed at reducing displacement and energy demand [25]. Layout decisions—ranging from tank and machinery placement to the allocation of electric machines and energy-storage systems—directly affect weight management, longitudinal distribution and stability margins, and therefore effective resistance under real operating conditions [26], [27]. Hull form, GA, structure, materials and propulsion must consequently be co-designed rather than addressed sequentially.

The adoption of parametric models for structural reinforcement and hull-element verification represents a further essential component of this integrated approach. Recent studies demonstrate how parametric structural optimisation, coupled with performance models and classification-society rules, can significantly reduce both structural weight and material usage while maintaining regulatory compliance [28]. More broadly, these developments point toward the need for an integrated digital design chain encompassing parametric hull and GA definition, rapid hydrodynamic evaluation, stability and weight assessment, propulsion-system simulation and emission evaluation [29].

In light of the above, the most convincing methodological perspective for the design of passenger vessels intended for coastal commuting is not the abandonment of traditional naval-architectural principles, but their critical reinterpretation and integration with

---

advanced digital tools [30]. The design spiral retains its value as a conceptual framework for iterative refinement and verification; however, its effectiveness is renewed only when supported by parametric models, systems-engineering methodologies and concurrent workflows capable of accelerating exploration, improving transparency and supporting sustainability-oriented decision-making in early-stage design.

In this perspective, the evolution of the ship design process outlined above highlights the need for methodologies capable of managing complexity through integration rather than through the traditional decomposition into loosely connected disciplinary stages. The strong interdependence between hull geometry, internal layout, propulsion architecture, structural configuration and regulatory compliance requires preliminary design processes in which these aspects are evaluated concurrently within a coherent, traceable and computationally supported framework.

Building on this conceptual framework, the present research proposes an integrated and parametric methodology for the preliminary design of passenger vessels intended for sustainable coastal transport. The original contribution lies in the development of a computational design pipeline that enables the automatic generation, verification and evaluation of complete vessel configurations during the concept-design phase. Unlike traditional approaches, in which hull form, general arrangement, propulsion selection and structural considerations are addressed sequentially, the proposed methodology embeds these elements within a single parametric environment, allowing their mutual interactions to be explicitly represented and assessed from the earliest design iterations.

Within this methodology, the GA is treated as a primary design driver rather than as a downstream consequence of hull definition. A rule-based and parametric GA model is developed to generate admissible internal layouts consistent with functional, regulatory and accessibility requirements, while simultaneously interacting with hull geometry, structural constraints and propulsion-system integration. In parallel, propulsion and energy systems are modelled as parametric and modular entities, enabling the evaluation of hybrid and low-emission architectures in direct relation to spatial availability, weight distribution and operational profiles. Particular emphasis is placed on solutions aligned with sustainability objectives, including the adoption of series-hybrid propulsion architectures and recyclable structural materials.

---

The methodology is implemented within a parametric modelling environment and coupled with DoE techniques to enable a systematic exploration of the multidimensional design space. Feasibility is no longer assumed implicitly but is enforced through automated checks addressing regulatory compliance, geometric consistency, stability, weight distribution and system integration. This approach allows an initially broad set of generated variants to be progressively filtered into a compact subset of technically admissible and operationally meaningful configurations, suitable for comparative analysis and informed decision-making.

The proposed framework is validated through a case study focused on coastal passenger transport in the Gulf of Trieste. The case study demonstrates the capability of the methodology to generate coherent vessel configurations, analyse key trade-offs between performance, capacity and sustainability, and support transparent early-stage design decisions under realistic operational and regulatory constraints.

The remainder of this thesis is organised as follows. Chapter 1 introduces parametric design as a paradigm for systematic ship exploration and discusses its theoretical and methodological foundations. Chapter 2 analyses the principal technological constraints and design choices related to propulsion systems, hull forms and structural materials, providing the rationale for the solutions adopted in this work. Chapter 3 presents the integrated parametric workflow and details the structure of the computational design pipeline. Chapter 4 describes the case-study application and the validation of the methodology, while Chapter 5 discusses the results, trade-offs and design implications emerging from the analysis. Finally, the conclusions summarise the main findings and outline directions for future research.

## Chapter 1

### Parametric Design as a Paradigm for Ship Exploration

In recent years, ship design has faced a significant increase in complexity, primarily driven by the evolution of the regulatory framework, which has introduced increasingly stringent and often interdependent requirements imposed by certification and control authorities [1]. This intensification of regulatory constraints has progressively reduced the available design space and made the exploration of morphological, functional, and structural alternatives more demanding, exacerbating the conflict between technical constraints and market demands [31].

At the same time, the evolution of shipowners' expectations has imposed an unprecedented level of integration among aesthetics, design quality, and engineering performance. Clients increasingly demand solutions capable of harmonizing aesthetic criteria and operational requirements within a framework of efficiency and sustainability [1].

In this context, the ability to generate, evaluate, and compare a wide range of technically feasible configurations becomes a strategic necessity. Parametric design thus assumes the role of a paradigm able to systematically extend the space of explorable alternatives while ensuring consistency with regulatory and performance requirements [32].

The conceptual shift from the manual definition of a single geometry to the definition of a shape space governed by parameters, constraints, and relationships transforms the design process into a generative and evaluative procedure. This shift accelerates trade-off analysis and improves the traceability of design decisions [32].

The complex demands of shipowners, often in apparent contradiction with the limits imposed by ship physics, safety regulations, and structural requirements, render the search for a single ideal solution ineffective. Instead, design practice requires the construction and assessment of a family of admissible solutions, each representing a different balance among performance, cost, accessibility, comfort, and regulatory compliance [33].

Traditional design methods, although effective in producing compliant solutions, are less suited to generating, within market-driven time frames, a broad and comparable set of

alternatives. This limitation is largely due to the intensive effort required for manually modelling differentiated geometries and the subsequent need for repeated verification steps [8] (Figure 3).

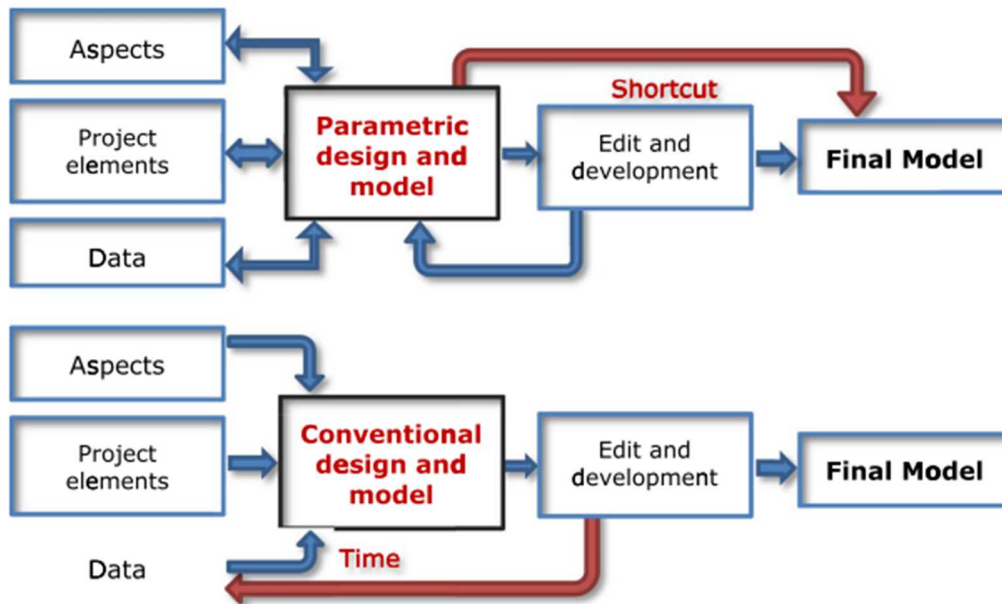


Figure 3 Comparison of parametric and conventional design workflows

### 1.1. Process Logic and Parametric Design Thinking

Parametric design is not merely a set of geometric techniques; it entails a redefinition of design practice and the cognitive processes that support it. According to the paradigm known as Parametric Design Thinking (PDT), the designer ceases to be a mere form-maker and becomes the architect of a system of rules, variables, and constraints capable of generating coherent forms based on boundary conditions [34].

Technically, the implementation of a parametric system requires the formalization of three essential elements:

- the selection of control parameters, geometric or performance-related;
- the definition of mathematical relationships and constraints linking these parameters to the geometric and functional entities of the project;
- the implementation of algorithmic mechanisms capable of translating variations in the parameters into coherent and reproducible geometric variations [34].

Figure 4 shows the intersection of cognitive design knowledge, digital design process models, and parametric design tools, highlighting the integrated nature of parametric design methodologies.

This methodological shift entails a reorganization of the design information flow: initial parameters are no longer rigid constraints, but dynamic components of the generative code from which geometry emerges. Any design modifications are addressed by updating the algorithmic module, which automatically regenerates configurations consistent with the new constraints, significantly reducing the number of manual iterations and improving the overall efficiency of the process [35].

PDT thus emerges as an intersection among cognitive models of design knowledge, parametric models and digital tools/processes, and operational models governing the project sequence, from concept generation to final validation [34], [36].

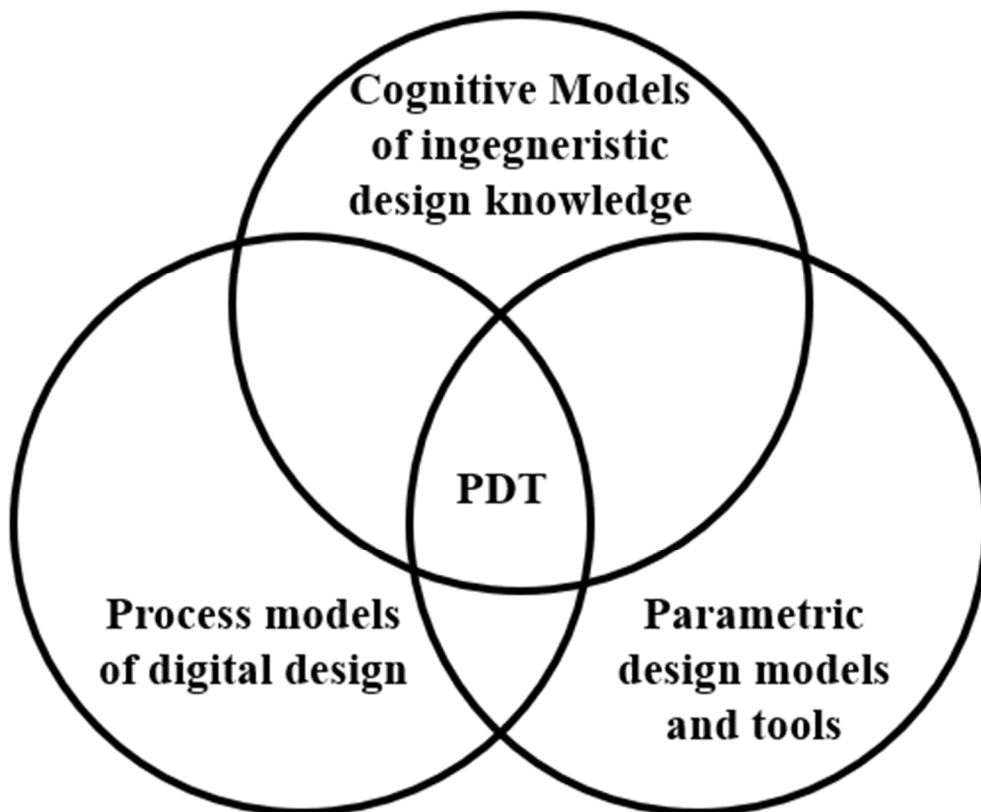


*Figure 4 Schematic representation of Parametric Design Thinking*

## 1.2. Parametric Methodology Applied to Ship Design

The adoption of parametric methodologies in naval architecture is steadily increasing due to their ability to effectively explore the design space and support multi-objective analyses combining performance, economic, and environmental criteria [37].

The resulting iterative efficiency makes it possible to correlate each parametric variation with measurable numerical responses and to integrate such responses into optimization loops and informed decision-making procedures [38].

### 1.2.1. General Characterization of Parametric Techniques: FPA vs. FFD

In hull-form modelling, the literature identifies two complementary yet distinct approaches for shape variation and optimization: the Fully Parametric Approach (FPA) and Free Form Deformation (FFD) [39].

The FPA constructs geometry starting from the explicit definition of primary design parameters, high-level design variables, such as length overall ( $L_{OA}$ ), maximum beam ( $B_{OA}$ ), prismatic coefficient ( $C_P$ ), or longitudinal centre of buoyancy ( $LCB$ ) [40], [41].

Rules are then formalized to convert these parameters into fundamental curves (waterlines, buttocks, sections) and NURBS surfaces, ensuring that variations in engineering parameters propagate deterministically and coherently across the entire geometry (Figure 5).

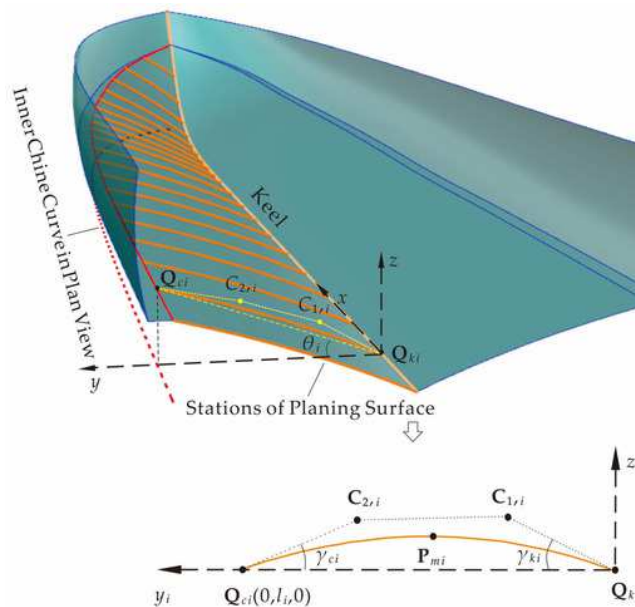


Figure 5 Example of the FPA [41]

A key advantage of the FPA lies in its direct engineering control: the parametric structure is inherently linked to hydrodynamic and stability coefficients, ensuring robustness in generating buildable geometries and facilitating integration with resistance and stability analysis modules [42].

This makes FPA particularly effective for targeted optimization of specific hull typologies, such as planing hulls, where dimensional ratios and shape coefficients critically influence performance [43].

The FFD, by contrast, is a deformation-based technique that modifies a reference (parent) geometry by manipulating the nodes of a non-uniform control lattice [44]. Displacing lattice nodes produces continuous morphological variations throughout the enclosed geometry (Figure 6).

This technique is especially suited to exploratory phases and to the massive generation of variants, and may also be integrated with Reduced Order Modelling (ROM) techniques to restrict geometric variation to a low-dimensional subspace [45].

However, the increased geometric freedom of FFD is also its primary criticality: without embedded plausibility filters and engineering constraints, the resulting deformations may produce non-physical or non-buildable configurations, requiring subsequent validation and filtering steps [29]. The geometric implications and the effectiveness in design space exploration of these two methodological paradigms are clearly visualized in Figure 7, which compares the optimized hull forms resulting from the FPA and FFD. The comparison highlights how the FPA method generates smooth and disciplined geometric variations, preserving the structural plausibility of the hull lines, whereas the FFD approach induces more irregular and aggressive deformations, especially in the forward sections. These differences visually confirm the contrasting nature of the two methods: controlled, engineering-driven variation in FPA versus broader but less constrained exploration in FFD.

For this reason, methodological choices are strategic: FFD enables broad and rapid exploration during the concept phase, especially when integrated with CFD/FEM mesh-based pipelines, while FPA is preferable for trade-off studies constrained by buildability and regulatory compliance [39]. In both industry and academia, hybrid strategies are increasingly

adopted, combining FFD or ROM-based approaches for initial variant generation with FPA for refinement and engineering verification of promising solutions [29].

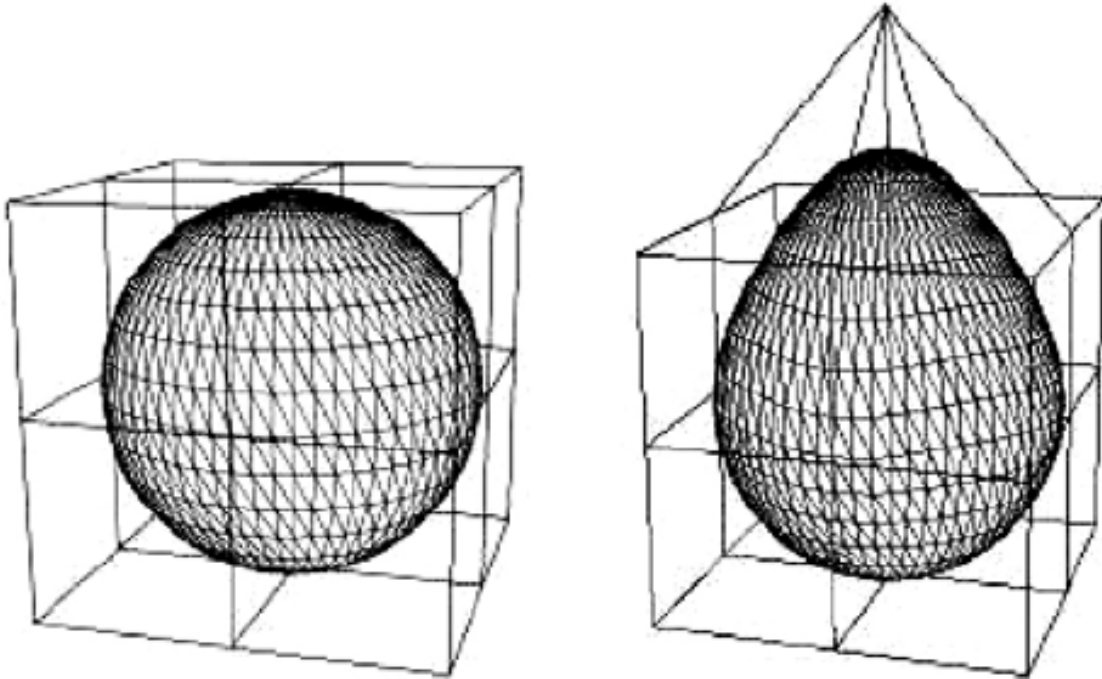


Figure 6 Example of the FFD [46]

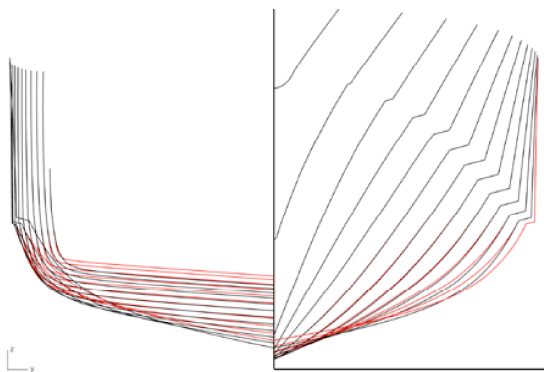


Figure 26: Stations of the FPA optimized hull (red) and the reference hull (black)

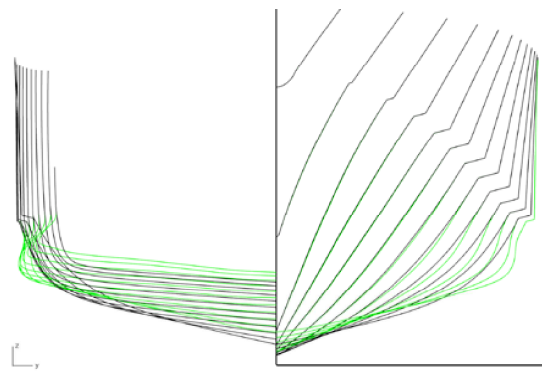


Figure 27: Stations of the FFD optimized hull (green) and the reference hull (black)

Figure 7 Methodological comparison of hull form generation using the FPA and FFD [39]

### 1.2.2. The Mathematical Formalism of Non-Uniform Rational B-Splines

The mathematical foundation supporting both FPA and the controlled geometric transformations of FFD is provided by the formalism of Non-Uniform Rational B-Splines (NURBS) [32].

NURBS surfaces are the industrial standard for modelling complex geometries and for accurately representing conic and quadric surfaces (such as cylinders, spheres, and cones), while offering the continuity, smoothness, and local control required for hull-form fairing [32], [47].

A NURBS curve  $C(u)$  of degree  $p$  is defined as:

$$C(u) = \frac{\sum_{i=0}^n N_{i,p}(u) w_i \mathbf{P}_i}{\sum_{i=0}^n N_{i,p}(u) w_i}$$

Where:

- $\mathbf{P}_i$  are the control points;
- $w_i$  are the associated weights;
- $N_{i,p}(u)$  are the B-spline basis functions of degree  $p$ ;
- $u$  is the non-dimensional curve parameter.

The basis functions  $N_{i,p}(u)$  are recursively defined via the Cox–de Boor formula and depend on the knot vector

$$U = \{u_0, u_1, \dots, u_m\}$$

The non-uniformity of the knot vector and the rational use of weights are key features that grant NURBS their exceptional flexibility.

For hull surfaces, the NURBS formalism extends to the bivariate surface:

$$S(u, v) = \frac{\sum_{i=0}^n \sum_{j=0}^m N_{i,p}(u) M_{j,q}(v) w_{i,j} \mathbf{P}_{i,j}}{\sum_{i=0}^n \sum_{j=0}^m N_{i,p}(u) M_{j,q}(v) w_{i,j}}$$

where the control-point matrix  $\mathbf{P}_{i,j}$  and weights  $w_{i,j}$  define the hull geometry [48].

The integration of NURBS-based modelling with optimization techniques, Design of Experiments, and surrogate modelling represents current best practice for reducing the

computational cost of hydrodynamic evaluations and obtaining reliable Pareto fronts [29], [49].

### *1.2.3. Critique of Commercial Computer-Aided Preliminary Ship Design Systems and Methodological Justification*

Although several dedicated ship design platforms integrate both parametric and analysis functionalities, such as Paramarine, CAESES/FRIENDSHIP Framework, Maxsurf, NAPA and GHS, these tools are typically oriented toward modelling the external hull form and its related analyses. They are less equipped for native, integrated parametric modelling of the General Arrangement (GA), onboard systems, and the packing and proximity rules required for passenger vessels.

Recent advances in generative networks for hull forms, such as ShipHullGAN, demonstrate remarkable geometric generation capabilities but do not fully address the integration of onboard subsystems and regulatory constraints typical of passenger-ship design [15].

Moreover, the proprietary, and often “black-box”, nature of many commercial solutions hinders extensibility and the implementation of custom modules typical of a Systems Engineering approach. This limits the possibility of constructing open and modular pipelines capable of covering hull, GA, structure, regulations and systems [29].

These considerations justify the methodological choice of pursuing, in this work, an integrated and modular parametric pipeline that overcomes the rigidity of commercial CAPSD tools by embedding feasibility filters and regulatory constraints directly into the generation phase, while enabling direct connections with hydrodynamic, structural, and systems-analysis modules.

### **1.3. Grasshopper: A Methodological Environment for Parametric Prototyping**

Among general-purpose parametric modelling environments, Grasshopper for Rhinoceros stands out as a highly extensible visual platform based on NURBS geometry and node-based logic, enabling the construction of algorithmic diagrams for geometric generation without textual programming [50]. Figure 8 illustrates a parametric definition in Grasshopper (right) generating and controlling a 3D geometry (left) within the Rhinoceros environment. This showcases the immediate visual feedback and direct link between the algorithmic definition and the resulting NURBS-based model.

Grasshopper is not a specialized ship software; however, its modular nature and the availability of numerous plugins make it an effective environment for experimenting with both FPA and FFD strategies, and for developing hybrid frameworks that combine rapid design exploration with engineering verification.

Grasshopper enables the construction of modular parametric pipelines, in which subsystems such as hull geometry, general arrangement, structural elements, and onboard systems can be modelled as independent but interconnected modules. Changes in a high-level parameter propagate automatically throughout the network, drastically reducing the number of manual iterations required and ensuring consistency across all project aspects.

Compared with traditional commercial ship CAD platforms, Grasshopper offers several advantages. It provides greater flexibility in defining parametric relationships, enables rapid prototyping and systematic design space exploration, and supports hybrid approaches that combine FPA and FFD strategies within the same environment. While commercial CAPSD tools often focus on hull form and related analyses, Grasshopper facilitates the early incorporation of constraints and feasibility filters and enables seamless integration with specialized analysis modules, enhancing both design efficiency and reliability.

However, for large-scale parametric studies and multi-objective optimizations involving hundreds of variants, Grasshopper alone may not provide sufficient computational efficiency. In such cases, integration with external computation strategies, surrogate models, and multifidelity workflows is necessary to ensure computational sustainability and feasibility for industrial-scale applications [14].

In summary, Grasshopper represents a versatile parametric environment that combines the generation of complex NURBS-based geometries with advanced workflow management, optimization capabilities, and modular integration, bridging the gap between rapid conceptual exploration and rigorous engineering validation in contemporary naval architecture.

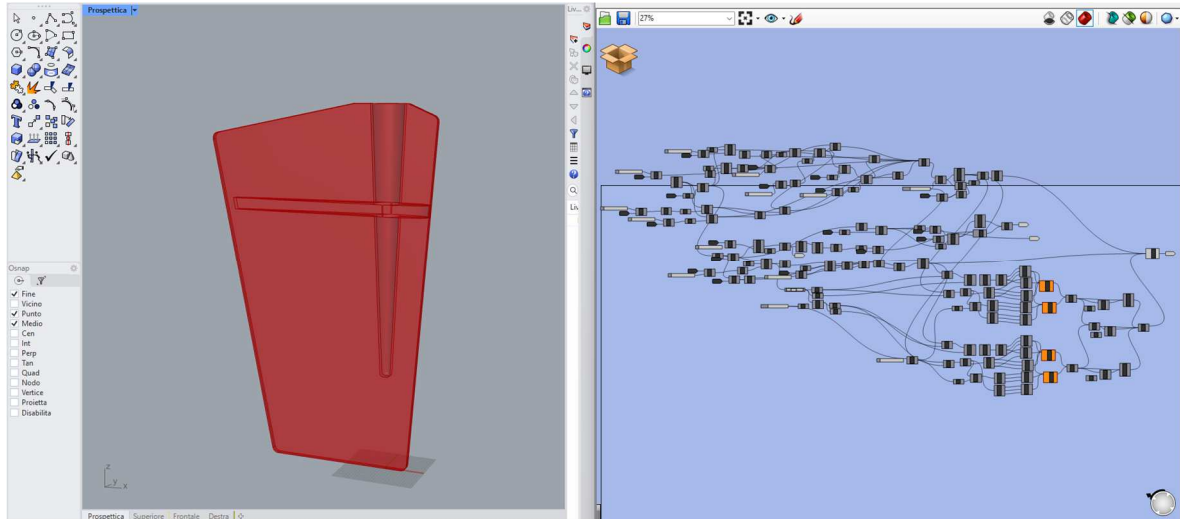


Figure 8 Integration of Grasshopper and Rhinoceros for parametric modelling

## Chapter 2

### Methodological Constraints and Technological Choices

Building on the analysis developed in Chapter 1, which introduced the transition toward a parametric design paradigm capable of exploring wide geometric and functional domains within reduced timeframes, the present chapter formalises the methodological constraints and technological choices adopted for the preliminary configuration of passenger vessels intended for daily coastal transport. This vessel category is characterised by a strong interdependence between regulatory requirements, environmental objectives, operational needs and producibility constraints, which must be addressed coherently within an integrated design framework.

Coastal passenger transport, often underrepresented in naval architecture literature, has become a critical element in the European strategy for the decarbonisation of local mobility. In many urban and peri-urban areas, passenger vessels are expected to integrate with land-based public transport networks, alleviate road congestion, and operate under increasingly stringent limits on atmospheric and acoustic emissions. This calls for a fundamental rethinking of the design approach: it is no longer sufficient to optimise a single discipline (hull form, propulsion, structural layout); rather, the entire ship system must be orchestrated according to a multi-objective, multi-constraint logic consistent with an integrated parametric pipeline.

Within this framework, Chapter 2 pursues two main objectives:

- To critically analyse the principal technological choices concerning propulsion systems, structural materials, and hull morphologies, linking them to the parametric tools introduced in the previous chapter;
- To justify the final selections adopted in the virtual prototypes developed throughout the research, ensuring methodological coherence, traceability, and reproducibility.

Accordingly, the chapter formalises the ensemble of design constraints and technological options that underpin the definition of the virtual prototypes presented in this work. Three closely interconnected themes are addressed:

- a) Propulsion: a comparative review of series-hybrid and parallel-hybrid architectures;
- b) Hull typologies: the identification of the most suitable hull form for coastal commuting, balancing hydrodynamic efficiency, seakeeping, manoeuvrability, and producibility;
- c) Structural materials: a technical, environmental, and life-cycle assessment of GRP, aluminium alloys, and HDPE.

Throughout the chapter, each design choice is justified not only in terms of its technical performance but also with respect to its compatibility with the integrated parametric pipeline (PDT) that will be presented in the methodological chapter, thereby ensuring that constraints and technologies are coherently embedded within the entire digital design process.

## **2.1. Methodology for the Selection of the Propulsion System**

The definition of the propulsion system for passenger vessels operating in coastal service constitutes a multi-objective engineering problem, in which decisions taken at the Concept Design stage have irreversible consequences on hydrodynamic efficiency, propulsive performance, operational expenditure (OPEX), mass distribution, and volumetric integration within the GA [1]. The increasing need to comply with environmental regulations and to reduce emissions [51] further amplifies the complexity of the design space, often rendering non-integrated, sequential approaches sub-optimal.

In response to these challenges, the present work frames propulsion-system selection as a dynamic module within a digital design pipeline. Within the broader context of Integrated Ship Design, this approach requires propulsion architectures to exhibit modularity and parametric decomposability, enabling real-time coupling with geometric-generation algorithms and feasibility checks [52], [53].

Such a methodological stance ensures that propulsion choices are not treated as late-stage constraints but rather as active design variables, capable of influencing and being influenced by the iterative exploration of the vessel's parametric configuration.

### *2.1.1. Technical Analysis and Critical Review of Propulsion Architectures*

In the preliminary technological assessment, two main classes of propulsion systems were considered and evaluated in terms of efficiency, onboard integration, volumetric requirements, operational flexibility, and compatibility with a parametric design pipeline:

1. Series-hybrid system;
2. Parallel-hybrid system.

For each architecture, the fundamental operating principles, advantages, limitations, and relevant performance metrics for passenger transport vessels are examined.

### *2.1.2. Series Hybrid: Architectural Principles and Controlled Power Flow*

The series-hybrid architecture is defined by the elimination of the direct mechanical coupling between the internal combustion engine (ICE) and the propeller. The ICE is connected exclusively to an electrical generator (GS), converting all fuel chemical energy into electrical power, which in turn feeds an AC or DC bus (Figure 9). This electrical link acts as a central distribution node, supplying power to the propulsion electric motor (EM), the onboard auxiliary loads (hotel load), and the energy storage system (ESS) [54], [55].

Mechanical power therefore undergoes a double conversion summarised as

$$\text{Mechanical} \rightarrow \text{Electrical} \rightarrow \text{Mechanical}$$

Such process theoretically introduces efficiency losses. However, in practice these losses are largely compensated by the operational and control advantages achieved [56].

A defining characteristic of this architecture is its installation flexibility [7]. By removing the constraint of rigid coaxial alignment, heavy components, particularly the GS and the ESS, can be positioned optimally within the vessel to balance longitudinal and vertical centres of gravity (*LCG* and *KG*, respectively). This freedom in layout is essential for both effective virtual prototyping and maintaining geometric feasibility within a parametric GA [53], [57].

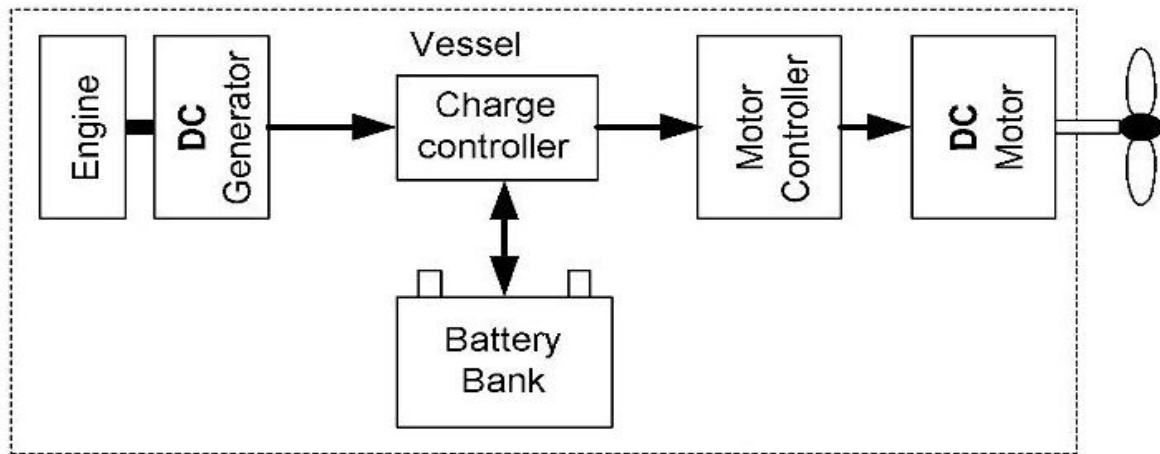


Figure 9 Series Hybrid architecture [58]

### Efficiency Optimisation Through Advanced Control Strategies

The primary engineering advantage of the series-hybrid system lies in the implementation of advanced power management systems (PMSs). These strategies allow the GS to operate consistently at its Optimal Operating Point (OPPT), corresponding to the minimum Brake Specific Fuel Consumption (BSFC) [55]. In contrast, in conventional mechanical systems, the ICE must operate across the full load range, often in thermally inefficient regimes during low-load manoeuvres.

In the series architecture, the ESS serves as a dynamic buffer, handling load transients and performing peak shaving [59]. Instantaneous power demands from the propulsion system, especially during acceleration or deceleration, are supplied to or absorbed by the ESS, thereby shielding the GS from fluctuations. Real-time balancing is achieved as follows:

- if the instantaneous demand  $P_{\text{Prop}} + P_{\text{Aux}}$  is lower than the GS power at OPPT, surplus energy charges the ESS;
- if demand exceeds this threshold, the ESS supplies the deficit.

This isolation of the ICE not only maximises combustion efficiency but also improves onboard acoustic and vibrational comfort [24], [60].

An additional key operating mode is Zero Emission Mode (ZEM), in which the ICE is completely shut down and propulsion is powered solely by the ESS. Enabled by functional decoupling, ZEM is essential for operations in ports and environmentally sensitive areas and constitutes a primary sizing constraint for ESS capacity.

### *Design Implications and Engineering Challenges*

The intrinsic modularity of the series-hybrid system provides a major methodological advantage: each component (GS, EM, ESS) can be treated as a discrete parametric module with attributes such as mass, centre of gravity, and power rating feeding directly into selection and optimisation algorithms. This is crucial for enabling a parametric workflow that explores a wide configuration space while verifying volumetric and stability constraints in real time.

Despite its benefits, implementation introduces several engineering challenges. ESS thermal management is critical, as the high charge/discharge power required for peak shaving generates heat that, if not properly controlled, reduces cell lifespan and efficiency [61]. The PMS also entails significant algorithmic complexity; predictive control strategies are needed to anticipate load transients and optimise energy flow throughout the mission profile.

High-efficiency electrical components (motors and converters with  $\eta > 95\%$ ) are therefore essential to ensure that the thermal and efficiency gains of the GS outweigh the losses associated with double conversion [56]. Integrating such parametric and technical data early in the design process ensures that the selected series-hybrid system is optimised not only for operational efficiency but also for maintainability and long-term durability.

#### *2.1.3. Parallel Hybrid: Architectural Principles and Combined Mechanical-Electrical Power Flow*

Unlike the series system, the parallel-hybrid architecture does not feature full functional decoupling; instead, the two power sources operate in mechanical conjunction. Both the ICE and the EM are directly coupled to the propeller shaft, either directly or through a transmission assembly incorporating reduction gears and clutches (Figure 10) [62].

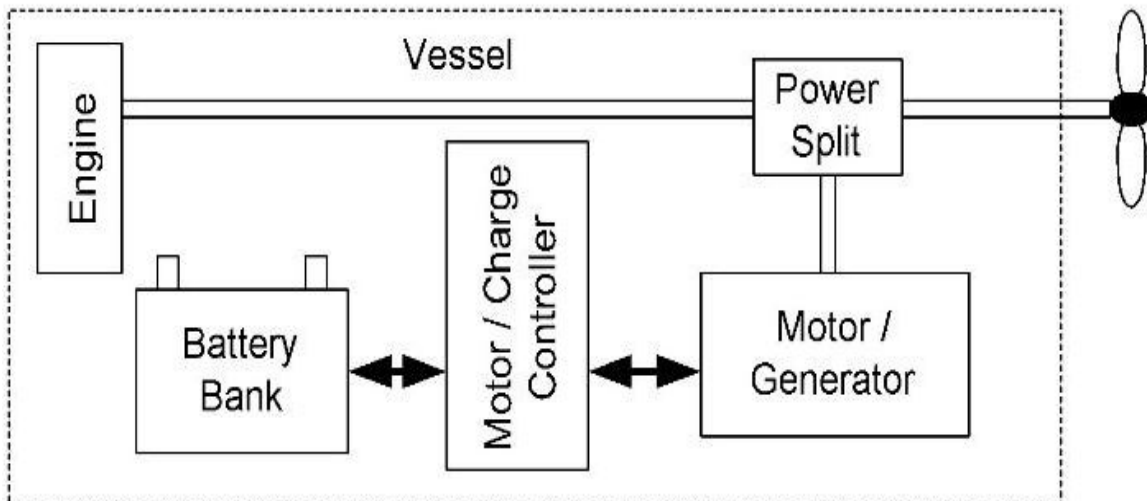


Figure 10 Parallel Hybrid architecture [58]

The core element of this configuration is a mechanical device, typically a planetary reduction gearbox or a clutching system, enabling:

- Pure mechanical mode (diesel–mechanical): the ICE provides the primary propulsion power, while the EM is disengaged or inactive;
- Pure electric mode (ZEM): the ICE is disengaged or shut down, and the EM is powered by the ESS or an auxiliary generator;
- Combined mode (power assist/boost): both ICE and EM operate simultaneously to deliver maximum propulsive power. The EM may also act as a generator, absorbing excess ICE power to recharge the ESS under specific operating conditions.

In this architecture, power flow is predominantly mechanical, with electrical power serving either as an auxiliary propulsion source or as a means of energy storage. System effectiveness depends on the speed and precision with which the clutches engage and disengage the two power sources, a process requiring a sophisticated PMS to avoid harmful mechanical transients.

#### Performance Advantages and Efficiency Strategies

The main scientific advantage of the parallel-hybrid system is its higher efficiency at elevated cruising speeds. Because the ICE is directly coupled to the shaft, its mechanical output is not subject to double-conversion losses, as occurs in the series-hybrid [62]. In

operating regimes requiring sustained high power, the parallel system maximises thermal efficiency and minimises electrical losses.

PMS strategies can leverage this architecture to enable:

- Power boost, using the EM to provide additional torque during acceleration or in rough sea states, reducing the need for ICE oversizing;
- Optimal gear selection, where the EM acts as a variable transmission device to keep the ICE near its optimal BSFC over a broader range of vessel speeds;
- Regenerative braking/charging, where the EM recharges the ESS during deceleration or when the ICE provides excess power, improving the overall energy balance.

### Engineering Limitations and Integration Challenges

Despite its advantages in high-power scenarios, the parallel-hybrid architecture presents limitations that reduce its suitability for small passenger vessels subject to strict GA and maintenance constraints.

1. Mechanical complexity and rigid layout requirements: Direct mechanical coupling imposes strict alignment constraints, significantly reducing flexibility in component placement. This conflicts with the need for GA optimisation and weight distribution control in parametric design processes. The presence of complex transmission subsystems (clutches, gears) increases mass, spatial requirements, and mechanical intricacy;
2. Reduced efficiency at partial load: Although efficient at high power output, the parallel-hybrid can be penalised at partial loads. The ICE operates over a wider range of regimes compared to the fixed OPPT of the series-hybrid, and mechanical losses from the transmission can further degrade efficiency at low vessel speeds typical of port operations;
3. Maintenance burden and reliability constraints: The increased mechanical complexity, high-power clutches, interconnected reduction gears, raises maintenance requirements (OPEX) and introduces additional potential points of failure. These factors must be carefully addressed in life-cycle assessments.

In conclusion, while the parallel-hybrid architecture excels in delivering high power and efficient cruising performance, its mechanical integration constraints and transmission complexity make it less suitable for small passenger vessels designed within an Integrated Parametric Design paradigm, where modularity and layout flexibility are decisive requirements.

### *2.1.4. Comparative Synthesis and Final Rationale for the Solution*

The quantitative and qualitative analysis of the alternative propulsion architectures converges robustly toward the selection of the series-hybrid system. This preference is not arbitrary; rather, it is scientifically motivated by the superior ability of this architecture to balance energy efficiency, installation flexibility, and methodological coherence with the PDT paradigm. In addition, the environmental implications of the two configurations further reinforce this choice.

Although both architectures can contribute to reducing the operational impact of coastal passenger vessels, the series-hybrid layout provides a more favourable platform for implementing energy-saving strategies and low-emission operating modes. Its capability to operate engines closer to optimal loading, integrate battery-assisted propulsion, and accommodate future alternative energy sources allows for a substantial reduction of fuel consumption and pollutant emissions.

In conclusion, the selection of the series-hybrid architecture results from the convergence of technical, operational, and environmental factors. Its combined advantages in layout flexibility, energy efficiency, and sustainable operation make it the most technologically and methodologically robust solution for coastal passenger transport within a PDT framework.

## **2.2. Hull Form Selection**

The definition of the hull geometry represents a pivotal stage in the design of high-speed and semi-displacement vessels, as it simultaneously influences resistance, seakeeping performance, manoeuvrability, integration of onboard systems, and construction constraints.

For small and medium-sized passenger craft, this choice cannot rely solely on minimising resistance at a single operating point; rather, it requires a multi-criteria evaluation that accounts for hydrodynamic performance, stability requirements, manoeuvring

characteristics, constructability, internal volumetric integration, and coherence with the adopted propulsion architecture (see Chapter 2.1).

Within this framework, the present chapter provides a critical analysis of the main morphological families employed in boat design, namely round-bilge and hard-chine configurations, by comparing them against the most established experimental systematic series, including the NPL High-Speed Round-Bilge Series (Bailey, 1976) (Figure 11) [63], the Series 62 in its DTMB (1962) (Figure 12) [64] and Delft (1982, 1993) [65], [66] developments, and the Semiplaning Systematic Series (SS) developed by Compton (U.S. Naval Academy, 1986) (Figure 13) [67].

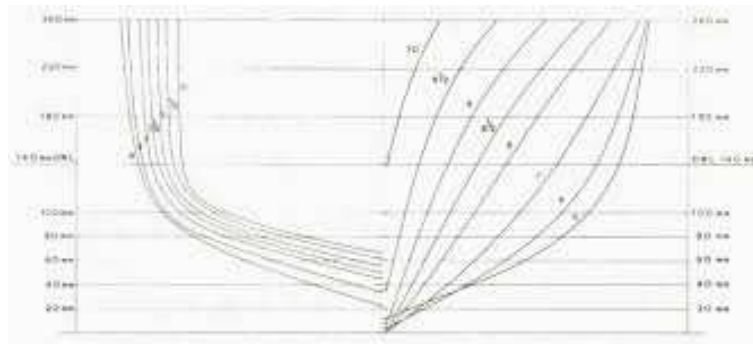


Figure 11 Body-plan of NPL High-Speed Round-Bilge Series (Bailey, 1976)

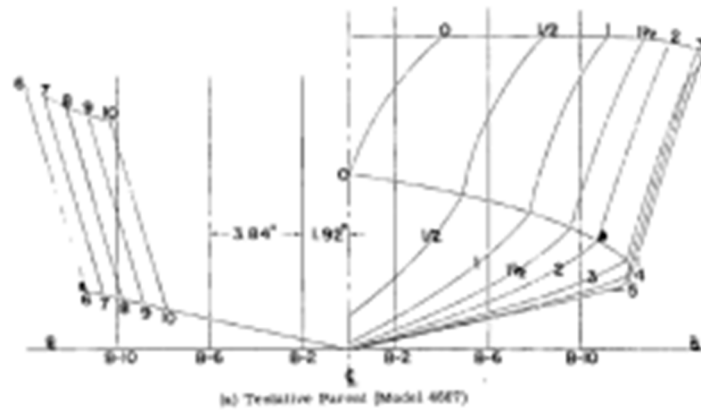


Figure 12 Body-plan of the Series 62 systematic set (Clement & Blount, 1962)

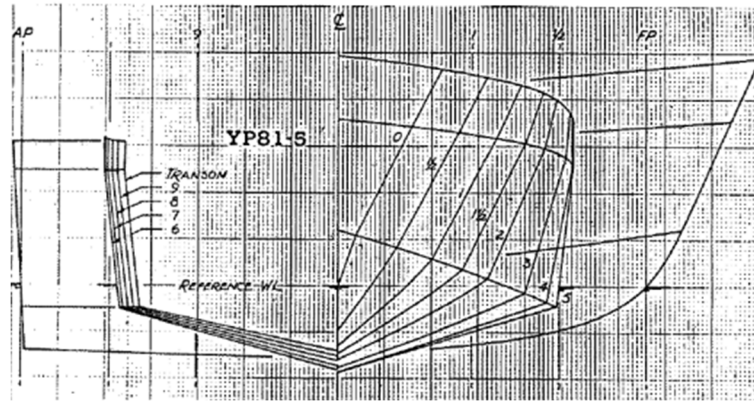


Figure 13 Body-plan of the Semiplaning Systematic Series (Compton, 1986)

These series are employed here as interpretative tools that help delineate the operational characteristics, strengths and limitations associated with each hull family, and to support an informed selection aligned with the design goals of the present work.

### 2.2.1. Operational Framework

The vessels within the national fleet considered in this study typically operate between 10 and 24 knots, with waterline lengths ranging from 15 to 24 metres. Under these conditions, the volumetric Froude number falls within the interval  $Fn_V \approx 0.6 - 4$ , positioning these craft in the semi-displacement regime, with partial transitions toward semi-planing behaviour. Within this dynamic range, hydrodynamic resistance arises from a composite interaction of viscous and wave-making phenomena, while trim and sinkage may vary significantly with speed and loading condition. Additional influences derive from the geometry of the transom, and the presence or absence of spray rails. These factors collectively demonstrate that the assumption of a round-bilge hull as universally optimal is overly reductive. The actual performance of a hull form is strongly conditioned by parameters such as the L/B ratio, the longitudinal position of the centre of buoyancy, the geometry and sharpness of the chines, and the vessel's operational environment, which — for passenger coastal vessels — often includes confined areas, repeated manoeuvres and wave climates. A rigorous comparison between competing hull morphologies must therefore be anchored in coherent design criteria and informed by systematic-series benchmarks.

From a hydrodynamic perspective, round-bilge hulls may display advantages at low Froude numbers owing to their reduced wetted surface and curvature continuity, which favour lower viscous resistance. However, hard-chine hulls exhibit distinct advantages in terms of

manoeuvring performance and dynamic stability, particularly at the low-to-medium speeds characteristic of coastal passenger operations [68]. The presence of a chine enhances the generation of lateral forces and promotes a more predictable response during rapid course corrections, while also contributing to improved directional stability during transient phases such as acceleration and deceleration. Classical experimental work on fast craft, including the contributions of Savitsky and Brown (1976) [69] and Blount and Fox (1975) [70], consistently demonstrates that the separation surfaces induced by the chine strengthen directional control in semi-displacement and semi-planing regimes. For vessels that must operate in constrained harbour areas or along irregular coastal routes, these qualities may become equally, if not more, decisive than minimal differences in bare-hull resistance.

Constructional and architectural considerations reinforce the preference for a hard-chine configuration. Developable plating is readily achieved with aluminium, light steel or composite materials, enabling shorter production times, reduced costs and greater repeatability, an advantage in fleet-oriented manufacturing contexts. The resulting internal geometry tends to be more regular and thus more conducive to the efficient arrangement of propulsion equipment, auxiliary systems or, where required, energy-storage modules. The overall mass distribution also benefits from clearer structural reference planes and more predictable positioning of concentrated weights, a factor of particular relevance when hybrid propulsion systems are adopted. Within the PDT, planar surfaces and well-defined edges facilitate robust geometric regeneration, minimise volumetric interference between subsystems and enable the effective integration of DoE procedures.

Although systematic series such as those previously cited provide invaluable guidance in understanding the hydrodynamic tendencies of different hull families, their applicability remains inherently constrained by the discrete nature of the experimental matrices from which they derive. The design problem addressed in this thesis involves specific constraints related to layout, construction and propulsion integration that cannot be adequately represented by the fixed geometries of historical systematic series. This motivates the adoption of a dedicated parametric formulation capable of spanning a broader and more flexible design space.

For these reasons, a hard-chine hull has been selected as the most suitable foundation for the present design study. This methodological choice allows explicit control over the key

geometric variables that govern hydrodynamic performance, supports the generation of coherent hull families tailored to the project requirements, and ensures a smooth integration into the PDT.

### **2.3. Structural Material Selection: Condition of the National Fleet and Prospects**

The selection of the structural material for small vessels intended for coastal passenger transport is not merely a technological issue; it is a decision that affects the entire life cycle of the craft and, consequently, the sustainability of the maritime mobility system as a whole. In the Italian context, this question is particularly critical: the existing fleet is large, on average old, and heavily dependent on glass-reinforced plastic (GRP). Recent data for the European boating sector indicate that around 90% of pleasure craft are built from glass fibre-reinforced composites [71], with an estimated abandonment rate on the order of 1–2% of the fleet in service. In Italy alone, tens of thousands of GRP boats are believed to be abandoned or out of use, with significant accumulations in sensitive lagoon and coastal areas [72].

The analysis of the national fleet of small coastal passenger vessels (typical lengths 15–24 m) reveals a situation that is broadly aligned with wider European trends: the vast majority of hulls are built in GRP, accompanied by a smaller but growing share of marine aluminium-alloy units and a residual number of steel craft. This picture is consistent with the specialist literature on the market for leisure craft and small workboats, where GRP composites account for up to approximately 80% of hulls below 20–24 m in length [73].

Recent Life Cycle Assessment (LCA) studies on composite manufacturing technologies for marine applications show, however, that while the widespread adoption of GRP has enabled a substantial reduction in production costs and a remarkable degree of formal freedom, it also generates significant criticalities in both production and end-of-life phases. The assessment of impacts associated with the manufacture of composite structures highlights the dominant contribution of materials (particularly fibres and resins) compared with process energy [74].

In this context, the choice of structural material for new coastal passenger vessels cannot ignore the inertia of the existing fleet, nor the need to avoid reproducing the same problem in the next generational cycle of hulls.

In parallel, the international debate on Green Boatbuilding [75] emphasises the central role of recyclable materials, low-energy production processes and design-for-end-of-life strategies, with growing attention to recyclable thermoplastic polymers and innovative materials such as high-density polyethylene (HDPE). This perspective is reflected, for example, in studies on green shipbuilding and concurrent green ship design [76], on the challenges of green shipbuilding and recycling [77], and on the role of design and material selection within green shipbuilding technologies [78], as well as in recent research exploring the potential of thermoplastic materials and the use of parametric tools to support their characterisation and structural optimisation [79].

However, the adoption of such alternative materials must also be reconciled with the specific geometric and hydrodynamic requirements of the hull. In particular, materials such as HDPE and, in some cases, marine aluminium alloys present limitations in terms of achievable curvature and formability, which may constrain the designer's ability to realise certain hull geometries. This introduces a strong interdependence between material selection and hull form design, making the choice of structural material a key decision that must be aligned with both functional and morphological objectives.

### *2.3.1. Glass-Reinforced Plastic: technological maturity and end-of-life criticalities*

For more than half a century, glass-reinforced plastic has been the reference material for small- and medium-sized hulls, thanks to a favourable compromise between weight, cost, mechanical strength and geometric freedom. The combination of glass fibres with thermoset resins (typically polyester or vinylester) enables complex geometries, large continuous surfaces and high-quality finishes, together with excellent corrosion resistance in the marine environment [73]. A particularly emblematic demonstration of the geometric freedom achievable with glass-fibre/thermoset composite construction is provided by MAMBO (Figure 14), the 3D-printed GRP boat developed by the Politecnico di Milano in collaboration with MICAD and Moi Composites. As documented in recent research on innovative composite manufacturing, MAMBO's hull showcases the ability of GRP materials to form continuous, highly sculpted surfaces that would be impractical with traditional metallic construction techniques.

Table 1 provides an overview of the typical mechanical properties of GRP materials commonly employed in small and medium-sized marine hull structures. These properties

have progressively fostered the standardisation of hand lay-up and vacuum-infusion processes and the diffusion of series production for leisure craft and coastal passenger vessels.

*Table 1 Typical mechanical properties of GRP laminates*

<b>Property</b>	<b>GRP – E-glass/Polyester or Vinylester</b>
<i>Density</i>	1.5–1.9 g/cm <sup>3</sup>
<i>Tensile Strength</i>	200–900 MPa (laminate dependent)
<i>Tensile Modulus</i>	15–25 GPa
<i>Compressive Strength</i>	150–350 MPa
<i>Flexural Strength</i>	250–500 MPa
<i>Flexural Modulus</i>	10–20 GPa
<i>Interlaminar Shear Strength</i>	20–40 MPa
<i>Elongation at Break</i>	1.5–3%
<i>Fatigue Resistance</i>	Moderate; dependent on laminate design and resin system
<i>Corrosion Resistance</i>	Excellent in marine environments
<i>Water Absorption</i>	0.1–0.5% (depending on resin type)



Figure 14 MAMBO prototype: an experimental GRP hull [<https://alumni.polimi.it/2020/10/14/la-prima-barca-al-mondo-in-fibra-di-vetro-stampata-in-3d-e-made-in-polimi/>]

LCA studies on GRP boats indicate, however, that while the production phase is indeed relevant in terms of embodied energy and emissions, it does not constitute the only critical node: the real discontinuity arises at end of life. Comparative LCAs on GRP hulls manufactured by hand lay-up and vacuum infusion show that process choices significantly affect the overall environmental balance, but they also confirm that the non-recyclable nature of thermoset matrices is a structural limitation for any recycling strategy [80].

From an end-of-life management standpoint, GRP behaves as a “problematic” material: as a thermoset composite, it cannot be remelted like a metal or a thermoplastic, and the technologies currently available for its recycling (pyrolysis, co-processing in cement kilns, solvolysis) are characterised by high plant complexity, significant energy consumption and an economic yield often insufficient to sustain stable industrial supply chains. An in-depth analysis by Önal and Neşer, based on LCA methodologies compliant with ISO 14040–14044, confirms that the end-of-life options currently implemented for GRP hulls are associated with non-negligible environmental impacts and very limited material recovery [81]. Evidence gathered from operators also points to a progressive increase in the number of hulls abandoned in marinas and yards, in the absence of economically viable models for demolition and composite-waste treatment.

In the national context, these considerations are particularly significant. The combination of a large, ageing fleet built almost entirely in GRP implies that, within a relatively short time frame, a substantial number of coastal passenger hulls (similar to the one shown in Figure 15) will reach the end of their service life simultaneously. In the absence of structured end-of-life management chains, there is a concrete risk of shifting the environmental and

logistical burden from the operational phase to the disposal phase, with potential impacts on ports and coastal areas.



*Figure 15 Typical example of an ageing GRP coastal passenger vessel*

### 2.3.2. Marine aluminium alloys: recyclability and durability

Marine aluminium alloys (5xxx–6xxx series) represent the most mature metallic alternative to GRP for small and medium-sized hulls intended for coastal passenger transport. Structurally, they provide high specific strength, good toughness and ductile behaviour, with plate thicknesses generally lower than those of steel and beneficial effects on overall ship weight and fuel consumption.

Table 2 summarises the key mechanical properties of the most commonly employed marine-grade aluminium alloys., where H stands for strain-hardened and T for tempered.

Comparative LCA analyses on aluminium alloys and composite hulls for high-speed craft show that, when the entire life cycle is considered, the weight reduction afforded by lightweight structures can translate into significant reductions in fuel consumption and, consequently, operational emissions [82].

A crucial feature of aluminium in relation to circular-economy objectives is its potentially unlimited recyclability. Consolidated data from the International Aluminium Institute indicate that the production of secondary aluminium requires only about 5–10% of the energy needed to produce primary aluminium from bauxite, with a corresponding reduction in emissions associated with extraction and refining [83]. In ship LCA scenarios, the recycling credit associated with closing the aluminium loop can, in many cases, fully offset

the higher impacts of primary production compared with other materials, especially when the vessel's operational lifetime is long and the end-of-life recovery rate is high.

Sector-specific studies on shipbuilding confirm these findings. Comparative LCAs of different structural solutions for high-speed craft show that, although the production of aluminium hulls can exhibit slightly higher values in some impact categories relative to composites, the combined effect of weight reduction, lower fuel consumption and high recyclability makes aluminium competitive and, in many cases, favourable in terms of overall environmental impact [82].

A further advantage of aluminium in the context of this thesis is its full acceptance by major classification societies for passenger and high-speed vessels. RINA's rules for marine aluminium hulls have long provided consolidated criteria for structural design, production control and durability management in the marine environment [84], thereby reducing regulatory uncertainty associated with innovative solutions.

From an operational standpoint, aluminium offers additional advantages. Its metallic nature allows direct inspection of the structure, facilitates structural modifications over the ship's lifetime, and is fully compatible with conventional coating systems. The main drawbacks relate to susceptibility to galvanic corrosion, requiring careful design of joints and interfaces with dissimilar metals, and the need for skilled personnel to ensure welding quality. These aspects are, however, widely manageable within national shipyards, particularly in sectors already experienced in aluminium construction (patrol boats, fast ferries, workboats).

### *2.3.3. HDPE: thermoplastic potential and current regulatory constraints*

High-density polyethylene (HDPE) belongs to a family of thermoplastic materials that, in recent years, has attracted growing interest in the maritime sector, particularly for small workboats such as aquaculture vessels, anti-pollution craft, service boats and harbour workboats.

Figure 16 shows a typical HDPE workboat, illustrating the type of small utility craft for which this material has become increasingly popular.

Industrial case studies and experimental investigations reported in the literature confirm that HDPE hulls can offer low density, high impact resistance, immunity to corrosion and fouling, as well as the possibility of thermoplastic welding and remelt-based recycling at end

of life. Table 3 summarises the typical mechanical properties of HDPE used in the construction of small workboats and marine service craft.

*Table 2 Mechanical properties of marine-grade aluminium alloys*

<b>Property</b>	<b>5083-H116</b>	<b>5083-H321</b>	<b>5086-H116</b>	<b>6061-T6</b>	<b>6082-T6</b>
<i>Yield Strength (0.2% offset)</i>	~215 MPa	~ 240 MPa	~170 MPa	~275 MPa	~260 MPa
<i>Ultimate Tensile Strength</i>	~305 MPa	~ 330 MPa	~260 MPa	~310 MPa	~340 MPa
<i>Elongation (A50)</i>	10–12%	10–12%	12–14%	8–10%	8–12%
<i>Hardness (Brinell)</i>	~75 HB	~ 78 HB	~60 HB	~95 HB	~95 HB
<i>Modulus of Elasticity</i>	70 GPa	70 GPa	70 GPa	69 GPa	69 GPa
<i>Shear Strength</i>	~200 MPa	~ 200 MPa	~180 MPa	~200 MPa	~205 MPa
<i>Fatigue Strength (<math>5 \times 10^8</math> cycles)</i>	~95 MPa	~ 95 MPa	~85 MPa	~96 MPa	~90 MPa
<i>Density</i>	2.66–2.70 g/cm <sup>3</sup>	2.66–2.70 g/cm <sup>3</sup>	2.65–2.70 g/cm <sup>3</sup>	2.70 g/cm <sup>3</sup>	2.70 g/cm <sup>3</sup>
<i>Weldability</i>	Excellent	Excellent	Excellent	Good	Good
<i>Corrosion Resistance</i>	Very high	Very high	Very high	Moderate-to-good	Good



*Figure 16 Example of an HDPE workboat [<https://tidemanboats.com/>]*

The thermoplastic nature of HDPE introduces a conceptual advantage over thermoset composites: in principle, hull structures can be remelted and reprocessed into new shapes or components, drastically reducing the amount of unrecoverable waste. Recent experimental campaigns on virgin and recycled HDPE for marine applications show that, even after recycling cycles, the material retains mechanical properties compatible with structural uses at moderate load levels, albeit with some variation in elastic moduli and long-term response [85]. Other studies focusing on the structural response of HDPE panels and sandwich configurations under static and impact loading reveal a highly ductile behaviour and a notable energy-absorption capacity, with large plastic deformations but preservation of overall structural integrity [75]. These characteristics make HDPE particularly attractive for workboats and service craft, where damage tolerance and robustness in operation are at least as important as hydrodynamic performance.

Despite this potential, the use of HDPE in passenger vessels for public service remains, at present, limited. Operational experience documented in the literature concerns almost exclusively workboats, service craft and small specialised units, often certified according to CE standards or specific class notations, but not yet embedded within a comprehensive regulatory framework for conventional coastal passenger ships. From a regulatory standpoint, some classification societies, including RINA, have recently begun introducing dedicated chapters on HDPE hulls within their workboat rules [86], but fully developed and widely applied rules for passenger vessels engaged in regular public transport are not yet available.

In parallel, international experimental programmes and pilot projects are underway to characterise the structural behaviour, fire response and long-term durability of HDPE and

other thermoplastic structures, with the aim of providing classification societies with sufficient data to consider future extensions of their rules to passenger transport.

### *2.3.4. Critical synthesis*

Bringing together evidence on the existing fleet, structural performance and end-of-life scenarios leads to three main conclusions for national coastal passenger transport. GRP, while still dominant due to its industrial maturity, presents significant end-of-life issues, with no widely implemented or economically viable recycling solutions and the consequent risk of accumulating composite waste from an ageing fleet. HDPE offers strong potential in terms of recyclability and ductile performance, but its adoption remains limited to workboats, with evolving regulations and no consolidated experience in the passenger sector. Marine aluminium alloys currently stand out as the most suitable option for new low-impact passenger vessels, combining regulatory acceptance, favourable structural and weight performance, and high recycling rates. Consequently, the hull parametric modelling in this thesis will assume marine aluminium alloys as the baseline material.

Table 3 Typical mechanical properties of HDPE

<i>Property</i>	<b>HDPE</b>
<i>Density</i>	0.94–0.96 g/cm <sup>3</sup>
<i>Yield Strength (Tensile)</i>	20–30 MPa
<i>Ultimate Tensile Strength</i>	25–35 MPa
<i>Tensile Modulus</i>	0.8–1.5 GPa
<i>Flexural Strength</i>	20–30 MPa
<i>Flexural Modulus</i>	0.8–1.2 GPa
<i>Compressive Strength</i>	15–25 MPa
<i>Elongation at Break</i>	> 200%
<i>Impact Resistance</i>	Very high
<i>Fatigue Resistance</i>	Good, especially under low-stress cycles
<i>Water Absorption</i>	< 0.01%
<i>Corrosion/UV Resistance</i>	Excellent (UV-stabilised grades)
<i>Typical Melting Temperature</i>	130–135 °C
<i>Continuous Service Temperature</i>	–50 °C to +60 °C
<i>Maximum Short-Term Service Temperature</i>	~80–90 °C
<i>Brittleness Temperature</i>	–100 °C

## Chapter 3

### Methodological Workflow and Process Overview

In continuity with the considerations developed in Chapter 1 and in continuity with the methodological constraints and technological choices formalised in Chapter 2, this section presents the overall methodological workflow developed in this study. The proposed approach addresses the limitations of the traditional design spiral by adopting a Concurrent Engineering paradigm, in which the modules responsible for generation, verification, and evaluation operate in parallel rather than through a rigidly sequential process.

The original contribution of this research lies in the development of an integrated parametric model for the concept design of coastal passenger vessels, in which the automatic generation of geometric variants, the configuration of the general arrangement, structural modelling, propulsion-system selection, and regulatory verification operate within a single computational workflow. This architecture, based on Design of Experiments (DoE) techniques and on the formalisation of design constraints from the earliest stages, enables a systematic, traceable, and engineering-coherent exploration of the solution space, overcoming the limitations of traditional sequential paradigms. The full workflow underlying the integrated parametric model is implemented in Grasshopper, which serves as the computational environment for encoding geometric relationships, constraint logic and system interactions. This implementation ensures complete transparency, extensibility, and reproducibility of the modelling process.

The flow chart shown in Figure 17 represents the conceptual framework within which the entire parametric design process is structured, coherently organizing owner requirements, regulatory prescriptions, preliminary technological choices, and technical databases. The integration of these informational sets within a computational process makes it possible to effectively manage the interdependencies between heterogeneous domains, ensuring consistency and traceability throughout the entire design pipeline.

In the operational model thus defined, the owner's specifications establish the functional and performance framework within which the project must be situated, whereas the regulatory

constraints, pertaining to safety, stability, subdivision, structural requirements, and onboard systems, set the limits within which the generated configurations must remain to be considered certifiable. Preliminary design decisions, such as the hull typology, the propulsion arrangement, and the structural material, contribute to defining the technological architecture of the vessel and guide the evolution of the geometric, structural, and functional modules. In parallel, the integration of technical databases provides a structured set of dimensional and performance information relating to components and systems, ensuring that each generated variant is compatible with physically realizable elements rather than purely conceptual constructs.

This methodological phase plays a decisive role in establishing the logical relations and co-dependencies that govern the design process. The chain linking hull generation, structural modelling, engine room arrangement, general arrangement development, resistance analysis, propulsion system selection, and the assessment of weights, centres, and stability does not follow a linear sequence. Instead, it takes the form of a complex system of interconnected information flows that continuously feed into one another. Such a methodological configuration enables the timely activation of consistency and feasibility checks, reducing the risk of producing configurations lacking engineering significance and ensuring internal coherence among geometries, constraints, and functions. The overarching architecture thereby becomes the regulatory structure of the parametric process: it defines what must be generated, which constraints must be respected, and how intermediate results must be recombined to guide the production of subsequent configurations.

Based on this general framework, the integrated model is established, with its architecture illustrated in Figure 18. While the parametric methodology provides the logical foundation, the integrated model constitutes its algorithmic translation, formalizing the mechanisms through which variables, parameters, and constraints are transformed into complete three-dimensional configurations. The systematic exploration of the parametric domain is achieved through the application of DoE techniques, which are introduced in Chapter 3.4 and represent the core mechanism by which alternative configurations are generated and evaluated. The parametric and integrated pipeline relies on DoE techniques, which constitutes statistical methodologies aimed at systematically exploring the design space through the controlled sampling of independent variables. DoE allows for a drastic reduction in the number of evaluations required to achieve a meaningful representation of the

parametric domain, while ensuring a balanced distribution of input combinations. In this research, the DoE approach is implemented through Uniform Latin Hypercube Sampling (ULHS), which guarantees uniform coverage of the multidimensional space and prevents clustering phenomena that would undermine the significance of the exploration.

Once the parametric domain has been defined, the information derived from the owner's specifications, regulatory requirements, and preliminary design decisions is converted into a set of independent variables and subsequently into controllable parameters, which constitute the primary input of the system. Each parameter set generated through ULHS represents a distinct design configuration and triggers the activation of all modelling, verification, and evaluation modules described in the following sections. This formalization enables the transformation of heterogeneous qualitative constraints into a stable and manipulable computational domain within which automatic generation can be activated. Each point generated through ULHS represents a potential vessel configuration and triggers the construction of the three-dimensional model.

The resulting 3D model integrates all fundamental technical aspects of the concept design, hull, structure, systems, propulsion arrangements, engine room layout and general arrangement, according to computational logics that operate in parallel and mutually influence one another. The co-dependence between the general arrangement and the structural model is particularly significant: the former defines the functional distribution of volumes and spaces, while the latter governs their engineering materialization. This bidirectional relationship ensures that every configuration simultaneously satisfies functional, volumetric, and structural constraints.

Each 3D model generated is subsequently subjected to automatic checks that include geometric validations, regulatory compliance assessments, stability and trim analyses, verification of weight distribution, and evaluation of the feasibility of integrating propulsion and onboard systems. Only the configurations that pass all these checks are classified as admissible and stored within the space of valid solutions. For each accepted configuration, the pipeline automatically produces 3D models, 2D drawings, technical tables, and performance indicators, thereby forming the basis for comparative analyses, multi-objective evaluations, and subsequent optimization cycles.

Overall, the integration between the general methodology and the parametric model transforms preliminary design from a sequential, slow, and rigidly iterative process into a digital system capable of exploring the entire design space in a systematic, controlled, and traceable manner, thereby ensuring coherence among functions, structural constraints, and operational requirements.

The following sections therefore present a detailed analysis of the individual modules of the integrated model, progressing from the definition of parametric entities and constraints, through the DoE-based sampling strategy to the feasibility analysis framework presented in Chapter 3.5, which determines the set of admissible design solutions.

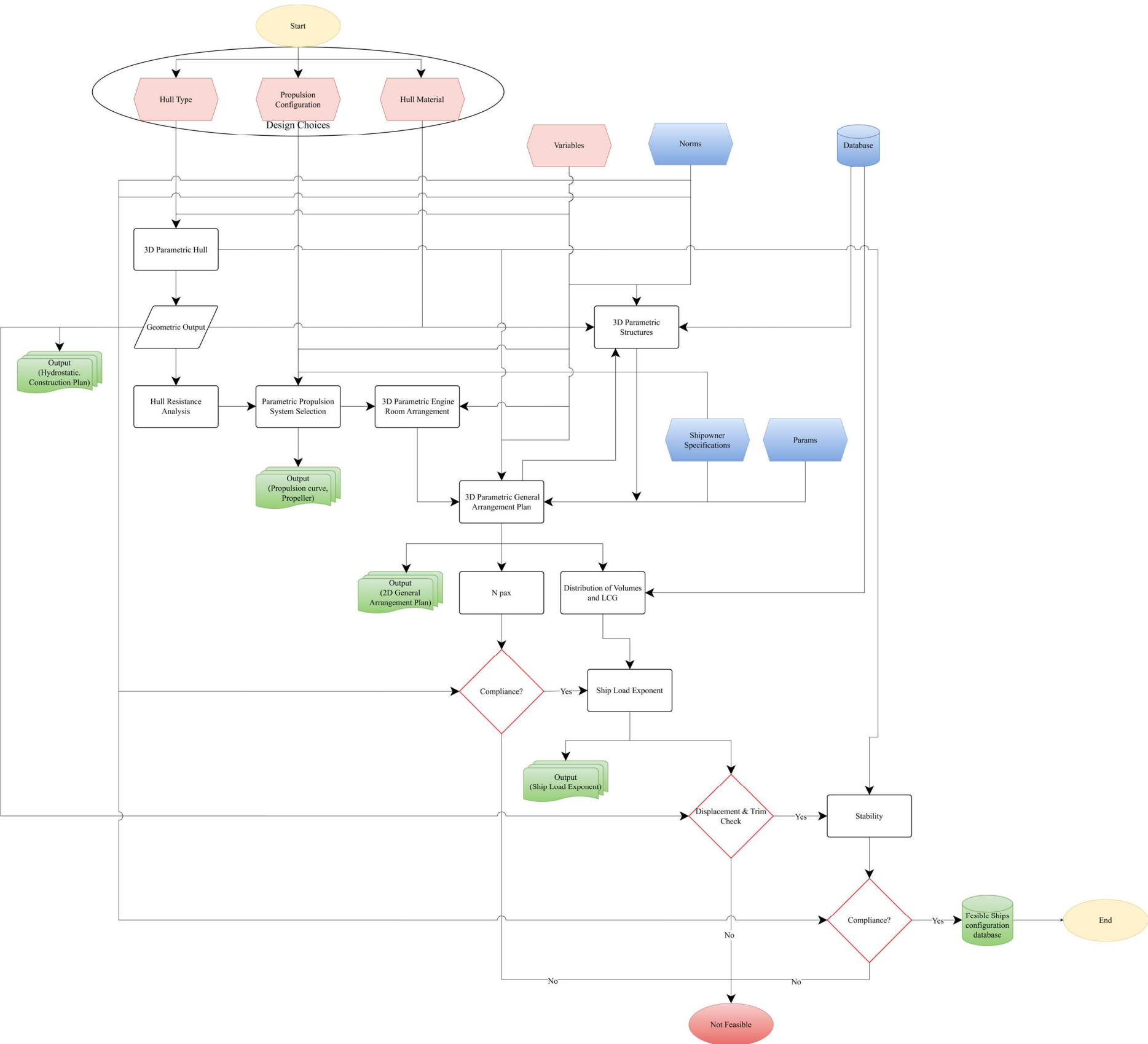


Figure 17 Information flow within the integrated parametric design model

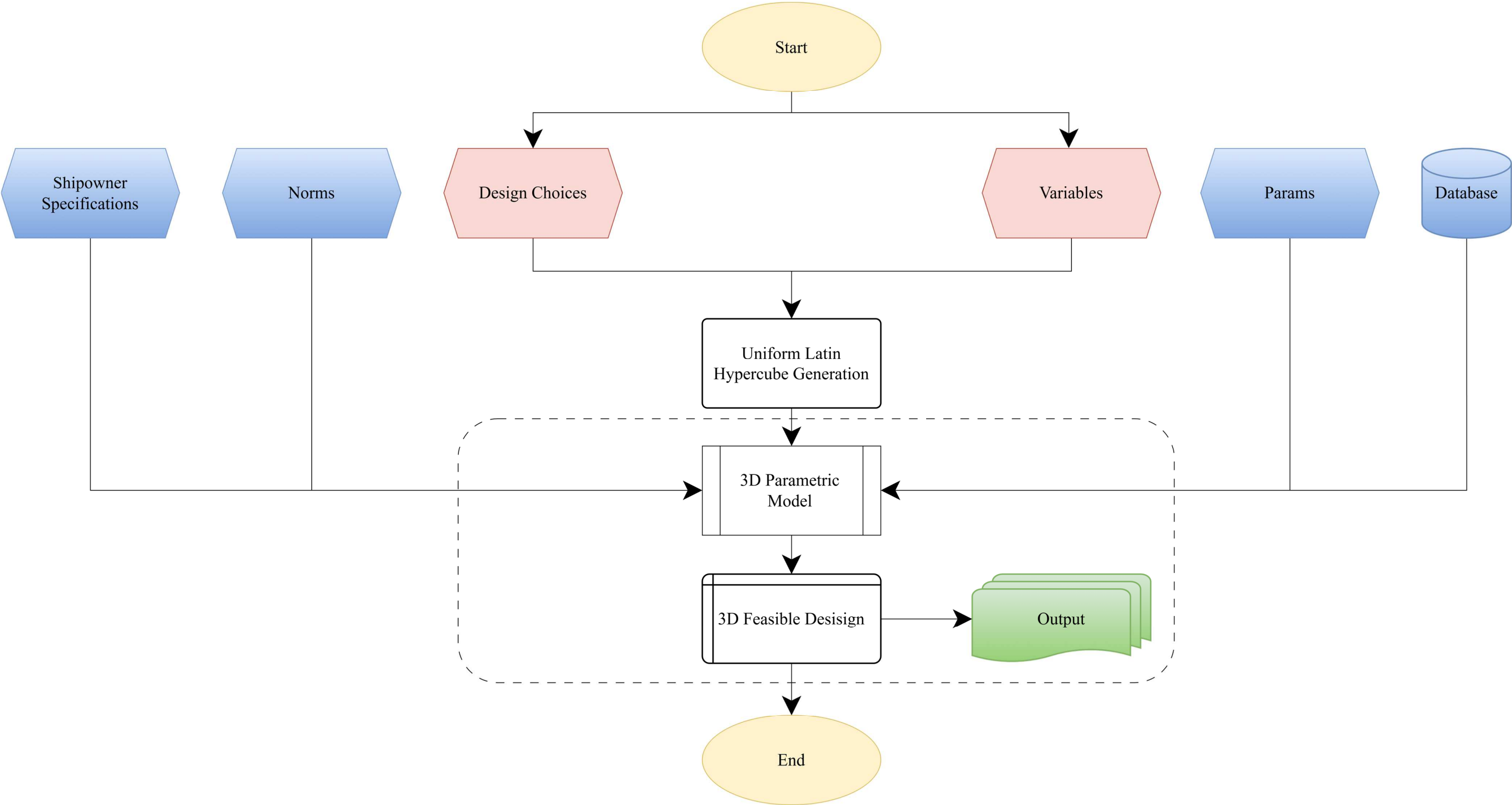


Figure 18 High-level schematic of the parametric design workflow

### 3.1. 3D Parametric Hull

In continuity with the methodological framework outlined above, the definition of the hull geometry represents one of the fundamental modules within the integrated parametric model. The hull is, in fact, the primary generative element of the three-dimensional model: it determines the external envelope of the vessel and directly influences the feasibility of the configurations produced by the system.

Within the proposed methodology, hull generation is not conceived as an isolated or preliminary operation; rather, it forms an integral part of the information flow that bidirectionally connects geometry, functionality, structural constraints, regulatory requirements, and propulsion systems. The parametric definition of the hull both feeds and is fed by the design domain explored through ULHS, within which each geometric configuration triggers automatic checks of technical, regulatory, and functional compliance. In this sense, the hull is not merely a product of the pipeline but one of the principal elements governing its internal coherence.

#### *3.1.1. Generating Curves and Their Role within the Integrated Pipeline*

The work of Pérez-Arribas (2014) [43] constitutes a significant methodological reference for the parametric generation of planing hulls, founded on the definition and manipulation of a set of fundamental curves, specifically the centre line, the chine line and the sheer line and on their subsequent interpolation through B-spline functions and NURBS surfaces (Figure 19). While the present study takes this conceptual framework as its theoretical foundation, the formulation of the parameters, equations and control-point strategies adopted for the definition of each generating curve has not been directly transposed from the original paper. Rather, based on the indications regarding the geometric role of the three reference lines, a dedicated parametric methodology has been developed to govern their construction within the computational environment.

In this research, therefore, the structural principles outlined by Pérez-Arribas have been integrated into a modelling logic specifically designed for Grasshopper and Python, enabling an interactive and dynamically controllable generation process. As illustrated in the article, the geometry of a single-chine, step-less hull can be effectively represented by the three generating curves (Figure 20), within which the surface of the vessel can be decomposed

and subsequently reconstructed on the basis of the design parameters. Building upon this conceptual basis, the present work develops original parameterisation schemes for the centre line, chine line and sheer line, ensuring that the resulting B-spline surfaces rigorously satisfy the imposed geometric constraints while maintaining full mathematical control over the hull morphology.

The definition of the curves has been simplified by assuming, as an initial condition, the presence of a vertical and flat transom, such that the x-coordinate of the aft endpoint of each curve is taken to be zero (Figure 21). Should the transom instead exhibit an inclination, the formulation can be readily adapted by introducing a translation of the aft endpoint along the X-axis, the magnitude of which is a function of the transom angle itself. This generalization allows the method to retain its validity even in the presence of raked or flared transoms, thereby preserving the parametric structure of the geometric definition.

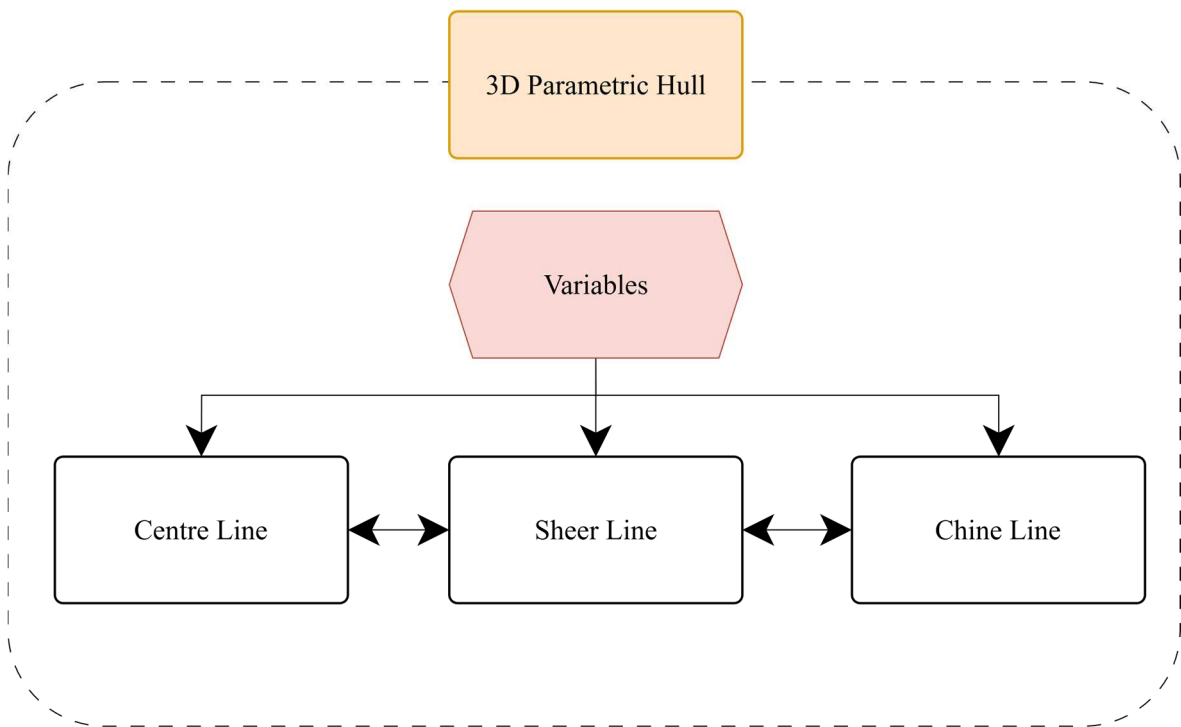
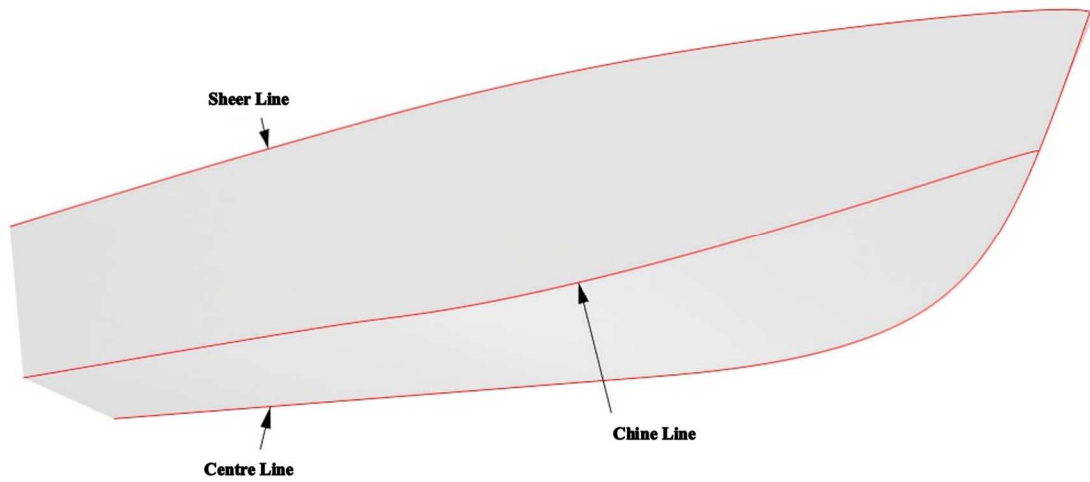


Figure 19 Logical framework of the parametric hull definition



*Figure 20 Generating curves of the parametric hull geometry*

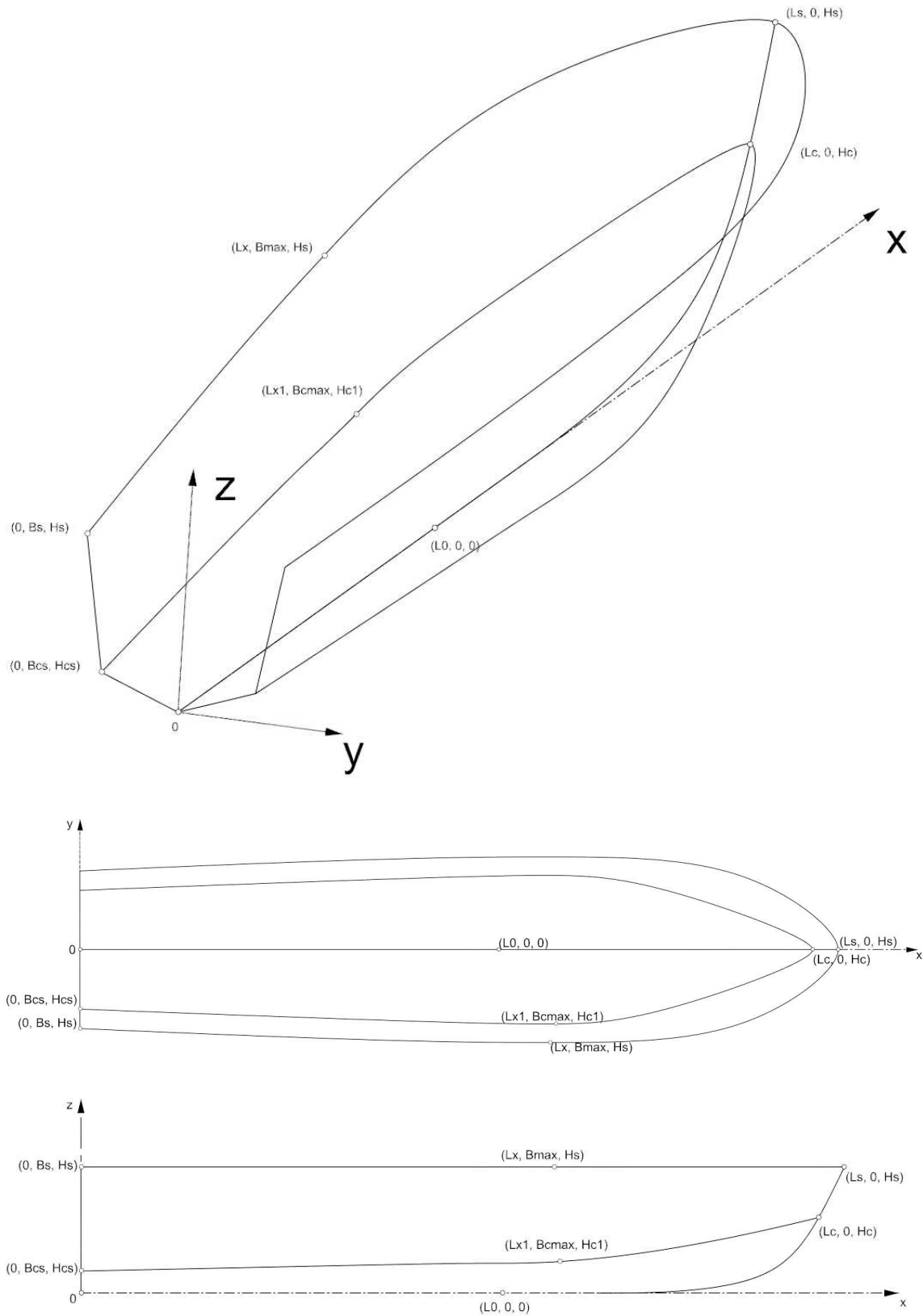
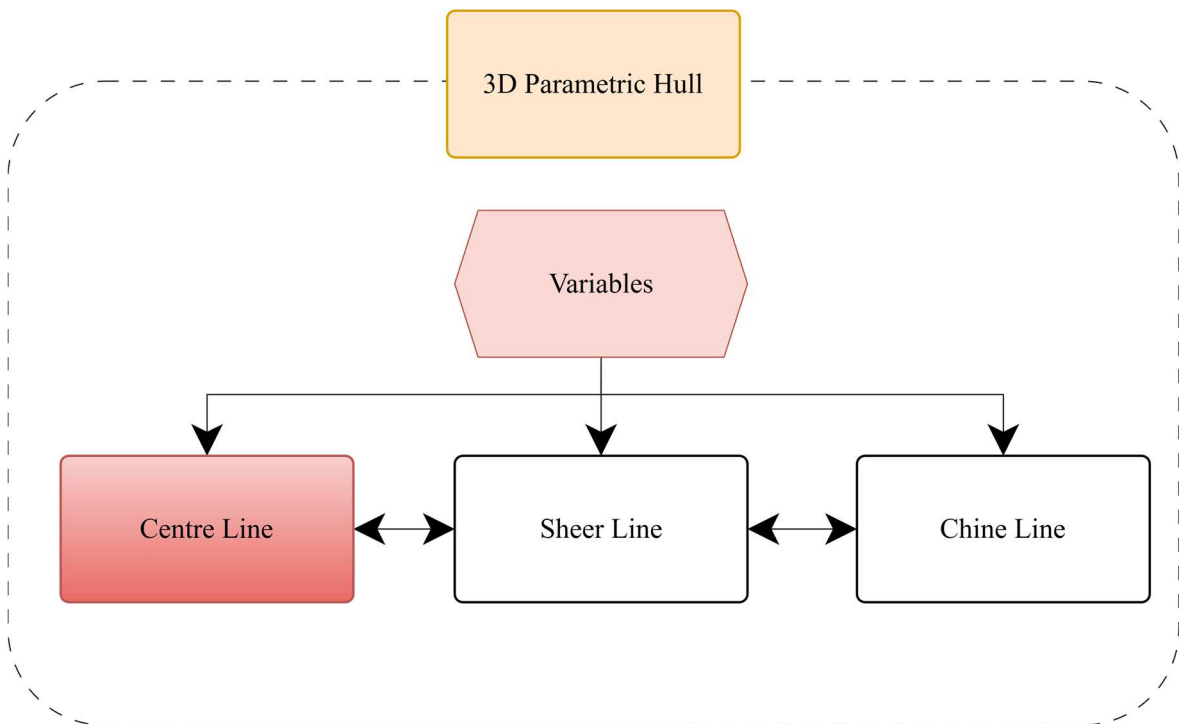


Figure 21 Geometric definition of the hull generating curves

*Parametric Definition of the Centre Line*

The definition of the centre line (Figure 22) represents one of the central aspects of hull modelling, particularly in the case of planing and semi-displacement vessels, where the geometry of the centre line directly influences the vessel’s trim, hydrodynamic response, and manoeuvring behaviour. In the parametric system developed, this profile is constructed through the identification of a set of key points on the centre plane, which are subsequently used as nodes or control points for generating an interpolated NURBS curve (Figure 23).



*Figure 22 Logical framework of the parametric hull - Centre Line Module*

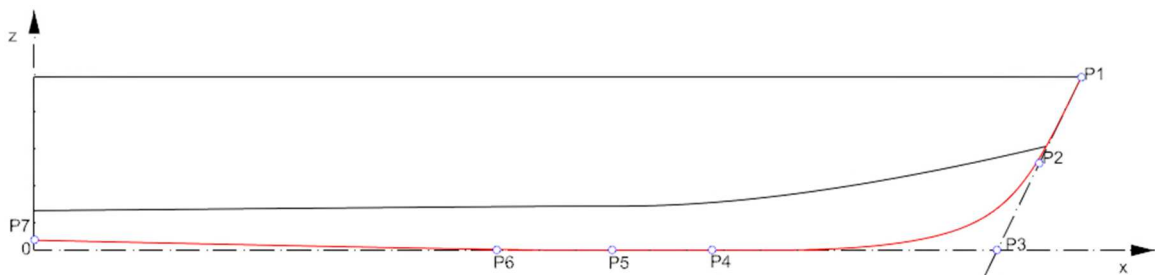


*Figure 23 Longitudinal layout of the control points defining the Centre Line*

The forward portion of the keel is defined through two principal points. The first point (P1) corresponds to the uppermost extremity of the bow, located at the intersection between the overall length and the maximum sheer height. This point identifies the position of the bow apex and serves as the geometric reference from which the stem line is established.

The second point (P2) is an auxiliary point which, together with P1, determines the direction of the stem. Its position is governed by a stem angle and by a control coefficient that regulates the inclination and the “fullness” of the forward region. The straight line connecting these two points represents, in design terms, the guiding line of the stem.

The geometry of the lower portion of the centre line is defined by introducing a point (P5) located on the baseline, which is considered the starting point of the functional section of the keel. Its longitudinal distance from the bow is controlled by a parameter that allows the onset of the lower curvature to be shifted forward or aft.

By extending the direction of the stem line downward until it intersects the baseline, point P3 is identified. This point represents the ideal intersection between the projection of the stem and the keel, defining the position at which the bow “closes” geometrically toward the bottom. It constitutes a particularly significant constraint for the vessel’s trim and for directional stability at low speeds.

The local behaviour of the curve in the forward region and in the area immediately aft is governed by two additional control points (P4 and P6).

The first point (P4) is located between the beginning of the keel and the theoretical forefoot, according to a ratio defined by a design coefficient. It allows the curvature in the forward portion to be modulated, determining the continuity and tangency of the B-spline at the transition between the straight or quasi-straight segment of the keel and the more inclined region toward the bow.

The second control point (P6) is positioned aft of the keel’s starting point, at a distance determined by a dedicated parameter. Its role is to govern the tangency of the curve toward the central part of the hull, contributing to a fluid and controlled development of the longitudinal profile.

The aft end of the keel is represented by a point located on the transom plane (P7), whose vertical coordinate is not necessarily zero. Instead, it is determined as a function of the rocker angle, that is, the upward curvature of the keel toward the stern. This rise, appropriately limited according to the maximum allowable draft, constitutes an essential design element for planing hulls, as it significantly influences flow detachment, longitudinal trim, and the reduction of residual resistance at high speeds.

In the context of passenger vessels, which typically operate in a semi-displacement regime, the precise definition of the keel assumes even greater importance. For such craft, directional stability, particularly at low speeds, is fundamental for passenger comfort and safety. Since the parametric configuration described does not include any appendages along the centre line, the resulting hull tends to exhibit reduced directional steadiness during low-speed manoeuvring.

To mitigate this effect, it is advisable to introduce a skeg, also modelled parametrically, which enhances straight-line stability and improves the vessel's dynamic response (Figure 24).

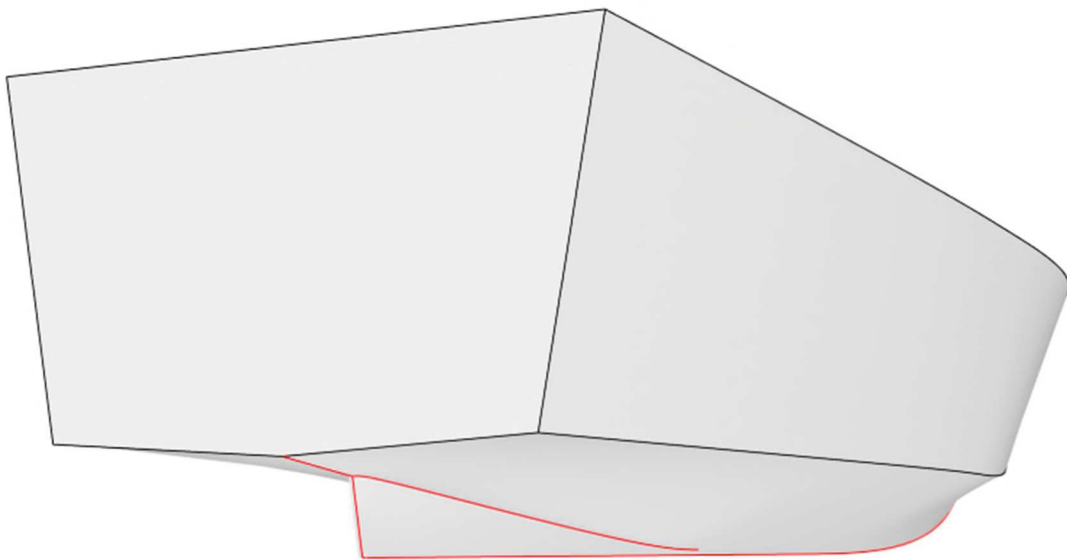


*Figure 24 Aft view of the hard-chine hull featuring a parametrically modelled skeg*

*Parametric Definition of the Sheer Line*

The sheer line (Figure 25) represents the upper boundary of the hull. Its three-dimensional parametric definition is obtained through the generation of a series of appropriately computed control points, which are subsequently used to construct an interpolating NURBS or B-spline curve (Figure 26).

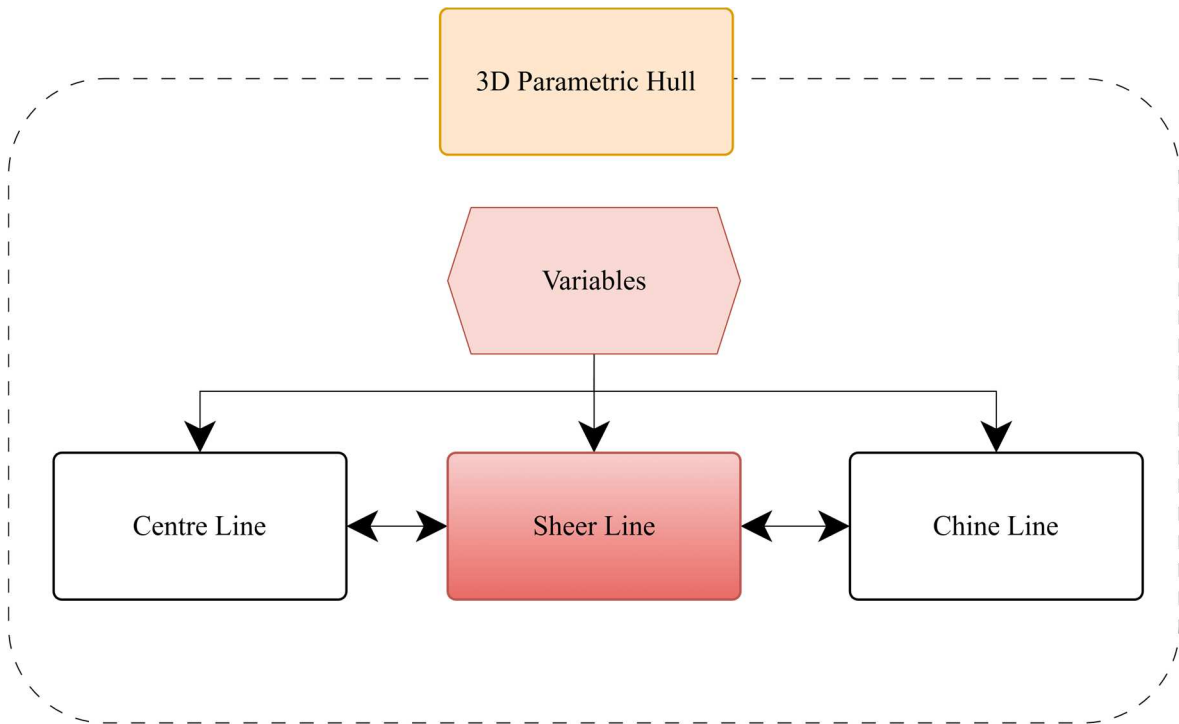


Figure 25 Logical framework of the parametric hull - Sheer Line Module

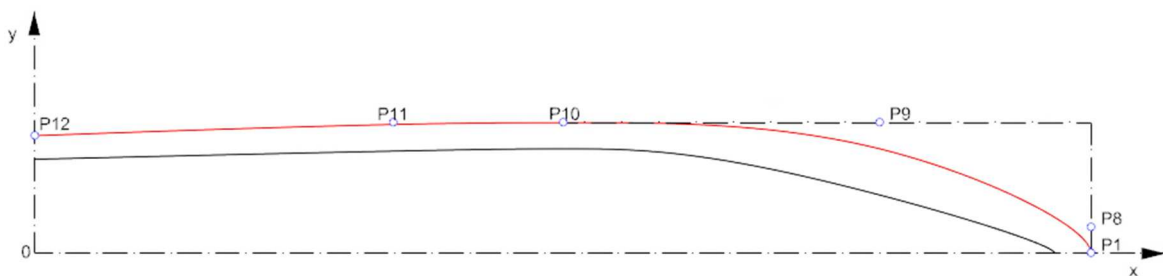


Figure 26 Plan view of the control-point layout defining the Sheer Line

These points are determined by assuming the forward extremity of the sheer line (P1), coincident with the uppermost point of the bow, as a known quantity. This point provides the maximum vertical reference for the entire line and serves as the basis for defining the heights of the overall profile.

The first point in the sequence (P8) is positioned longitudinally at the bow extremity and functions to define the width of the sheer line at this specific location. Its transverse position is modulated by a factor that controls the narrowing of the gunwale in the forwardmost region. This point therefore governs the tangency and the final fairing of the sheer line toward the bow apex, contributing to the definition of the hull's formal elegance.

The point P10 defines the section of maximum beam and constitutes a fundamental reference for the overall shape of the sheer line. Its longitudinal position is established by a coefficient that allows the maximum beam to be shifted either forward or aft. The transverse coordinate corresponds exactly to the maximum half-beam, representing the point of greatest lateral expansion.

The final point in the sequence (P12) is located on the transom plane. It defines the sheer width at the stern and the height of the gunwale in that section. Its transverse position is determined as a fraction of the vessel's maximum half-beam, modulated by a dedicated coefficient.

To govern the shape of the sheer line between the stern and the point of maximum beam, as well as between the latter and the bow, two additional intermediate control points (P9 and P11) are introduced.

The aft control point (P11) is positioned between the transom and the section of maximum beam, with its location determined by a coefficient that defines its setback from the stern. This point allows the tangency and degree of curvature in the aft portion of the sheer line to be modulated, influencing the shape of the lateral tuck and contributing to the overall harmony of the line.

The forward control point (P9), by contrast, is located between the section of maximum beam and the bow extremity. Its distance from the bow is governed by a parameter that regulates the "fullness" of the sheer line in the forward portion of the hull. Through this point, the transition between the most expansive section and the natural narrowing of the

bow is controlled, an element crucial for ensuring a balanced profile from both a hydrodynamic and a formal standpoint.

#### *Parametric Definition of the Chine Line*

The chine line (Figure 27) represents one of the fundamental geometric components in the characterization of planing hulls, defining the longitudinal edge responsible both for generating dynamic lift and for modulating the deadrise angle. The curve is modelled through a set of three-dimensional control points governed by specific parameters, thereby ensuring a coherent, continuous construction that remains compatible with the constraints imposed by the keel and the sheer line.

In this formulation, the chine line is obtained as the spatial intersection between two parametric 2D curves, one defined in the plan view (Figure 28) and the other in the longitudinal view (Figure 29).

In the plan view, the chine originates at the bow with point P13, obtained from the intersection between the chine curve and the vessel's centre plane. This point determines the forwardmost position of the chine and provides the reference for the subsequent widening of the hull. From here, the first control point (P14) defines the initial divergence of the chine from the stem line; its transverse coordinate is modulated by a factor that regulates the forward tangency of the chine and its degree of opening in the bow region.

Proceeding aft, point P15 controls the forward fullness of the curve. Through a specific coefficient, this point adjusts how gradually the chine transitions from the narrow bow entry to the broader mid-body of the hull. The following point (P16) corresponds to the maximum transverse extent of the chine and constitutes a fundamental reference for the overall plan-view shape. Its position is governed by parameters that determine both the longitudinal location of this maximum and the associated half-beam.

Two additional control points (P17 and P18) regulate the development of the chine toward the stern. Point P17 modulates the tangency and curvature aft of the maximum-beam region, while P18 establishes the chine width at the transom through a coefficient that sets its proportion relative to the vessel's maximum half-beam.

In the longitudinal view, the chine line is again defined starting from P13, which fixes the chine height at the stem and establishes the reference from which the vertical profile

develops. The next control point (P19) governs the initial curvature of the chine in the forward portion of the hull; its vertical coordinate results from a balance between the required bow height and the rise imposed by the deadrise angle.

Point P20 identifies the chine height in the mid-length region. Its longitudinal coordinate is intentionally aligned with that of P16, ensuring that the maximum transverse development in the plan view corresponds to a clearly defined height in profile. Its vertical position is computed to maintain coherence with the hull geometry at mid-length and with the deadrise angle prescribed for that section.

Moving aft, point P21 defines the curvature and tangency of the chine as it approaches the stern, controlled by a parameter that governs its setback relative to mid-length. Finally, point P22, located on the transom plane, establishes both the height and the terminal slope of the chine at the stern. Its elevation is determined by reconciling the required transom deadrise with the maximum sheer height, ensuring continuity and formal harmony at the aft boundary.

The combination of these points generates a 3D NURBS curve that is continuous and sufficiently flexible to allow precise control over the hull form.

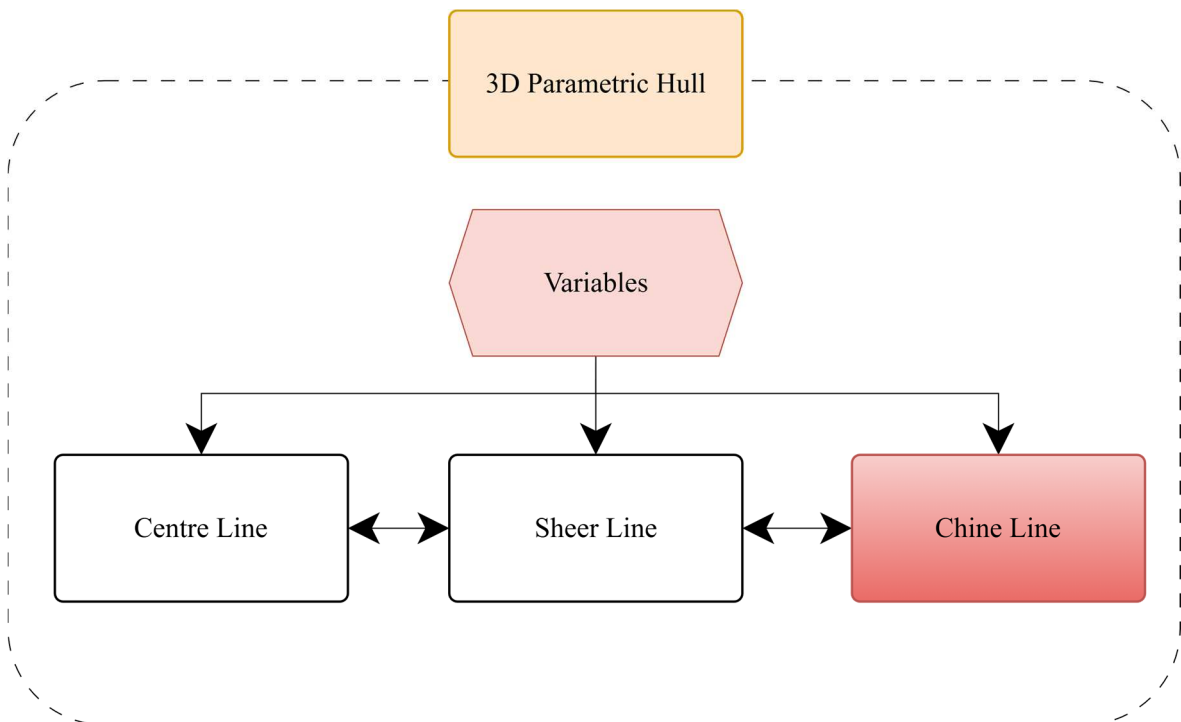


Figure 27 Logical framework of the parametric hull - Chine Line Module

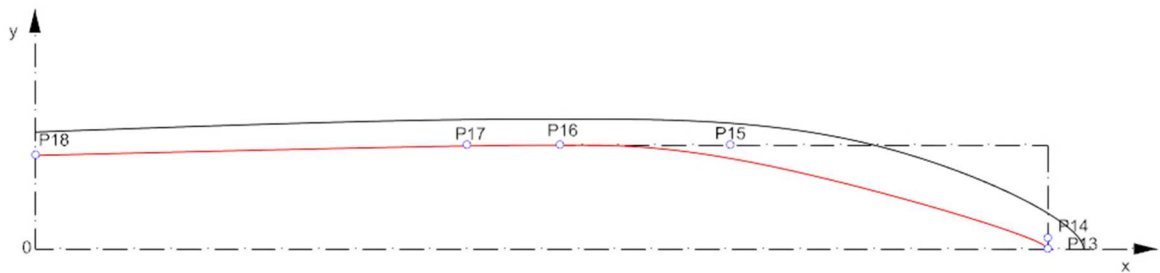


Figure 28 Plan view of the control-point layout defining the Chine Line

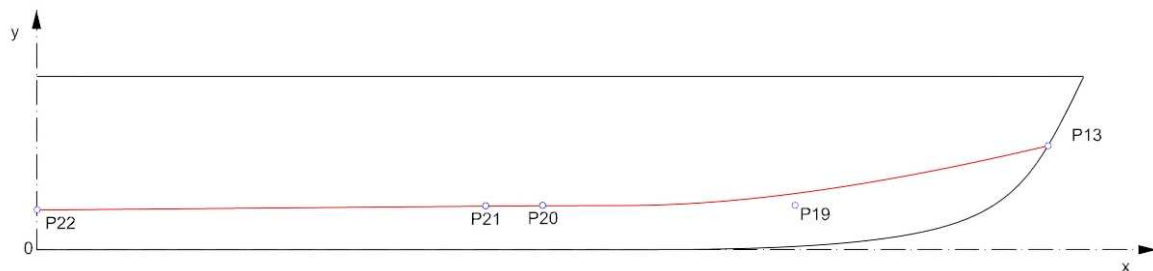


Figure 29 Longitudinal layout of the control points defining the Chine Line

The curve must satisfy two fundamental constraints:

1. it must never exceed the maximum lateral extension defined by the sheer line;
2. it must always remain above the construction baseline.

To satisfy these constraints, the system adopts a strategy based on the generation of two distinct NURBS curves, which are subsequently extruded to form surfaces. The intersection of the extruded surfaces defines a 3D curve that is coherent with the hull geometry and automatically compliant with the imposed constraints. This approach makes it possible, on the one hand, to avoid the intrinsic instability associated with point-based references and, on the other, to ensure greater computational robustness, particularly in the presence of variable parameters and frequent update operations.

The modelling of the spray rail is implemented as a direct continuation of the chine, through a simple lateral translation of the chine line control points by an amount equal to the width of the spray deflector (Figure 30). This translation, always directed inward so as not to exceed the geometric limits imposed by the sheer line, allows the step surface to be correctly defined (Figure 31). When no translation is applied, the model automatically returns to a

configuration without a step, thereby ensuring continuity and simplicity in the management of the parametric model.

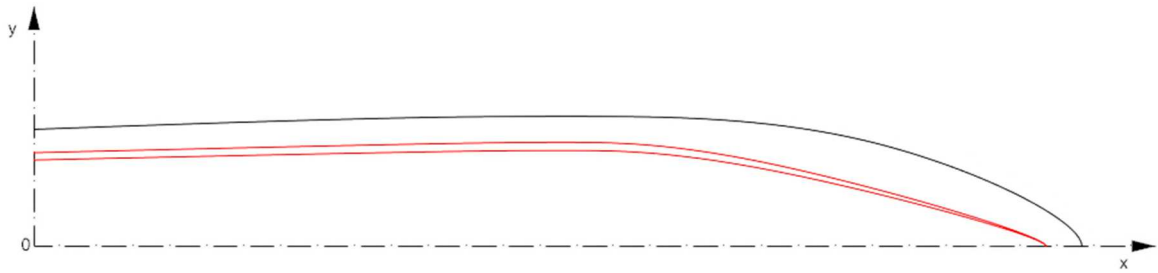


*Figure 30 Plan view of Spray Rail NURBS*

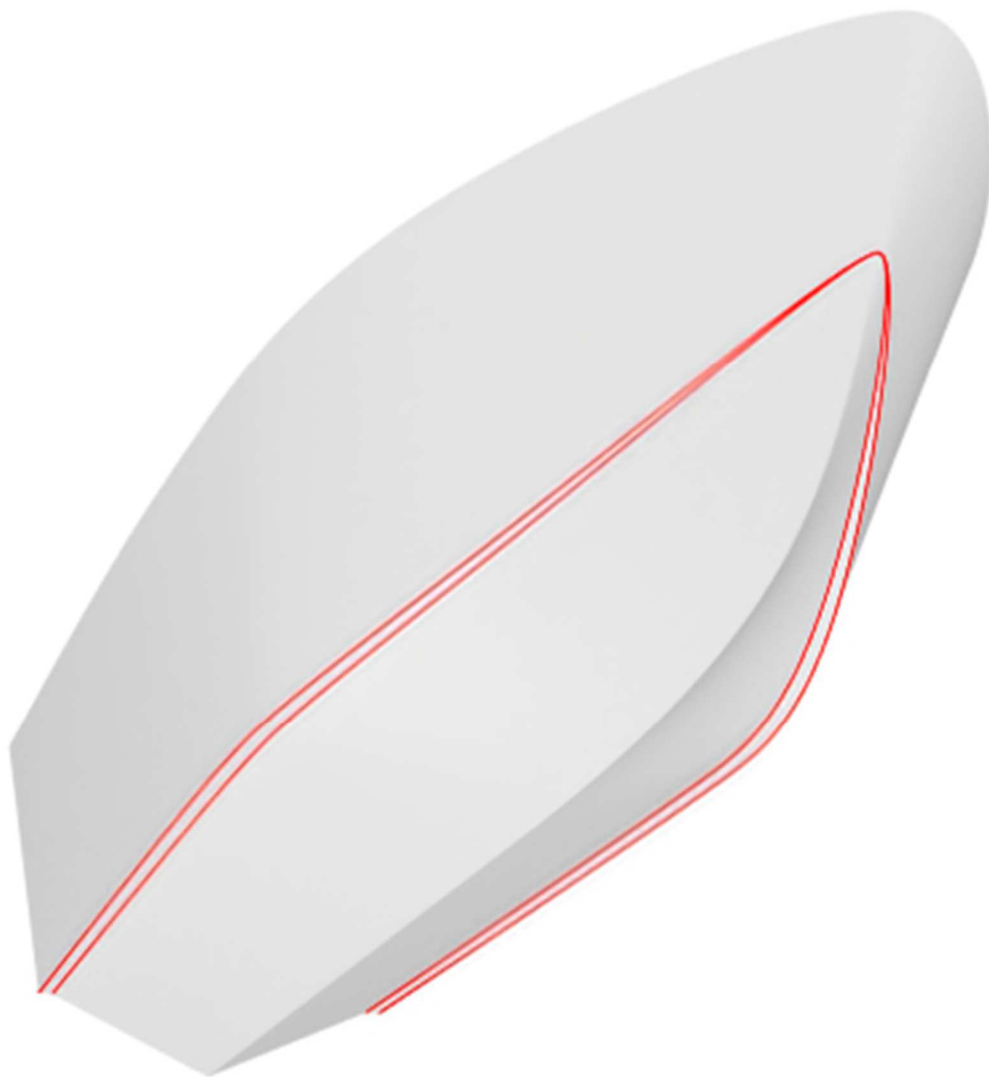


*Figure 31 Spray rail geometry obtained through parametric offset of the chine line*

### *3.1.2. Identification of the Design Variables*

The parametric definition of the fundamental hull lines, the centre line, the sheer line, and the chine line, potentially extended to include the spray rail, enables the generation of complex geometries from a controlled set of variables. These variables constitute the operative core of the Parametric Design Thinking and represent the elements through which the designer can explore, modify, and optimize the hull form in relation to operational requirements and design constraints.

Each variable directly affects the three-dimensional position of the control points defining the principal curves and, consequently, the final shape of the hull surfaces. The variables that can be modified within the PDT are grouped according to the type of line to which they belong. As a result, the tables presented below gather the complete set of variables used to parameterize the centre line (Table 4), sheer line (Table 5), and chine line (Table 6). They constitute the quantitative formalization of the parametric domain explored by the integrated model.

Table 4 Variables adopted in the parametric formulation of the hull centre line

Variable		Geometric Role	Affected Coordinates
<i>Length overall</i>	<i>LOA</i>	Defines the bow extremity	X
<i>Sheer Height</i>	<i>SH</i>	Controls the vertical position of the upper bow point	Z
<i>Bow Angle</i>	<i>BA</i>	Rake angle of the bow	X, Z
<i>Control coefficient for point P2</i>	<i>C2</i>	Governs bow fullness	Z
<i>Coefficient for positioning point P5</i>	<i>C1</i>	Governs the longitudinal position of the point at zero elevation	X
<i>Coefficient</i>	<i>CTPR</i>	Control of bow tangency (initial curvature)	X
<i>Coefficient</i>	<i>CTPP</i>	Control of stern tangency	X
<i>Rocker Angle</i>	<i>RA</i>	Governs the upward rise of the keel toward the stern	Z
<i>Design draft</i>	<i>T</i>	Design draft	Z

Table 5 Variables adopted in the parametric formulation of the hull sheer line

Variable		Geometric Role	Affected Coordinates
<i>Beam overall</i>	<i>BOA</i>	Maximum beam of the hull	Y
<i>Beam Transom Coefficient</i>	<i>BTC</i>	Sheer width at the transom	Y
<i>Max Beam Position</i>	<i>BP<sub>MAX</sub></i>	Longitudinal position of the maximum beam	X
<i>Bow Fullness Factor</i>	<i>BFF</i>	Bow-side fullness factor	X
<i>Coefficient</i>	<i>CTPP</i>	Stern tangency control	X
<i>Bow Tangent Factor</i>	<i>TF</i>	Control of bow tangency	Y

Table 6 Variables adopted in the parametric formulation of the hull chine line

Variable		Geometric Role	Affected Coordinates
<i>Chine Height Factor Bow</i>	<i>CHF</i>	Chine height factor at the bow	Z
<i>Max Chine Position</i>	<i>MAXCP</i>	Longitudinal position of the point of maximum chine projection	X
<i>Max Chine Coefficient</i>	<i>MAXCC</i>	Maximum chine width	Y
<i>Chine Tangent Factor</i>	<i>TFC</i>	Control of bow tangency	Y
<i>Chine Fullness Factor</i>	<i>CFF</i>	Chine fullness in the forward area	X
<i>Chine Transom Coefficient</i>	<i>CTC</i>	Chine width at the transom	Y
<i>Coefficient</i>	<i>CTPP</i>	Stern tangency control for the chine	X
<i>Deadrise Angle at stern</i>	$\vartheta_T$	Chine height factor at stern	Z
<i>Deadrise Angle</i>	$\vartheta$	Chine height factor at midship	Z
<i>Spray rail width</i>	<i>SRW</i>	Spray rail width	Y

### 3.1.3. Output

The overall workflow through which the parametric hull model propagates its geometric information to the subsequent analytical and drafting modules is summarised in Figure 32. The diagram illustrates how the 3D hull (Figure 33) acts as the primary geometric output from which all downstream processes, construction plan extraction, hydrostatic computation, and resistance analysis, are automatically derived within a unified modelling pipeline.

This technical drawing (Figure 34), traditionally developed through manual phases of geometric reconstruction, is here generated by defining the fundamental curves of the hull and their associated construction. The innovative and useful feature is represented by the possibility of updating the drawing automatically: any modification to the fundamental curves instantly produces new sections, new waterlines, and an updated 2D drawing layout. The integration of the construction plan within the pipeline therefore enables the production

of geometric outputs that are consistently aligned with the current hull configuration, reducing time, errors, and informational discontinuities compared with traditional processes.

The extraction process is governed by a set of user-defined inputs that specify the distribution of the reference planes. The number of transverse stations and longitudinal sections is defined by the user, while for the waterlines, the spacing between planes is selected. The developed code automatically detects and highlights the waterline corresponding to the design draft, ensuring its correct representation in both the 3D model and the final drawing.

This mechanism allows for the immediate generation of a coherent set of technical views that correspond exactly to the underlying 3D geometry, without the need for corrective manual intervention. The automated drafting procedure includes a structured series of operations aimed at producing technical drawings fully compliant with naval architecture standards. In particular, the system provides complete technical plans that can be exported in vector formats compatible with external CAD software.

In parallel, the same parametric geometry feeds the module dedicated to the extraction of hydrostatic parameters, enabling real-time assessment of the effects of design choices on the vessel's equilibrium configuration (Table 7). The system computes all hydrostatic coefficients, displacement and buoyancy centres directly from the parametric hull, updating these quantities immediately whenever the geometry is modified.

These results are obtained through a dedicated Grasshopper script that determines the submerged portion of the hull at the design draft. A solid of height equal to the design draft is generated and intersected with the hull surface; the resulting immersed volume is then analysed to extract its geometric properties. All computed parameters are automatically processed and transferred to an Excel worksheet, ensuring full consistency between the modelled geometry and the hydrostatic data used in the subsequent design stages.

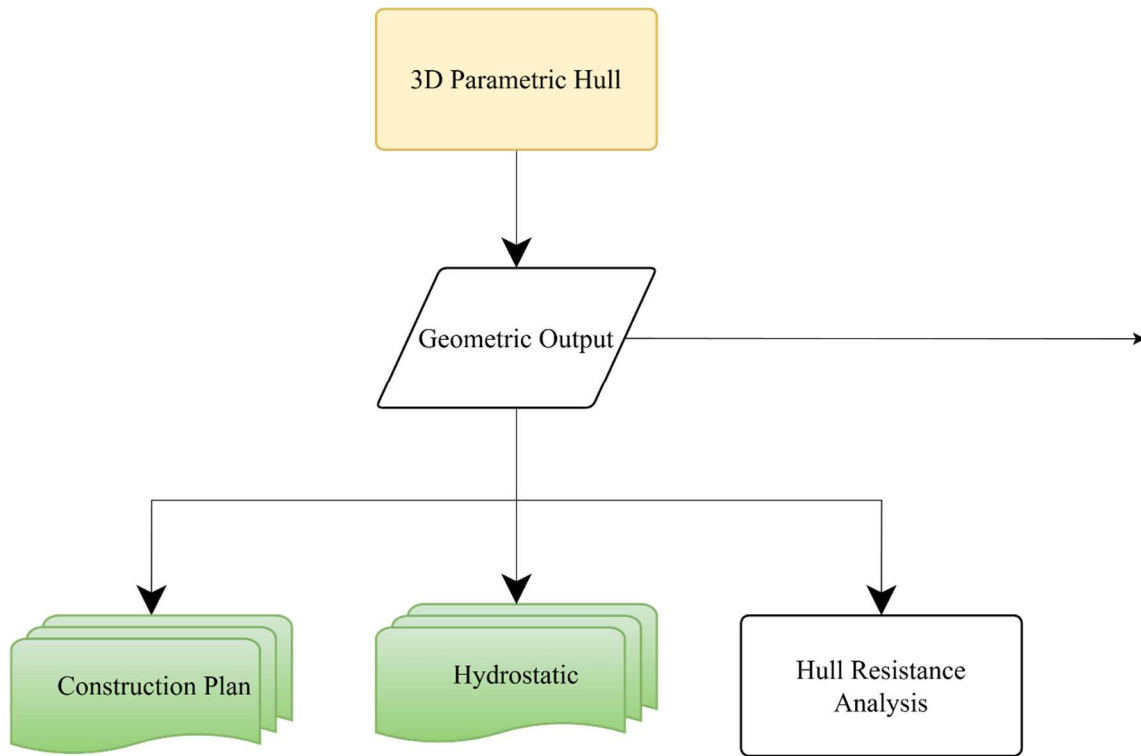


*Figure 32 Logical framework of the Hydrostatic output*

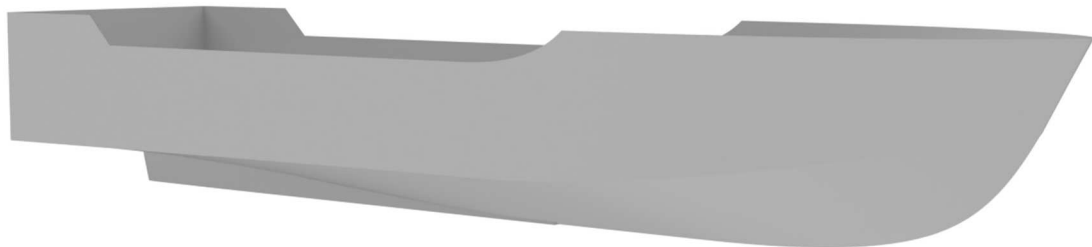


*Figure 33 Geometric output*

Table 7 Summary of the main hydrostatic characteristics computed for the hull geometry

<b>Parameter</b>	<b>Symbol</b>	<b>Unit</b>	<b>Value</b>
<i>Draft</i>	$T$	(m)	XXXX
<i>Volume</i>	$\nabla$	(m <sup>3</sup> )	XXXX
<i>Displacement</i>	$\Delta$	(t)	XXXX
<i>Length Overall</i>	$L_{OA}$	(m)	XXXX
<i>Beam Overall</i>	$B_{OA}$	(m)	XXXX
<i>Waterline Length</i>	$L_{WL}$	(m)	XXXX
<i>Waterline Beam</i>	$B_{WL}$	(m)	XXXX
<i>Wetted Surface Area</i>	$WSA$	(m <sup>2</sup> )	XXXX
<i>Waterplane Area</i>	$WPA$	(m <sup>2</sup> )	XXXX
<i>Block Coefficient</i>	$C_B$	(\)	XXXX
<i>Waterplane Area Coefficient</i>	$C_{WP}$	(\)	XXXX
<i>Longitudinal Centre of Buoyancy</i>	$LCB$	(m)	XXXX
<i>Vertical Centre of Buoyancy</i>	$KB$	(m)	XXXX
<i>Longitudinal Centre of Flotation</i>	$LCF$	(m)	XXXX
<i>LCB as Percentage of <math>L_{WL}</math></i>	$LCB \%$	(%)	XXXX
<i>LCF as Percentage of <math>L_{WL}</math></i>	$LCF \%$	(%)	XXXX
<i>Transverse Metacentric Radius</i>	$BM_t$	(m)	XXXX
<i>Longitudinal Metacentric Radius</i>	$BM_l$	(m)	XXXX

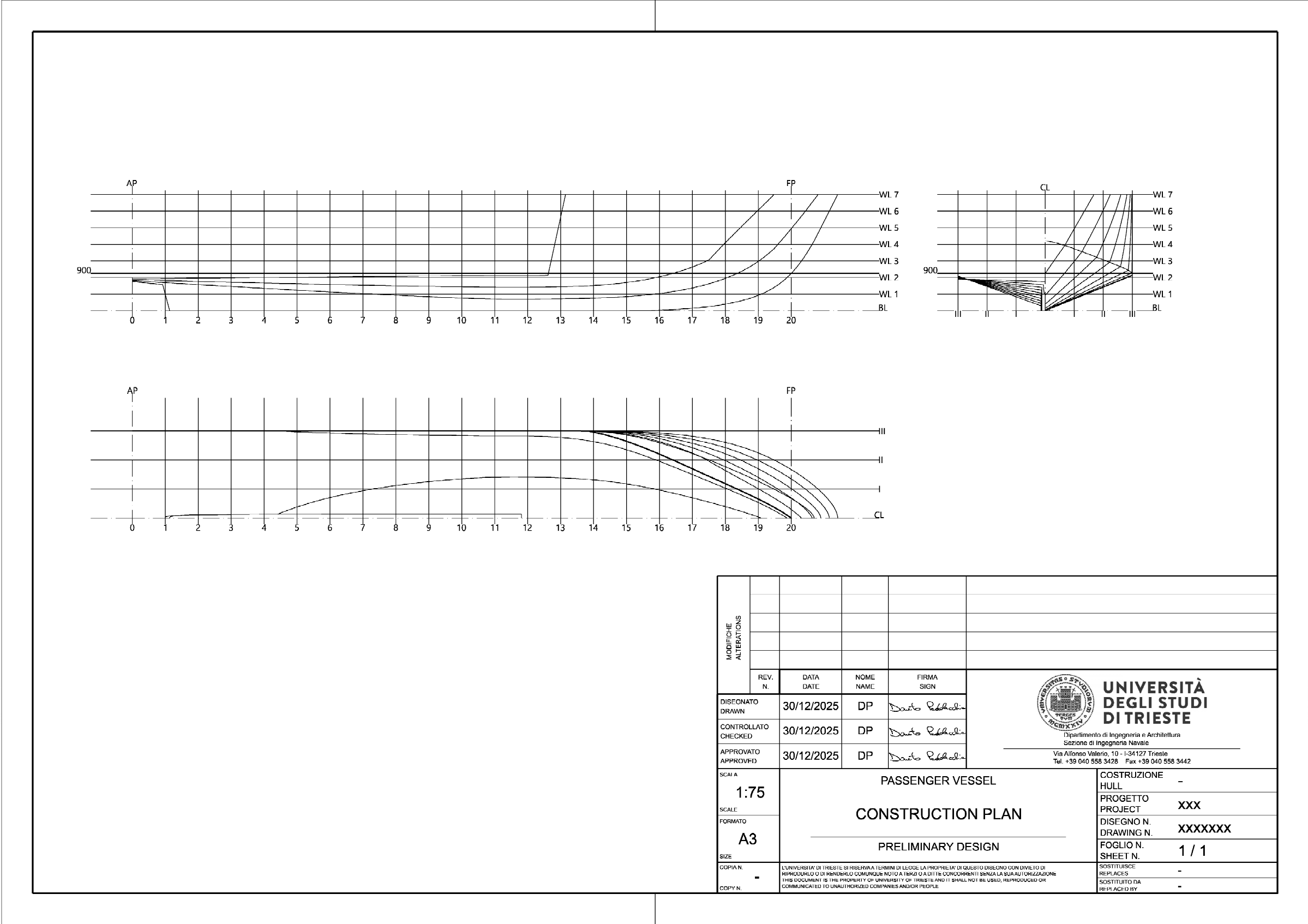


Figure 34 Construction Plan

### **3.2. Resistance, Propulsive selection and System Integration**

A critical aspect in the design of coastal passenger vessels concerns the misalignment between the design speed traditionally adopted during the engineering phase and the actual operational speeds imposed by local harbour authorities. Industrial practice frequently leads to vessels being dimensioned for service speeds in the order of 20–24 kn, selected to guarantee manoeuvrability margins and schedule resilience. In service, however, these craft often operate under speed limits as low as 8–12 kn, particularly in lagoon environments, port approaches and environmentally sensitive coastal corridors.

This discrepancy results in a structural inefficiency of conventional diesel-mechanical propulsion chains. Operating at reduced speed forces the propeller–engine system into regimes characterised by poor propeller loading, low engine mean effective pressure, increased specific fuel consumption, accelerated wear and higher emissions. The propulsion system is therefore driven far from its optimal thermodynamic and hydrodynamic operating conditions, undermining both efficiency and environmental sustainability.

Within this framework, the thesis adopts a site-specific, operation-driven design methodology, in which local speed-limit profiles are incorporated as primary design inputs rather than downstream constraints. By embedding the real mission profile at the earliest design stages, the hull form, propeller characteristics and power-generation system can be dimensioned coherently with the vessel’s actual operating envelope. In this context, the adoption of a series-hybrid propulsion architecture represents a structurally consistent solution: the decoupling between the internal combustion engine and the propeller allows the generator sets to operate close to their optimal efficiency point across the entire operating range, while the electric motor ensures correct propeller loading even in low-speed segments dictated by regulatory constraints.

Within the parametric pipeline (Figure 35), the estimation of propulsive performance and the selection of energy systems play a central role in the process of generating and validating design configurations. The methodological framework adopted does not merely produce resistance values and the corresponding power requirements; rather, it establishes an integrated information flow that enables the coherent sizing of the propeller, propulsion motors, power-generation systems, and energy-storage units, while maintaining full compatibility with geometric, regulatory, and installation constraints.

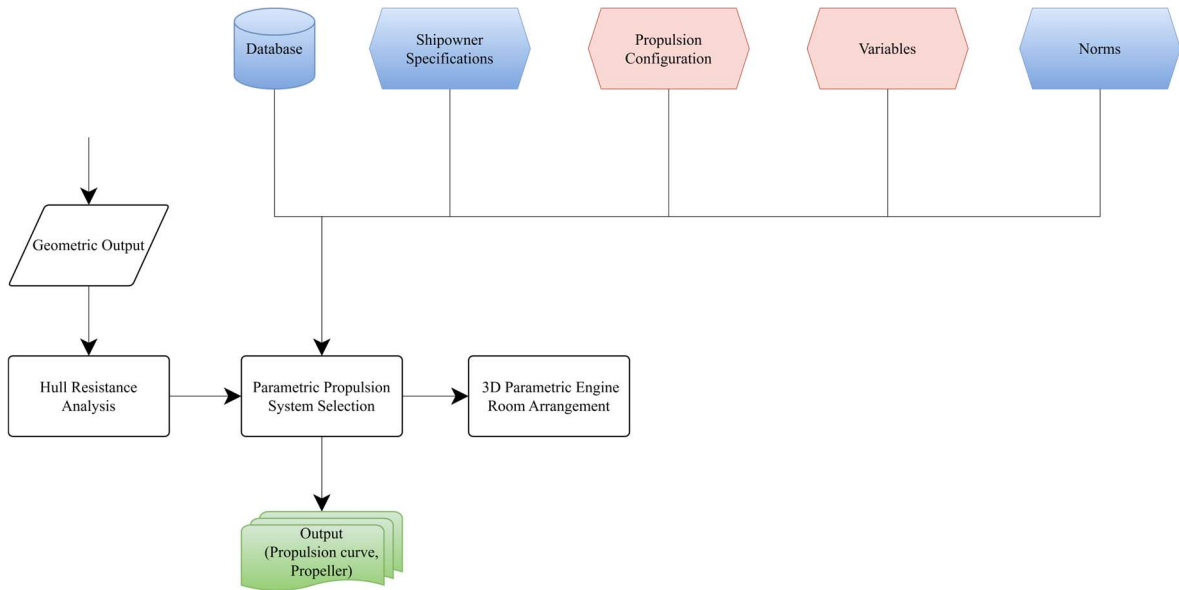


Figure 35 Logical framework of the Resistance, Propulsive selection and System Integration

The hull geometry, which is the output of the parametric model, serves as the foundation for estimating the resistance, obtained through a computational model appropriate for the project’s preliminary stage. Methodologically, what is significant is the framework’s ability to automatically update the resistance as the geometry changes, thereby ensuring continuous consistency between the hull form and the hydrodynamic performance.

Although the conclusions of Chapter 2 highlight the intrinsic limitations of classical systematic series—stemming from the discrete nature of their experimental matrices and their inability to fully represent the specific constraints of layout, construction and propulsion integration addressed in this thesis—these methods have nevertheless been implemented within the framework. This choice is motivated by the fact that hull forms generated through the parametric formulation may, in specific configurations, fall within the variability ranges of the underlying geometric parameters of the available systematic series. When this occurs, the corresponding resistance prediction methods can provide useful and physically consistent estimates, serving both as a reference and as a comparative benchmark.

In particular, the framework includes empirical formulations derived from the main experimental systematic series discussed in Chapter 2, such as the NPL High-Speed Round-Bilge Series, the Series 62 (DTMB and Delft developments), and the Semiplaning Systematic Series by Compton. In addition, resistance prediction models drawn from the scientific literature and tailored to specific hull morphologies and operating regimes have

been incorporated, including the Savitsky method for planing conditions [87], and the Simple Mathematical Model proposed by Radojčić [88] for hard-chine hulls operating in the semi-displacement regime.

A key methodological feature of the proposed approach is that the selection of the resistance prediction method is explicitly left to the designer. Depending on the hull morphology, operating regime and proximity to the validity domain of a given model, the user can choose the most appropriate formulation among the available options. The framework then automatically updates the resistance estimates as the hull geometry evolves, ensuring continuous coherence between geometric definition and hydrodynamic performance assessment. This flexibility allows the parametric design environment to accommodate multiple interpretative models while preserving consistency throughout the preliminary design process.

In particular, the resistance, estimated at the design speed defined by the owner, constitutes the essential input for the subsequent phase focused on the preliminary assessment of the propeller's operating conditions. In a parametric system, propeller sizing is not addressed as an isolated sequential problem, but rather as an integrated process that relates the required propulsive power, the reference speed, the general characteristics of the propeller series considered, and the installation constraints imposed by the hull geometry. The model's aim is to identify preliminary configurations that are technically consistent and compatible both with the required power and with the spatial constraints of the hull. In this context, the role of technical databases is crucial: they provide a structured set of parameters related to propeller series, representative performance curves, dimensional ranges, and hydrodynamic characteristics suitable for use in the preliminary design phase.

Operationally, the thrust corresponding to the estimated resistance is used to define an admissible propeller diameter range through cavitation-based criteria, implemented using Keller's formulation [89] and verified against the geometric constraints of the hull. Within this feasible range, systematic propeller series databases are employed to determine rotational speed and open-water efficiency.

The parametric process therefore employs the power required at the design speed to identify feasible propeller–engine configurations, based on the information provided by the databases and in compliance with the geometric and installation constraints. This selection

is not carried out through manual comparison, but through a script that automatically evaluates the feasibility of each option and verifies the compatibility between the available power and the spatial requirements.

In parallel with propeller selection, the analysis adopts the series-hybrid architecture as the reference configuration, as outlined in the Chapter 2. This option guides the definition of the propulsion and energy-generation system components and is coherently represented in the Integrated Power System (IPS) single-line diagram shown in the Figure 36. The design speed, the required power, and the autonomy targets defined by the owner represent the primary inputs for selecting the propulsion electric motors, generator-sets, and energy-storage systems. The corresponding databases (Table 8, Table 9 and Table 10) contain dimensional, performance, and energy-related information on the components, enabling the parametric system to automatically compare the required power with the available options and to identify compatible components.

A particularly significant stage of the pipeline is the three-dimensional integration of components within the parametric model. For each selected element—propeller, electric motors, generators, and battery modules—the system automatically imports the overall dimensions and masses in the form of simplified volumes. In addition, fuel tanks, fresh-water tanks, and black-water tanks are positioned within the engine room, with their respective capacities defined according to the owner’s requirements. All these data feed two parallel processes: the verification of installation compatibility within the technical spaces, and the computation of weights and centres of gravity, which are subsequently employed for the vessel’s stability assessments.

The integration of component volumes into the 3D model ensures that the preliminary design phase does not generate solutions that are unfeasible from a spatial or regulatory standpoint, and preserves consistency among the propulsion system, onboard installations, and the overall naval architecture.

In Figure 37, the elements highlighted in green represent the three-dimensional modelling of the propulsion system and the engine room, shown as one of the possible configurations generated by the parametric model.

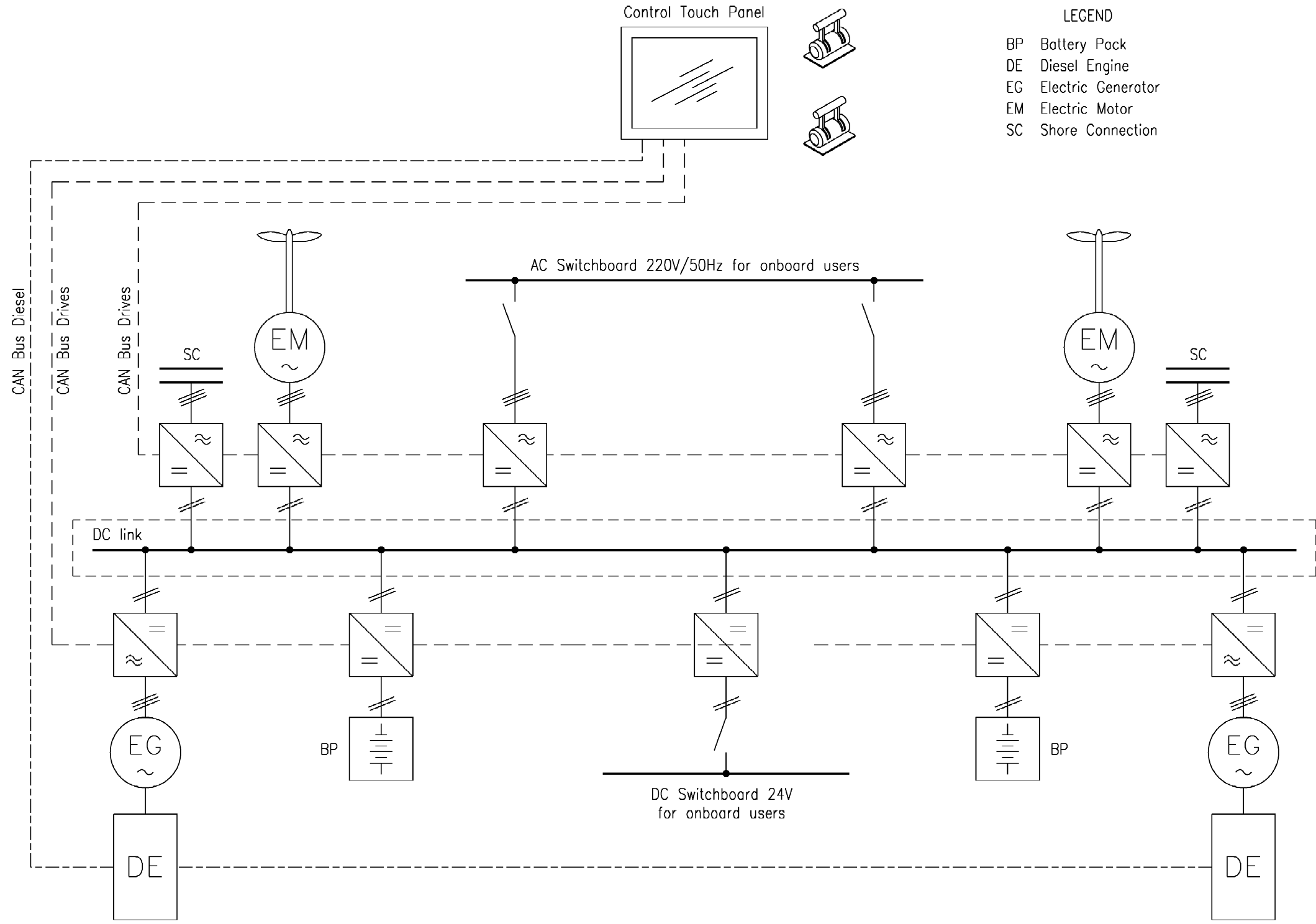


Figure 36 Integrated Power System (IPS)

Table 8 Structure of the electric motor database

<b>Voices</b>	<b>Value</b>
<i>Manufacturer</i>	XXXX
<i>Model</i>	XXXX
<i>Rated Power (kW)</i>	XXXX
<i>Maximum Power (kW)</i>	XXXX
<i>Rated Rotational Speed (rpm)</i>	XXXX
<i>Maximum Rotational Speed (rpm)</i>	XXXX
<i>Length</i>	XXXX
<i>Main dimension (mm)</i>	<i>Breadth</i>
	<i>Height</i>
<i>Weight (kg)</i>	XXXX
	<i>Longitudinal Centre of Gravity</i>
<i>Centre of Gravity (mm)</i>	<i>Transversal Centre of Gravity</i>
	<i>Vertical Centre of Gravity</i>

Table 9 Structure of the batteries database

<b>Voices</b>	<b>Value</b>	
<i>Manufacturer</i>	XXXX	
<i>Model</i>	XXXX	
<i>Nominal Capacity (kWh)</i>	XXXX	
<i>Maximum Discharge Power (kW)</i>	XXXX	
<i>Nominal Voltage (V)</i>	XXXX	
<i>Energy Density (Wh/kg)</i>	XXXX	
	<i>Length</i>	XXXX
<i>Main dimension (mm)</i>	<i>Breadth</i>	XXXX
	<i>Height</i>	XXXX
	<i>Weight (kg)</i>	XXXX
	<i>Longitudinal Centre of Gravity</i>	XXXX
<i>Centre of Gravity (mm)</i>	<i>Transversal Centre of Gravity</i>	XXXX
	<i>Vertical Centre of Gravity</i>	XXXX

Table 10 Structure of the generator-sets database

<b>Voices</b>	<b>Value</b>
<i>Manufacturer</i>	XXXX
<i>Model</i>	XXXX
<i>Rated Power (kW)</i>	XXXX
<i>Maximum Power (kW)</i>	XXXX
<i>Rated Rotational Speed (rpm)</i>	XXXX
<i>Maximum Rotational Speed (rpm)</i>	XXXX
<i>Length</i>	XXXX
<i>Main dimension (mm)</i>	<i>Breadth</i>
	<i>Height</i>
<i>Weight (kg)</i>	XXXX
<i>Longitudinal Centre of Gravity</i>	XXXX
<i>Centre of Gravity (mm)</i>	<i>Transversal Centre of Gravity</i>
	<i>Vertical Centre of Gravity</i>
<i>Fuel Consumption at Rated Load (g/kWh)</i>	XXXX

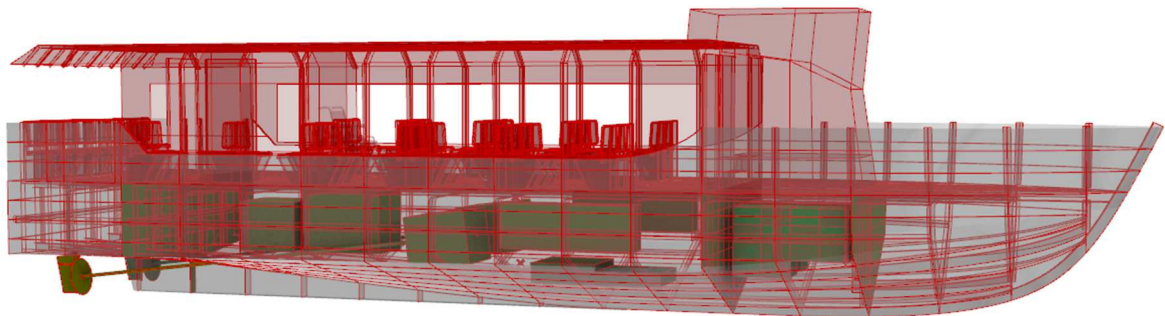


Figure 37 3D model of the propulsion system and engine room

### 3.2.1. Identification of the Design Variables

To define the set of variables that govern the resistance estimation process and the preliminary selection of the propulsion system, the parametric model relies on three

fundamental groups of information: the specifications provided by the shipowner, the design choices adopted in the preliminary phase, and the set of variables that feed the resistance–propeller module. Table 11, Table 12, Table 13 and Table 14 respectively present these categories of data, forming the methodological basis for the coherent generation and evaluation of the design configurations.

*Table 11 Shipowner specifications relevant to resistance and propeller selection*

<b>Category</b>	<b>Description</b>
<i>Design speed</i>	Target speed requested by the owner under standard operating conditions
<i>Zero Emission Mode speed</i>	Maximum allowable speed selected by the owner when operating in Zero Emission Mode

*Table 12 Preliminary Design choices relevant to resistance and propeller selection*

<b>Category</b>	<b>Description</b>
<i>Propulsion architecture</i>	Shaft line, hybrid-series architecture

*Table 13 Parametric variables involved in the propulsion module*

<b>Domain</b>	<b>Variables</b>
<i>Hull geometry</i>	Length, beam, draught, wetted surfaces, volumes, form coefficients
<i>Operating conditions</i>	Design draft
<i>Propeller parameters</i>	Maximum installable diameter, clearance from hull and appendages
<i>Engine room clearances</i>	Available length, heights and widths, technical corridors, volumetric space for equipment

Table 14 Main categories of technical data extracted from the propulsion and energy-system databases

Domain	Variables
<i>Propeller database</i>	Geometric and performance parameters derived from systematic propeller series
<i>Electric propulsion motors database</i>	Technical data for electric propulsion motors
<i>Diesel-generator sets database</i>	Information on power-generation units
<i>Battery systems database</i>	Energy and construction parameters of battery modules

3.2.2. Output

The process concludes with the structured export of results, which includes resistance curves (Figure 38), the propulsive power required at the design speed, preliminary propeller configurations (Table 15), the selected propulsion options (Table 16 and Table 17), and the possible compatible energy systems (Table 18 and Table 19). The data are stored in tabular form to enable comparative analyses and to serve as the methodological foundation for the application phases and the case study, in which the technical details, formulas, and hydrodynamic models adopted will be presented.

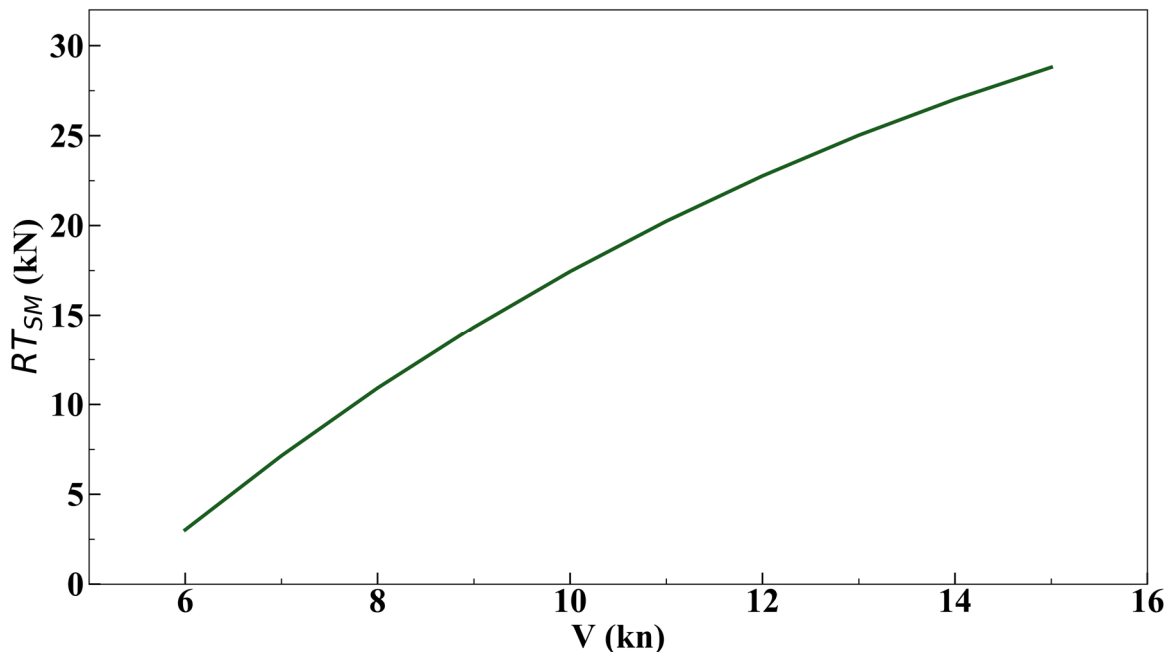


Figure 38 Speed–resistance curve

Table 15 Preliminary Propeller Configuration

<b>Parameter</b>	<b>Symbol</b>	<b>Units</b>	<b>Value</b>
<i>Propeller diameter</i>	$D_{PROP}$	(m)	XXXX
<i>Rotational speed</i>	$n$	(rpm)	XXXX
<i>Number of blades</i>	$Z$	(\)	XXXX
<i>Expanded area ratio</i>	$EAR$	(\)	XXXX
<i>Open-water efficiency</i>	$\eta_0$	(\)	XXXX

Table 16 Main characteristics of the selected propulsion motors

<b>Manufacturer and model</b>	<b>Quantity</b>	<b>Rated power (kW)</b>	<b>Total power (kW)</b>
xxxx	XXXX	XXXX	XXXX

Table 17 Main characteristics of the selected diesel-generators

<b>Manufacturer and model</b>	<b>Quantity</b>	<b>Rated power (kW)</b>	<b>Total power (kW)</b>
xxxx	XXXX	XXXX	XXXX

Table 18 Main characteristics of the selected battery Energy Storage System (ESS)

<b>Manufacturer and model</b>	<b>Quantity</b>	<b>Single module energy capacity (kWh)</b>	<b>Total energy capacity (kWh)</b>
xxxx	XXXX	XXXX	XXXX

Table 19 Power demand and endurance in Zero Emission Mode at the reference operating condition

Parameter	Units	Value
Battery power demand at 8 kn in ZEM	(kW)	xxxx
Hotel and auxiliary loads	(kW)	xxxx
Total power demand	(kW)	xxxx
Endurance at 8 kn in ZEM	h	xxxx

### 3.3. 3D General Arrangement Plan and Structures

In continuity with the FPA adopted, the process for generating the three-dimensional general arrangement and the structural model is conceived as an integrated and systematically organized system.

Unlike sequential modelling, where the general arrangement precedes the structural model or vice versa, the framework herein proposed assumes that the two domains are logically and functionally co-dependent. This principle, already highlighted in the flow chart shown in Figure 39, constitutes the fundamental methodological element: the definition of functional spaces and the structural materialization of the vessel evolve simultaneously and mutually influence each other at every stage of the generation process.

The foundation is the 3D parametric system, within which the hull geometry, deck locations, compartment subdivision are represented, together with the definition of technical volumes and service spaces.

In particular, the general arrangement is not conceived as a set of simple 2D drawings, but rather as a dynamic volumetric representation built around a controlled set of parameters that govern the position, dimensions, and interrelationships of the spaces. This approach enables the automatic and reproducible generation of multiple configurations, all consistent with regulatory constraints, owner requirements, and preliminary design choices.

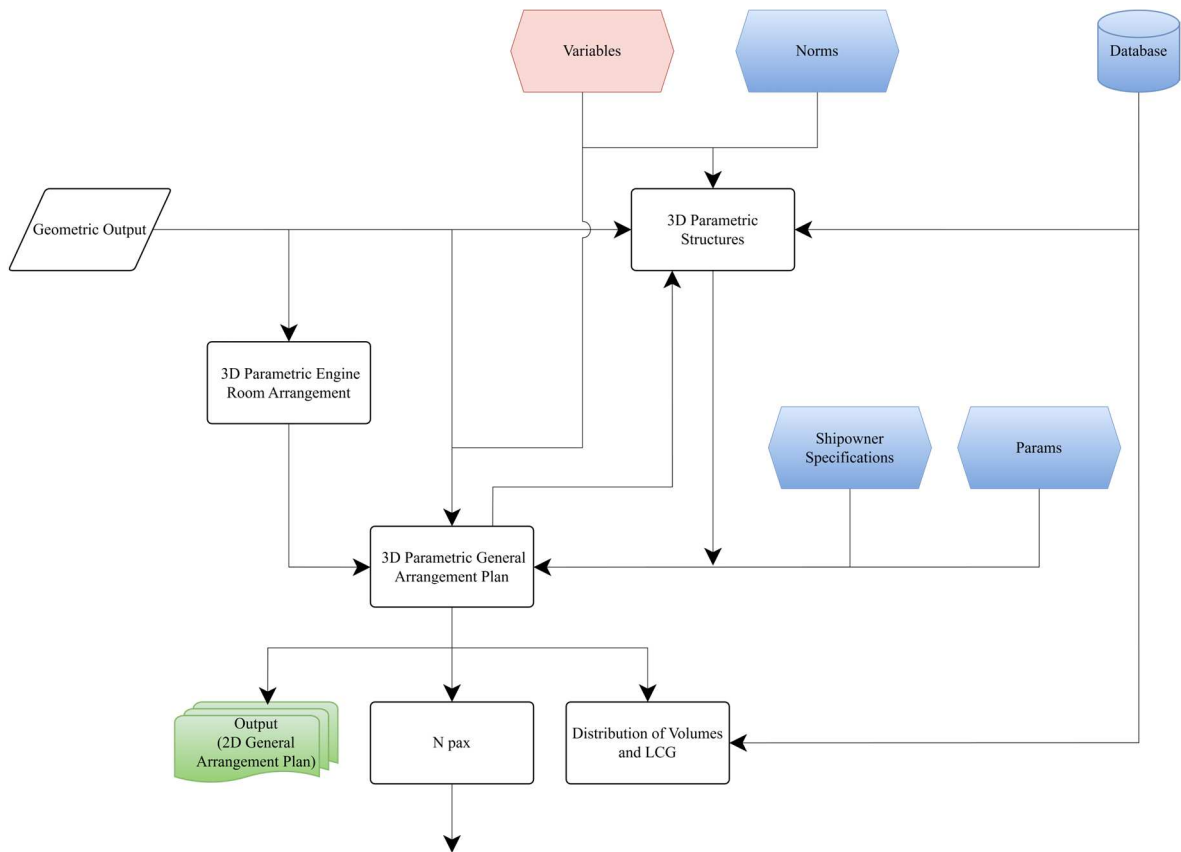


Figure 39 Logical framework of the 3D General Arrangement Plan and Structures

Within the pipeline, the general arrangement represents the element that governs the functional identity of the vessel, translating mission requirements into articulated spatial distributions. The methodology assumes that every technical compartment, passenger area, systems volume, and access path is defined by geometric parameters that control its extent, height, longitudinal and transverse position, as well as its connections to adjacent spaces. As also highlighted in the scientific literature [6], parametric modelling of the general arrangement enables the abandonment of the traditional approach, historically characterized by early design decisions that are difficult to modify, in favour of a logic in which any geometric variation is automatically reflected in the articulation of volumes and in the internal spatial relationships.

In this context, the general arrangement does not merely express the functional intentions of the spaces; it becomes an active computational node capable of interacting with both the structural and systems domains. The influence is bidirectional: on the one hand, the general arrangement defines the position and extent of bulkheads, the distribution of decks, and the subdivision of compartments; on the other hand, the structural model establishes the

engineering constraints within which these functions can be allocated. Elements such as keelsons, deck beams, stringers, floors, and main bulkheads are not treated as purely geometric entities, but as structural components that impose physical limits on the internal configuration. This bidirectional relationship represents one of the distinctive features of the adopted methodology: the general arrangement expresses functional requirements, while the structural model provides their engineering materialization within the three-dimensional domain.

The parametric structural model is constructed on the basis of general ship design rules, regulatory constraints and dimensional parameters governing the full set of load-bearing elements. In particular, the Rules for the Classification of Ships with Aluminium Alloy Hulls issued by RINA are adopted as the primary regulatory reference for the definition of structural layouts, scantlings and verification criteria [84]. Rather than being implemented as a static post-processing check, regulatory requirements are embedded directly into the parametric logic of the tool and actively guide the generation of the three-dimensional structural arrangement.

At the highest level, the designer is required to select the structural philosophy of the hull, choosing between a longitudinal or transverse framing system. This choice determines the subsequent organisation of the internal structure and activates the corresponding rule-based constraints. For transverse framing solutions, the spacing of ordinary transverse frames is defined by the user within an admissible interval that is consistent with the selected regulatory framework for aluminium structures. The parametric model enforces these bounds, ensuring that the adopted spacing remains compliant with rule prescriptions throughout the design exploration.

When a longitudinal framing system is selected, additional hierarchical rules are applied. Ordinary transverse frames are generated at the prescribed spacing, while every second frame is automatically defined as a reinforced transverse frame, in accordance with common classification practice for longitudinally framed aluminium hulls. The placement of watertight and non-watertight bulkheads is then discretised and constrained to coincide exclusively with these reinforced transverse frames. As a result, bulkhead positioning becomes a variable but rule-consistent design choice, preventing geometrically feasible yet structurally incoherent configurations.

A similar logic governs the definition of longitudinal stiffening. The user selects the spacing of ordinary longitudinal stiffeners, after which the model allows the designer to define the frequency at which reinforced longitudinals are introduced. Depending on their location and structural role, these reinforced elements may correspond to bottom girders, centreline girders or deck girders. This hierarchical subdivision reflects standard classification practice and ensures continuity between local stiffening and primary supporting members.

From a geometric standpoint, each structural decision results in a progressive “slicing” of the three-dimensional hull surfaces. The parametric model generates intersection curves on the bottom, side shell and deck surfaces corresponding to the selected frame and stiffener positions. These curves act as reference rails for the extrusion of structural profiles. Cross-sectional shapes for ordinary stiffeners and primary members are retrieved from dedicated databases and instantiated along these rails, guaranteeing geometric consistency, repeatability and spatial compatibility across the entire structure.

In parallel with the geometric generation, the tool performs rule-based structural checks. Design loads are evaluated as a function of the vessel’s principal dimensions, material properties, local plate thicknesses and the longitudinal position along the hull. For each structural element, the minimum required thicknesses and section moduli prescribed by the rules are computed and automatically compared against the properties of the selected catalogue profiles database (Table 20 and Table 21). This process allows immediate verification of compliance at the preliminary design stage and highlights non-conforming configurations as the geometry evolves.

*Table 20 Aluminium alloy T-beam Catalogue*

<b>Profile ID</b>	<b>h (mm)</b>	<b>b (mm)</b>	<b>t<sub>w</sub> (mm)</b>	<b>t<sub>f</sub> (mm)</b>
<i>T 60×40×5</i>	60	40	5	5
<i>T 80x50x5</i>	80	50	5	5
<i>T 100x60x6</i>	100	60	6	6
<i>T 120x60x6</i>	120	60	6	6
<i>T 140x70x7</i>	140	70	7	7
<i>T 160x80x8</i>	160	80	8	8

Table 21 Aluminium alloy Flat Bar Catalogue

<b>Profile ID</b>	<b>b (mm)</b>	<b>t (mm)</b>
<i>FB 40x5</i>	40	5
<i>FB 50x6</i>	50	6
<i>FB 60x6</i>	60	6
<i>FB 80x8</i>	80	8
<i>FB 100x8</i>	100	8
<i>FB 120x10</i>	120	10
<i>FB 150x10</i>	150	10

The methodological pipeline also ensures that each generated configuration is verified for regulatory compliance. The modelling of minimum room heights and corridor widths has been carried out in direct compliance with applicable regulations [90], [91]. These requirements are embedded in the geometric definition itself, so that only compliant configurations can be generated, without the need for any a posteriori validation or checking.

Following the 3D modelling of the entire vessel, the methodology also enables the preliminary execution of several additional assessments, including the calculation of the equipment number, a parameter through which the number and category of anchors, as well as the required chain mass, are determined for the unit. Although this evaluation is not an integral part of the structural scantling process, it naturally fits within the methodological workflow because it depends on the ship's geometry, the estimated weights, and the overall configuration resulting from the parametric modelling.

### 3.3.1. Identification of the Design Variables

To provide a structured overview of the parameters governing the generation of the three-dimensional general arrangement and the corresponding structural model, the following tables (Table 22, Table 23, Table 24 and Table 25) summarise the functional, geometric, and regulatory variables, incorporating both the technical data retrieved from the databases and the choices defined by the shipowner. These elements collectively define the bidirectional relationship between spatial organisation and structural materialisation within the parametric framework.

Table 22 Design variables associated with owner requirements and preferences

<b>Category</b>	<b>Description</b>
<i>Number of decks</i>	Relevant to vertical distribution and structural subdivision
<i>Number of toilets</i>	Influences spatial allocation and weight estimation
<i>Presence of special areas (bike racks, spaces for reduced mobility, light cargo)</i>	Impacts functional layout and spatial constraints
<i>Possible aesthetic or functional preferences</i>	May affect arrangement choices and internal configurations

Table 23 Summary of design variables and their implications

<b>Category</b>	<b>Description</b>
<i>Longitudinal and transverse location of spaces (toilets, embarkation)</i>	Governs spatial distribution and circulation
<i>Type of seating (bus-style or island-type)</i>	Influences functional layout and seat density
<i>Free heights</i>	Regulates usability and compliance with standards
<i>Corridor dimensions</i>	Determines circulation efficiency and safety compliance
<i>Number and placement of bulkheads</i>	Influences compartmentalization and structural continuity
<i>Spacing of longitudinal and transverse members</i>	Defines structural grid and scantling logic
<i>Deck positioning</i>	Affects overall arrangement and weight distribution
<i>Functional distribution of spaces</i>	Ensures correct allocation of mission-related functions
<i>Spatial constraints associated with onboard systems</i>	Governs equipment placement and integration feasibility

Table 24 Regulatory requirements governing space design and layout

<b>Category</b>	<b>Description</b>
<i>Compartmentalization rules</i>	Define subdivision and safety boundaries
<i>Minimum room-height requirements</i>	Ensure habitability and compliance
<i>Dimensions and clearances for corridors</i>	Guarantee accessibility and evacuation paths
<i>Accessibility and safety regulations</i>	Govern arrangement of spaces and equipment
<i>Passenger-related prescriptions</i>	Define constraints on comfort, circulation, and capacity

Table 25 Regulatory-derived parameters for structural design

<b>Category</b>	<b>Description</b>
<i>Available structural profiles</i>	Inputs for structural modelling and scantling
<i>Commercial plate thicknesses</i>	Defines feasible structural configurations
<i>Linear weights of materials</i>	Essential for weight and CoG estimation
<i>Dimensional envelopes of seats, furnishings, and technical modules</i>	Constrain spatial allocation and GA layouts
<i>Standard equipment for onboard systems</i>	Used in systems integration and volume allocation
<i>Weight of bathrooms and windows</i>	Contributes to mass estimation and distribution
<i>Standardized dimensions for doors, windows, and furnishing modules</i>	Support geometric compatibility and regulatory checks

### 3.3.2. Output

At the end of each iteration, the system automatically exports a set of outputs derived from the three-dimensional model: complete 3D models (Figure 40 and Figure 41), 2D GA plans (Figure 42), and technical tables relating to weight exponent (Table 26 and Table 27).

Among the outputs of fundamental importance are the number of passengers that can be accommodated on board and the number of seats that can be arranged across the different configurations.

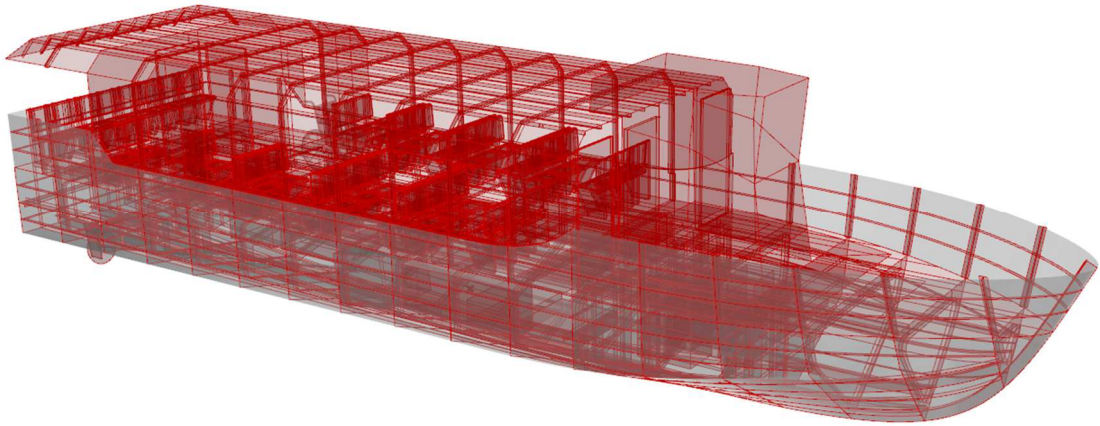


*Figure 40 View 1 of the complete 3D model*

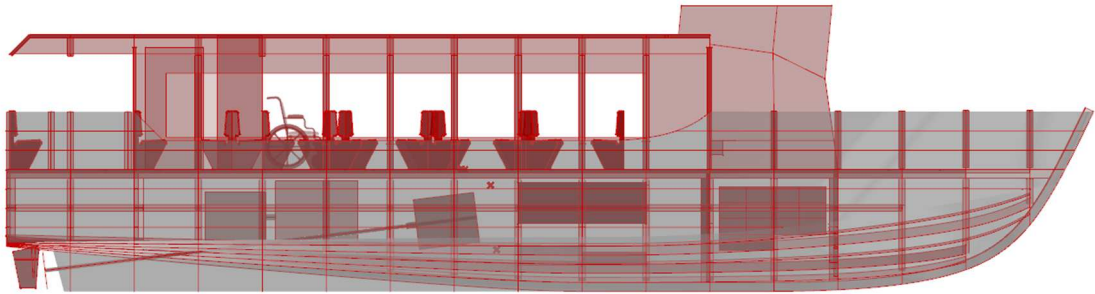
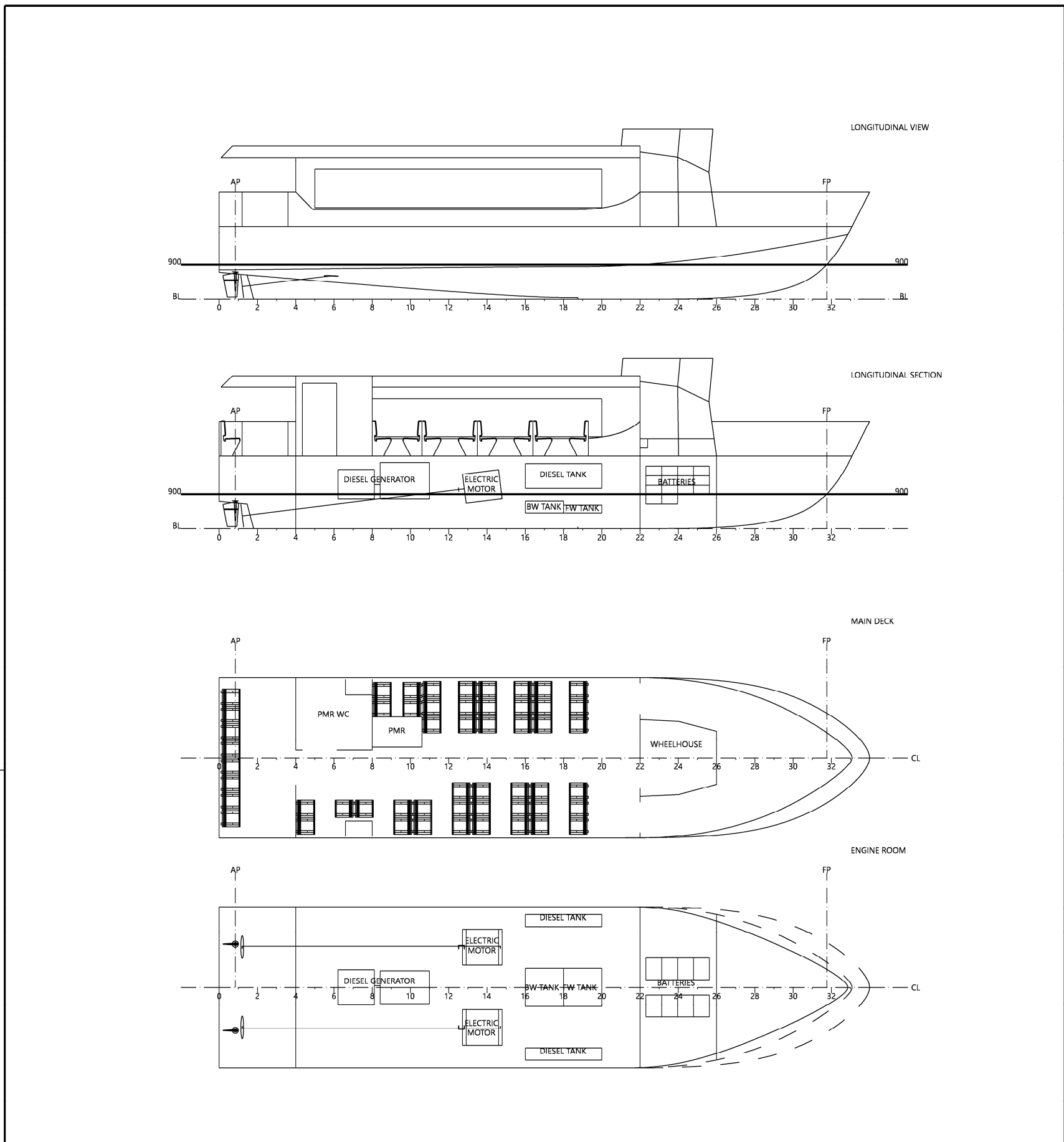


*Figure 41 View 2 of the complete 3D model*




MODIFICHE ALTERATIONS	REV. N.	DATA DATE	NOME NAME	FIRMA SIGN	 <b>UNIVERSITÀ DEGLI STUDI DI TRIESTE</b> Dipartimento di Ingegneria e Architettura Sezione di Ingegneria Navale Via Alfonso Valerio, 10 - I-34127 Trieste Tel. +39 040 558 3428 Fax +39 040 558 3442	
	DISEGNATO DRAWN	30/12/2025	DP	<i>Donato Padolecchia</i>		
CONTROLLATO CHECKED	30/12/2025	DP	<i>Donato Padolecchia</i>			
APPROVATO APPROVED	30/12/2025	DP	<i>Donato Padolecchia</i>			
SCALA <b>1:100</b>	<b>PASSENGER VESSEL</b>				COSTRUZIONE HULL	-
SCALE	<b>GENERAL ARRANGEMENT PLAN</b>				PROGETTO PROJECT	<b>XXX</b>
FORMATO <b>A3</b>	<b>PRELIMINARY DESIGN</b>				DISEGNO N. DRAWING N.	<b>XXXXXXX</b>
SIZE					FOGLIO N. SHEET N.	<b>1 / 1</b>
COPIA N. -	L'UNIVERSITA' DI TRIESTE SI RISERVA A TERMINI DI LEGGE LA PROPRIETA' DI QUESTO DISEGNO CON DIVIETO DI RIPRODURLO O DI RENDERSLO COMUNQUE NOTO A TERZI O A DITTE CONCORRENTI SENZA LA SUA AUTORIZZAZIONE THIS DOCUMENT IS THE PROPERTY OF UNIVERSITY OF TRIESTE AND IT SHALL NOT BE USED, REPRODUCED OR COMMUNICATED TO UNAUTHORIZED COMPANIES AND/OR PEOPLE.				SOSTITUISCE REPLACES	-
COPY N.					SOSTITUITO DA REPLACED BY	-

Figure 42 2D GA plans

Table 26 Lightship condition: weight and centre of gravity summary

<b>Item</b>	<b>W (t)</b>	<b>LCG (m)</b>	<b>TCG (m)</b>	<b>KG (m)</b>
<i>Structures</i>	-	-	-	-
<i>Superstructures</i>	-	-	-	-
<i>  Outfit</i>	-	-	-	-
<i>  Glasses</i>	-	-	-	-
<i>Anchor and</i>	-	-	-	-
<i>  Chains</i>	-	-	-	-
<i>Main Deck</i>	-	-	-	-
<i>  Floor</i>	-	-	-	-
<i>  Seats</i>	-	-	-	-
<i>  Tanks</i>	-	-	-	-
<i>(Structure)</i>	-	-	-	-
<i>Rudders</i>	-	-	-	-
<i>Propellers</i>	-	-	-	-
<i>  WC</i>	-	-	-	-
<i>Wheelhouse</i>	-	-	-	-
<i>  Safety</i>	-	-	-	-
<i>  equipment</i>	-	-	-	-
<i>Propulsion</i>	-	-	-	-
<i>Lightship Total</i>	-	-	-	-

Table 27 Full Load condition: weight and centre of gravity summary

<b>Item</b>	<b>Quantity</b>	<b>Unit Weight (t) / Equivalent Value (l)</b>	<b>W (t)</b>	<b>LCG (m)</b>	<b>TCG (m)</b>	<b>KG (m)</b>
<i>Passengers</i>	-	-	-	-	-	-
<i>Port Fuel Tank</i>	-	-	-	-	-	-
<i>Starboard Fuel Tank</i>	-	-	-	-	-	-
<i>Fresh Water Tank</i>	-	-	-	-	-	-
<i>Black Water Tank</i>	-	-	-	-	-	-
<i>Departure Full-Load Total</i>	-	-	-	-	-	-

### 3.4. Parametric Sampling Techniques: Design of Experiments

The systematic exploration of the design solution space requires sampling techniques capable of representing the parametric domain in an efficient and statistically meaningful way. While the methodological framework defines the set of independent variables and constraints, the DoE provides the strategy through which this domain is explored. In the present study, the investigation of the design space is conducted using a space-filling DoE implemented through ULHS [92].

ULHS is particularly well suited to high-dimensional problems involving numerous geometric, functional, and systems-related parameters. As a multidimensional extension of Latin Square principles [93], the method partitions each variable into equiprobable intervals and ensures that every interval is sampled exactly once. This guarantees that each generated configuration occupies a unique region of the domain, preventing clustering and promoting a homogeneous distribution of points across the multidimensional space (Figure 43).

The distinguishing feature of ULHS compared to other sampling methods is its ability to preserve uniformity even as the dimensionality of the problem increases, thereby avoiding clustering and sparsely explored regions. This characteristic is particularly relevant in

parametric ship design [52], where the combination of geometric variables (length, beam, draft, form coefficients), functional variables (capacity, internal volumes, propulsion power), and structural variables (bulkhead arrangement, subdivision constraints, construction limits) naturally gives rise to highly complex design spaces.

The application of ULHS in the present study thus makes it possible to obtain a representative set of design configurations, each of which serves as the input for the automatic generation of the 3D model. This approach not only ensures a homogeneous coverage of the parameter space but also reduces the overall number of combinations that must be evaluated, thereby contributing to the computational efficiency of the entire parametric process.

It should be emphasised that, at the concept and preliminary design stage addressed in this research, the parametric domain was deliberately defined with relatively wide ranges. This choice reflects the exploratory nature of the design phase, in which the objective is not to focus prematurely on a narrow subset of solutions, but rather to obtain an initial and unbiased mapping of the feasible and unfeasible regions of the design space.

Within this context, the adoption of ULH sampling plays a key methodological role. ULHS was selected specifically to guarantee a uniform and space-filling coverage of the multidimensional domain, without introducing a priori assumptions on the relative importance or admissible ranges of individual variables. This approach allows the interactions between geometric, functional, regulatory and system-related parameters to emerge naturally from the feasibility filtering process, rather than being implicitly constrained by pre-filtered variable ranges.

As a consequence, the possible presence of a significant number of unfeasible configurations is not interpreted as an inefficiency of the method, but as an intrinsic outcome of an intentionally broad exploration aimed at aggressively screening non-viable or unrealistic solutions at an early design stage.

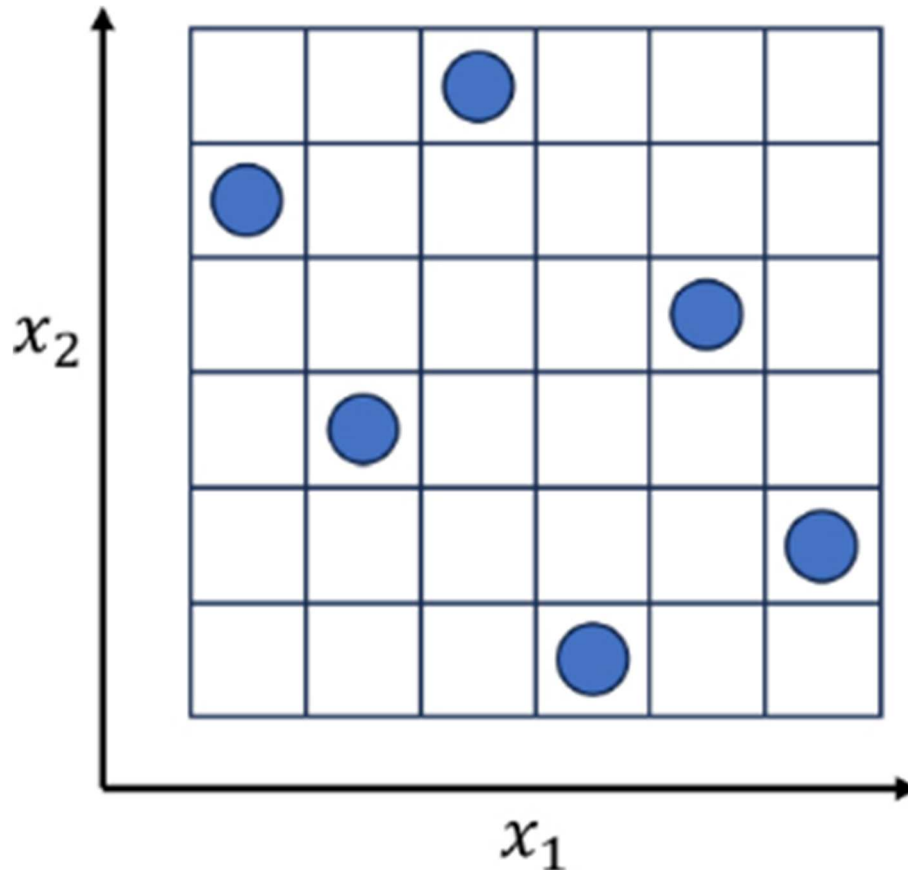


Figure 43 Uniform Latin hypercube sampling with two variables and six points [94]

### 3.5. Feasibility Analysis

At the conclusion of the entire generative process described in the preceding chapters, the parametric model performs a series of final checks whose purpose is to determine the technical feasibility of the configurations obtained. These checks, illustrated in the flow chart of the parametric modelling methodology (Figure 44), constitute the logical filter through which only those configurations that comply with operational requirements, regulatory constraints, and the stability and safety criteria required for a passenger vessel are selected. In this framework, the parametric process does not merely produce a set of alternative geometries; rather, it yields a set of technically admissible solutions validated according to formal and objective criteria.

The first validation concerns the number of passengers that can be transported, a crucial parameter for vessels intended for intermodal transport services. Indeed, the primary objective of such units is to reduce urban land-based traffic by offering transport capacities equivalent to those of a city bus. Consequently, every generated configuration must be able

to accommodate a minimum number of passengers sufficient to “empty” a land-based public vehicle in a single trip. This requirement, however, is not defined solely in functional terms: the passenger capacity must also comply with the limits imposed by current regulations, in particular the applicable Italian flag-state rules and the relevant class requirements.

The parametric model therefore compares the passenger capacity resulting from the three-dimensional general arrangement with regulatory limits regarding available surfaces, escape routes, room-height requirements, and minimum safety criteria. Configurations that fail to satisfy these constraints are automatically discarded by the pipeline.

Among the configurations that pass the passenger-capacity check, the system then proceeds to the evaluation of the weight–buoyancy balance and the longitudinal trim. This methodological phase constitutes an essential verification of the hydrostatic consistency and physical plausibility of the parametric model. By integrating the contribution of all estimated weights (structure, systems, furnishings, propulsion, energy systems, passenger load) and comparing them with the buoyant force generated by the submerged hull, the system determines whether the configuration falls within a predefined acceptability range.

This range is expressed in terms of:

- the weight–buoyancy difference,
- the relative position of the *LCG* with respect to the *LCB*.

The methodology considers as admissible only those configurations that satisfy these criteria within an established range, automatically eliminating those that exhibit implausible trim conditions, significant misalignments between centres, or equilibrium states that would compromise the vessel’s operability. This phase is particularly relevant because it integrates effects originating from all previously described modules: geometry, spatial arrangement, onboard systems, propulsion, and structure.

Configurations that also pass the hydrostatic equilibrium check are subsequently subjected to stability verification, conducted in accordance with the criteria prescribed by the class regulations, with specific reference to Parts B [91] and E [95] of the RINA rules for the stability of passenger vessels.

The combination of these checks ensures that only configurations satisfying the minimum stability requirements established by the regulatory framework for small passenger vessels

are classified as admissible. Configurations that do not comply are automatically excluded from the design pipeline, thereby ensuring that the exploration of the solution space generated by the parametric model remains within an engineeringly plausible, certifiable, and safe domain from the earliest design stages.

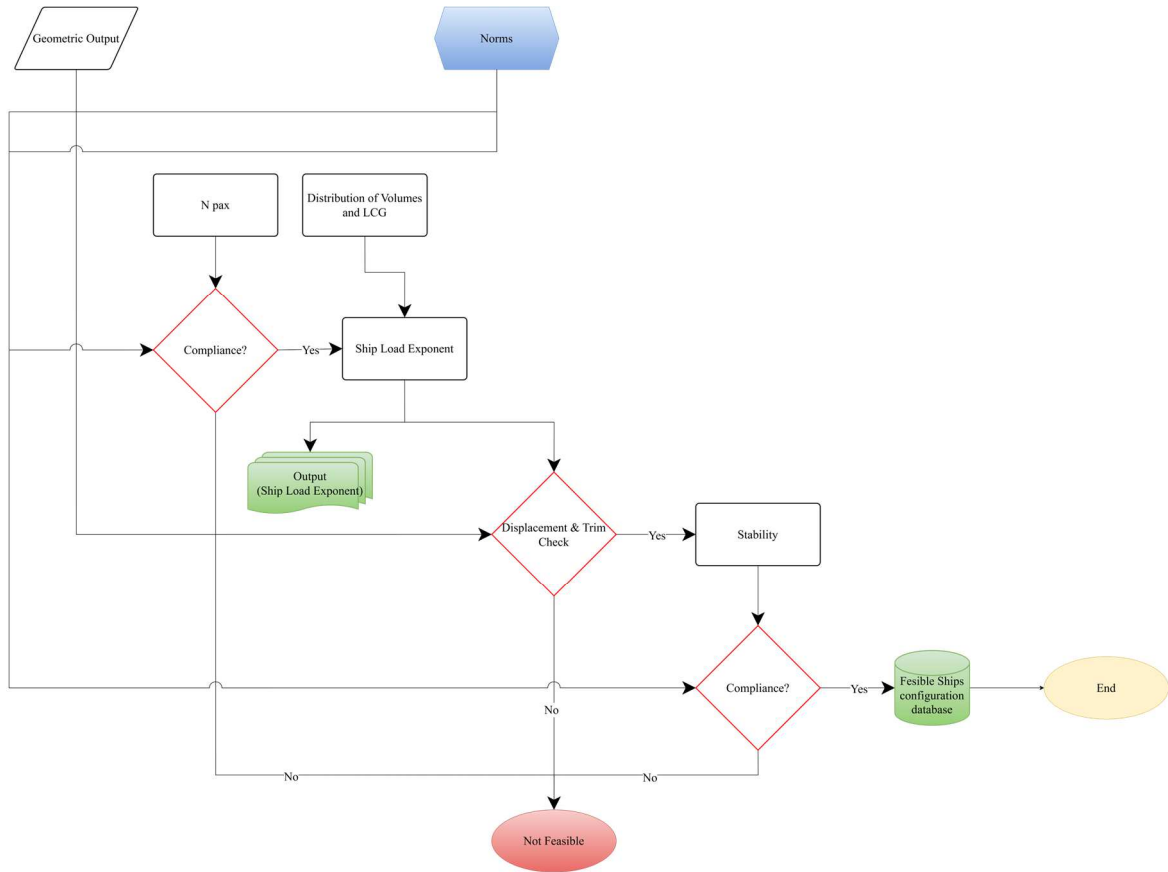


Figure 44 Logical framework of the Feasibility Analysis

## Chapter 4

### Case study–based validation of the proposed methodology

This chapter applies the integrated parametric methodology developed in the previous chapters to the definition of a set of ship configurations intended for passenger service in the Gulf of Trieste. The objective of the case study is twofold. On the one hand, it enables the operational robustness and engineering consistency of the computational workflow to be verified when applied to a real-world context characterised by heterogeneous technical, regulatory, and functional constraints. On the other hand, it allows the generation of a quantitatively significant set of feasible design solutions, providing an objective basis for the comparative evaluation of alternatives and for the identification of the most effective trade-offs in relation to the service objectives.

To ensure traceability throughout the chapter, the application of the methodology is organised around an initial baseline configuration (hereafter referred to as the *base model*), which serves as a reference starting point for the exploration of the design space rather than as a pre-validated solution.

The Gulf of Trieste, owing to its geographical configuration, the articulation of coastal urban nodes, and its increasing integration with land-based transport networks, represents a particularly suitable testbed for model validation. Daily mobility requirements, the presence of multiple centres of attraction distributed along the coastline, and the variability of routes and operational profiles associated with short- and medium-range services impose stringent requirements in terms of flexibility, efficiency, and reliability. These requirements directly affect the dimensional, architectural, and propulsion-related design choices of the ship system. In such a context, a traditional, sequential design approach, heavily reliant on manual iterations, proves inadequate for the systematic exploration of the full design space within timeframes compatible with service planning.

By contrast, the application of the methodology developed in Chapter 3 enables the set of operational and regulatory requirements specific to the Trieste context to be transformed into a controlled parametric domain. Within this framework, the base model is generated by

assigning initial values to the design variables derived from the operational requirements, while the parametric structure, constraints, and relationships remain those defined in the methodological phase. The base model is therefore geometrically coherent by construction, but it is not required to satisfy all feasibility criteria implemented in the verification modules. Within this domain, each point sampled through DoE techniques triggers the automatic generation of a complete three-dimensional configuration, including hull form, functional layout, propulsion system, onboard systems, and primary structural elements. The integration of verification modules—geometric, functional, regulatory, and propulsion-related—allows each configuration to be classified as admissible or non-admissible according to objective and traceable criteria, thereby drastically reducing the risk of generating solutions lacking engineering validity.

In this sense, feasibility is not imposed *a priori* but emerges from the interaction between parametric generation and the integrated verification workflow. In this way, the case study goes beyond serving as a mere application example and instead constitutes a true validation benchmark for the integrated parametric approach. The generation of a diverse set of solutions compatible with the constraints of the Gulf of Trieste effectively demonstrates the model’s ability to:

- coherently interpret complex operational requirements;
- translate them into geometric and functional variables and relationships;
- produce technically sound and verifiable design configurations.

#### **4.1. Case-study framework and definition of the parametric design domain**

This section introduces the case-study framework by first outlining the operational context of passenger transport services in the Gulf of Trieste and then formalising the resulting requirements into a coherent parametric design domain. These preliminary steps establish the boundary conditions and fixed inputs for the subsequent application of the integrated parametric methodology to hull definition, propulsion sizing, general arrangement modelling, and structural layout.

#### 4.1.1. Operational requirements for passenger transport services in the Gulf of Trieste

The definition of the operational requirements for the case study requires a thorough understanding of the geographical structure, mobility demand, and public transport supply characterising the Gulf of Trieste. This area can be described as a linear coastal system, in which the main settlements — Trieste, Barcola, Grignano, Sistiana, and Duino — are distributed along a relatively short maritime axis, with limited distances between landing points and a very close interaction between urban, suburban, and tourist mobility (Figure 45). The morphology of the Gulf, which represents the northernmost portion of the Adriatic Sea, is characterised by relatively shallow waters, with average depths generally below 20 metres and maximum values on the order of 35–40 metres [96]. This bathymetric structure, combined with the characteristics of the ports and small piers distributed along the coastline, imposes the adoption of vessels with limited draught, compact geometries, and high manoeuvrability. These aspects play a decisive role in the definition of the parametric design domain.

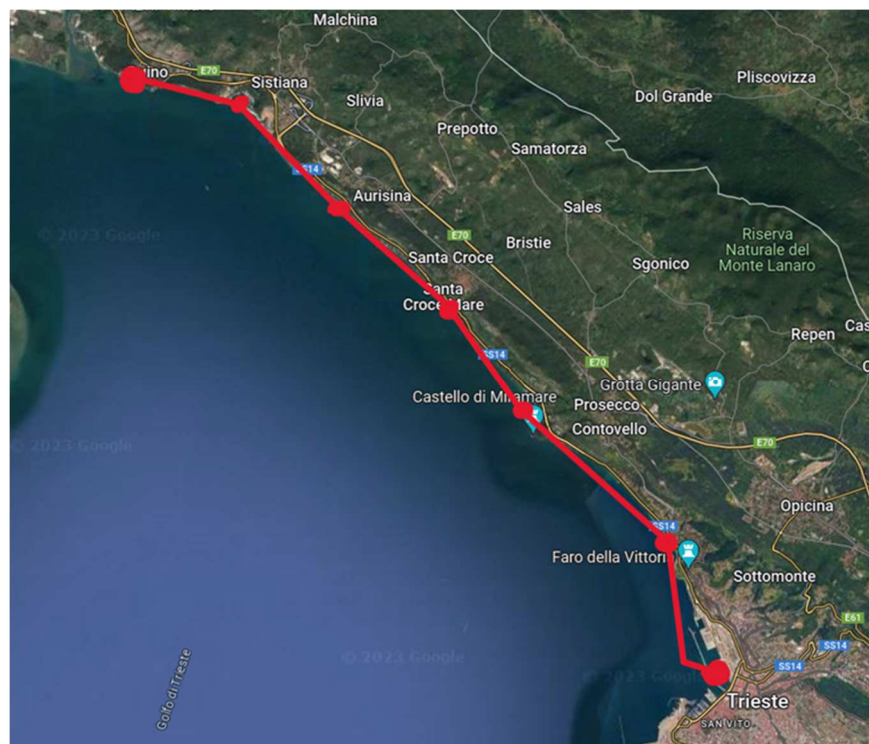


Figure 45 Linear coastal study area with the main settlements distributed along a short maritime axis

Mobility demand in the region confirms the relevance of a multimodal coastal transport system. The only maritime route operating year-round, the Trieste–Muggia line, has experienced a significant increase in recent years: from 89,493 passengers in 2019 to 131,125 in 2022, with an estimated value between 140,000 and 145,000 passengers in 2023, based on data released by the Friuli Venezia Giulia Regional Authority and reported by institutional media. This is complemented by the seasonal Trieste–Barcola–Grignano–Sistiana line, which has transported slightly more than 67,000 passengers per season over the last two years, showing a substantial stability in summer tourist flows (Table 28). Overall, regional maritime services reached approximately 351,000 passengers in 2023, compared to 211,000 in 2022, corresponding to an increase exceeding 60% according to officially presented regional data [97]. These figures indicate that the Gulf of Trieste represents one of the most significant hubs of regional maritime public transport, with a growing trend that further strengthens its role within the coastal mobility system.

By contrast, the road-based public transport offer along the same coastal corridor is considerably more intensive in terms of frequency and capacity. Public transport data provided by the Municipality of Trieste ([www.mobilitasostenibile.online.trieste.it](http://www.mobilitasostenibile.online.trieste.it)) indicate that the bus network serving the coastal area carries on the order of two million passengers per year along the main corridor alone, with pronounced peaks during the summer season and peak commuting hours. At the scale of the entire urban system, the public transport network operated by Trieste Trasporti ([www.triestetrasporti.it](http://www.triestetrasporti.it)) serves approximately 65 million passengers per year, through about 5600 daily services, highlighting the overall intensity of road-based mobility within the Trieste basin. During periods of maximum seasonal demand, additional services are introduced along the coastal corridor, resulting in more than one hundred bus passages per direction per day under peak conditions. This level of service provides a quantitative reference against which the potential role of a maritime passenger transport alternative can be assessed (Figure 46).

Table 28 Maritime services and annual passenger volumes

Maritime service	Annual passengers	Share of total FVG maritime public transport (%)
<i>Trieste–Muggia (year-round)</i>	145,000	39.9%
<i>Trieste–Sistiana (seasonal)</i>	67,000	19.1%

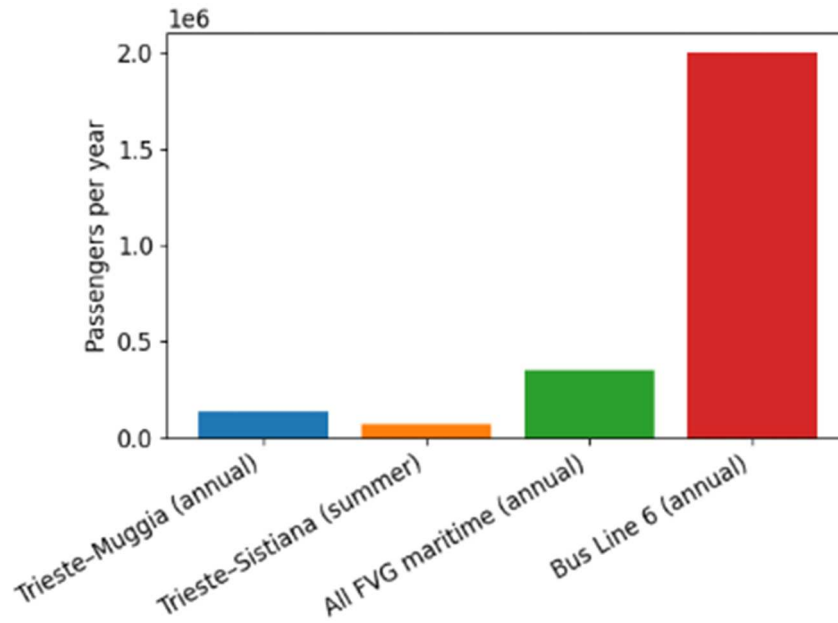


Figure 46 Annual passenger volumes for selected maritime services in Friuli Venezia Giulia and for Bus Line 6

Despite such a substantial service offer, the coastal corridor is frequently affected by congestion. Viale Miramare constitutes the main northern access route to the city and, particularly during the summer season, is subject to intense vehicular flows generated by commuting, seaside tourism, and traffic directed towards Miramare Castle. Local reports regularly document situations of slowed or blocked traffic, with significant impacts on the regularity and travel times of bus services, often caused by roadworks, accidents, or demand overloads. Under these conditions, even high-frequency services become vulnerable to delays, thereby losing part of their ability to guarantee reliable and predictable travel times.

In this context, maritime transport provides an alternative corridor that is structurally independent of road traffic conditions. The Trieste–Muggia line offers up to ten daily departures per direction on weekdays, while the Trieste–Sistiana line provides eight daily connections during the summer season, with evenly distributed departures throughout the day. Although the number of services is lower than that of road-based transport, the reliability of maritime travel times and the complete avoidance of terrestrial congestion represent factors of particular relevance for the sizing and design of new vessels intended for coastal public transport.

The combination of these elements — growth in maritime demand, summer congestion along the coastal corridor, high passenger loads on bus lines, and the need to ensure service

continuity during peak periods — defines the operational requirements for the design of new vessels. These units should be compact, characterised by limited draught and excellent manoeuvrability, capable of operating at moderate speeds along regulated coastal routes, yet able to achieve significantly shorter travel times than road transport under congested conditions. Passenger capacity should fall within a range between 50 and 149 persons, sufficient to serve both commuter and tourist demand. Moreover, the integration of zero-emission operating modes in environmentally sensitive areas must be considered an essential requirement in light of the ongoing energy transition.

Further insights arise from the analysis of the vessels currently operating in the Gulf (Table 29), primarily belonging to the fleet of Delfino Verde Navigazione ([www.delfinoverde.it](http://www.delfinoverde.it)). These units are powered by conventional internal combustion engines (ICE), which, while reliable, are associated with noise and environmental emissions that are not always compatible with protected areas or with the increasing emphasis on sustainable coastal transport. In addition, their dimensions and draught limit the ability to berth at small-scale landings or seasonal pontoons. Several locations — such as the port of Miramare Castle, Santa Croce, and Portopiccolo — which could potentially be served, are currently excluded from the maritime network precisely due to the size of the existing vessels. This highlights the need to design vessels smaller than those currently in service, capable of accessing a wider range of landing points and increasing the overall capillarity of the system.

Table 29 Main characteristics of vessels currently operating in the Gulf of Trieste

<b>Vessel</b>	<b><math>L_{OA}</math> (m)</b>	<b><math>B_{OA}</math> (m)</b>	<b>Passenger capacity</b>	<b>Propulsion</b>
<i>Delfino Verde AS</i>	25.5	6.5	212 pax	Diesel ICE
<i>Delfino Verde Gold</i>	27.2	6.0	150 pax	Diesel ICE
<i>Summer Breeze</i>	23.4	5.7	184 pax	Diesel ICE
<i>Delfino Verde Deluxe</i>	32.4	7.5	300 pax	Diesel ICE
<i>Delfino Verde GT</i>	31.0	7.0	330 pax	Diesel ICE

The following table summarises the main characteristics of the vessels currently operating in the Gulf, highlighting the dimensional limitations that motivate the need for smaller units.

These requirements, once formalised, constitute the basis for the definition of the parametric design domain and are translated into parametric variables and constraints in the following section.

#### 4.1.2. *Translation of operational requirements into parametric variables*

The set of operational requirements outlined in the previous section must be translated into a coherent system of independent variables, geometric constraints, and functional relationships, which together constitute the basis for the parametric exploration of the design domain. At this stage, the requirements related to the specific context of the Gulf of Trieste—such as the need for compact vessels, limited draught, the presence of small-scale landing facilities, seasonal variability in demand, and the requirement for low-emission navigation modes—are formalised so that they can be effectively interpreted and processed by the parametric workflow.

The morphological surveys, access restrictions associated with minor ports, and the functional requirements identified in Chapter 4.1.1 led to the *a priori* definition of several principal hull dimensions (Table 30). In particular, the overall length ( $L_{OA}$ ) was set equal to 17 m, a value representing an effective compromise between manoeuvrability requirements and the need to maintain an overall size compatible with small-scale landing facilities. The overall breadth ( $B_{OA}$ ) was fixed at 4.2 m, ensuring adequate transverse stability while allowing operations at berths characterised by limited lateral clearance. The draught was constrained to 0.90 m, in accordance with the minimum depths observed at several secondary landing sites within the Gulf, where seabed depths below one metre would prevent the operation of vessels with greater draught. These three parameters, directly derived from the operational requirements, therefore constitute prescriptive inputs to the model and are not subject to variation within the ULHS sampling process.

In addition to the dimensional constraints, the selection of the hull typology was also defined as a context-driven, imposed choice. For the present case study, a single-chine configuration with skeg was adopted, excluding the use of spray rails. This decision is motivated by multiple operational considerations. On the one hand, the single-chine profile allows for a

simplified hull construction while maintaining regular hydrodynamic behaviour at the expected operating speeds. In order to prioritise constructability, a deliberately simple hull form was assumed, with the maximum chine breadth set equal to the maximum hull breadth both at the position of maximum chine width and at the stern. On the other hand, the inclusion of a skeg enhances directional stability and low-speed manoeuvrability, conditions that are frequently encountered in the vicinity of ports and coastal landing points within the Gulf of Trieste. These features are therefore treated as fixed characteristics of the model, rather than as variables to be explored.

All remaining variables described in the methodological framework remain fully active and are subject to parametric sampling (Table 31). The presence of fixed dimensional constraints does not reduce, but rather sharpens, the role of these variables within the ULHS exploration, as it enables the search to be focused on solutions that are genuinely compatible with the objectives and constraints of the case study.

*Table 30 Principal hull characteristics and dimensions derived from the operational requirements*

<b>Parameter</b>	<b>Value</b>	<b>Units</b>
<i>Hull Type</i>	Single Chine	\
<i>Presence of Skeg</i>	Yes	\
<i>Length Overall</i> <i>L<sub>OA</sub></i>	17	m
<i>Beam Overall</i> <i>B<sub>OA</sub></i>	4.2	m
<i>Design Draft</i> <i>T</i>	0.9	m

Table 31 Definition and bounds of the geometric design variables adopted

Variable		Units	Lower Bound	Upper Bound	Step
<i>Chine Fullness Factor</i>	<i>CFF</i>	\	0.35	0.5	0.05
<i>Chine Tangent Factor</i>	<i>TFC</i>	\	0.1	0.2	0.05
<i>Max Chine Position</i>	<i>MAXCP</i>	\	0.45	0.55	0.05
<i>Deadrise Angle at stern</i>	$\vartheta_T$	deg	15	23	1
<i>Deadrise Angle</i>	$\vartheta$	deg	15	25	1
<i>Bow Angle</i>	<i>BA</i>	deg	10	50	1
<i>Coefficient for positioning point P5 of Center Line</i>	<i>CI</i>	\	0.4	0.6	0.05
<i>Coefficient</i>	<i>CTPR</i>	\	0	0.5	0.05
<i>Coefficient</i>	<i>CTPP</i>	\	0.3	0.8	0.05
<i>Max Beam Position</i>	<i>PB<sub>MAX</sub></i>	\	0.62	0.7	0.01
<i>Bow Fullness Factor</i>	<i>BFF</i>	\	0.5	0.7	0.05

#### 4.2. Resistance, Propulsive selection and System Integration

The selection of the design speed represents a fundamental step in translating the operational requirements into technical specifications for the vessel considered in the case study. In the context of the Gulf of Trieste, this parameter cannot be treated as a free variable, since coastal navigation is governed by a complex set of ordinances and regulations issued by the Trieste Harbour Master’s Office. These measures are aimed at ensuring navigational safety, limiting wake generation, and managing maritime traffic in the vicinity of urban and bathing areas. Regulations applicable to coastal waters, port areas, and environmentally sensitive zones impose reduced speed limits—often in the range of 3 to 5 kn—near landing points, beaches, and areas characterised by a high density of small craft [98]. Although these limits do not define a single uniform value across the entire Gulf, they establish a regulatory framework that effectively constrains the average sustainable speed along most coastal routes.

Within this framework, existing maritime services, such as those operated by Delfino Verde Navigazione, consistently adopt a typical operational speed of approximately 10 knots. This value represents a widely recognised compromise between safety, efficiency, and service continuity. It does not stem from a single regulatory requirement, but rather from the combined effect of three key factors. First, a speed of 10 kn ensures the containment of wave generation, which is essential to avoid interference with the stability of small craft operating along the coast and to prevent damage to lightweight infrastructure such as floating pontoons and leisure moorings. Second, routes within the Gulf develop close to the shoreline and cross areas with high maritime traffic density, where existing ordinances effectively enforce moderate navigation regimes. Finally, the hydrodynamic characteristics of the displacement vessels employed in the service—hulls without planing capability—make 10 knots an optimal balance from an energetic and performance perspective, avoiding disproportionate increases in resistance and fuel consumption.

Given its prescriptive nature and its central role in the sizing of the propulsion system, the design speed of 10 knots is therefore treated as one of the fundamental inputs of the case study, providing a key operational anchor around which the entire parametrisation of performance and energy consumption is developed.

Hydrodynamic resistance is estimated using the Simple Mathematical Model proposed by Radojčić *et al.* (Figure 47) [88], which is based on two dimensionless parameters: the slenderness ratio and the volume Froude number.

The model expresses the dimensionless resistance ratio as

$$\frac{R}{\Delta} = A \left( \frac{L}{V^{\frac{1}{3}}} \right) Fn_V^3 + B \left( \frac{L}{V^{\frac{1}{3}}} \right) Fn_V^2 + C \left( \frac{L}{V^{\frac{1}{3}}} \right) Fn_V + D \left( \frac{L}{V^{\frac{1}{3}}} \right)$$

from which the absolute resistance is obtained as

$$R_{hull} = \Delta \left( \frac{R}{\Delta} \right)$$

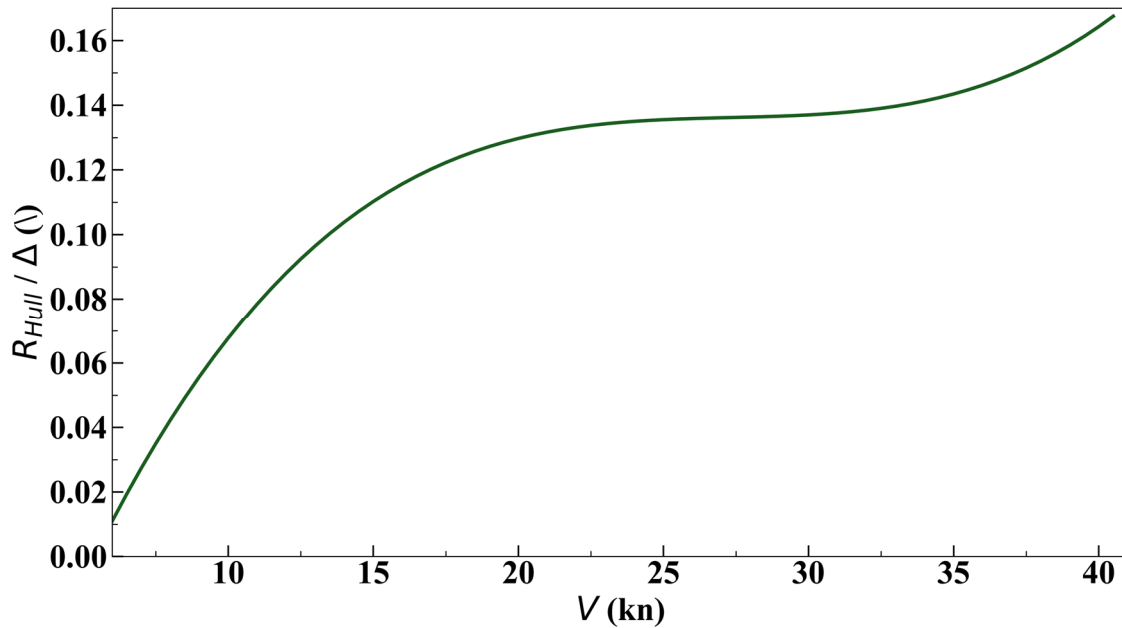


Figure 47 Speed–resistance curve of the reference hull configuration obtained through the Simple Mathematical Model [87]

Once the total resistance at the design speed of 10 kn has been calculated, it is converted into the thrust required at the propeller by applying the thrust deduction factor  $t$ , assumed from the literature for the adopted hull typology [99]. The resulting thrust is then processed within the propulsion-sizing module of the parametric workflow. Within this framework, cavitation-based criteria are used to define an admissible propeller diameter range, which is subsequently verified against the geometric installation constraints imposed by the hull. In particular, the propeller disk is required to remain fully above the keel line, and a minimum tip clearance equal to 15% of the propeller diameter with respect to the hull surface is enforced.

After determining a compatible diameter, and fixing the number of blades to  $Z = 4$  and the expanded area ratio  $EAR = 0.75$  — values typical for passenger vessels in this class, according to manufacturer guidelines provided by Eliche Radice Spa ([www.elicheradice.it](http://www.elicheradice.it)) — the propeller design is completed using data from the Wageningen B-series systematic propeller databases [100]. From these, the optimal rotational speed and the open-water efficiency  $\eta_0$  are derived. These parameters close the link between resistance and propulsion, enabling the determination of shaft power and the corresponding operating point of the traction motor within the series hybrid propulsion system.

In full consistency with the objectives of the case study, requirements related to Zero-Emission Mode (ZEM) autonomy—derived from propulsive power demand and onboard hotel loads—as well as the maximum speed in ZEM, set in this case to 8 knots, the capacity of the two fuel tanks, and the capacities of the freshwater and blackwater tanks, are treated as fixed design inputs. These parameters (Table 32) stem directly from the operator’s operational requirements and are not varied during the parametric exploration. What does vary, instead, is their volumetric allocation onboard, which changes according to the different geometric configurations generated by the parametric model and the selected propulsion system combinations. Similarly, the position of watertight bulkheads is not considered a fixed parameter: it may vary across the different configurations generated by the parametric model. As a consequence, the size and geometry of the engine room become a direct function of the applicable regulations. This aspect is examined in greater detail in the section dedicated to the 3D general arrangement and in the subsequent discussion on structural design.

The selection of electric motors, generator sets, and energy storage systems therefore remains variable, as it depends on the required power profile and on the solutions effectively available within the commercial component database (Table 33).

Alternative feasible engine room configurations adopted in the parametric design model are shown in Figure 48.

Table 32 Main operational and propulsion system parameters adopted in the study, including shipowner requirements

Parameter		Units	Value	Notes
<i>Design Speed</i>	$V_D$	kn	10	Shipowner requirement
<i>Max ZEM Speed</i>	$V_{ZEM}$	kn	8	Shipowner requirement
<i>Autonomy Requirement in ZEM</i>		h	3	Shipowner requirement
<i>Number of propellers</i>	$n_P$	\	2	
<i>Number of Blades</i>	$Z$	\	4	
<i>Expanded Area Ratio</i>	$EAR$	\	0.75	
<i>System Configuration</i>		\	Hybrid serial	
<i>Fuel Tank Capacity</i>		1	2 x 400	Shipowner requirement
<i>Fresh Water Tank Capacity</i>		1	1 x 200	Shipowner requirement
<i>Black Water Tank Capacity</i>		1	1 x 300	

Table 33 Discrete propulsion and energy system variables adopted in the parametric model

Variable	Value	Step
<i>Electric Motor</i>	From database	Discrete
<i>Generator Set</i>	From database	Discrete
<i>Battery System (number &amp; capacity)</i>	From database	Discrete
<i>3D Engine Room Arrangement</i>	Geometry dependent	

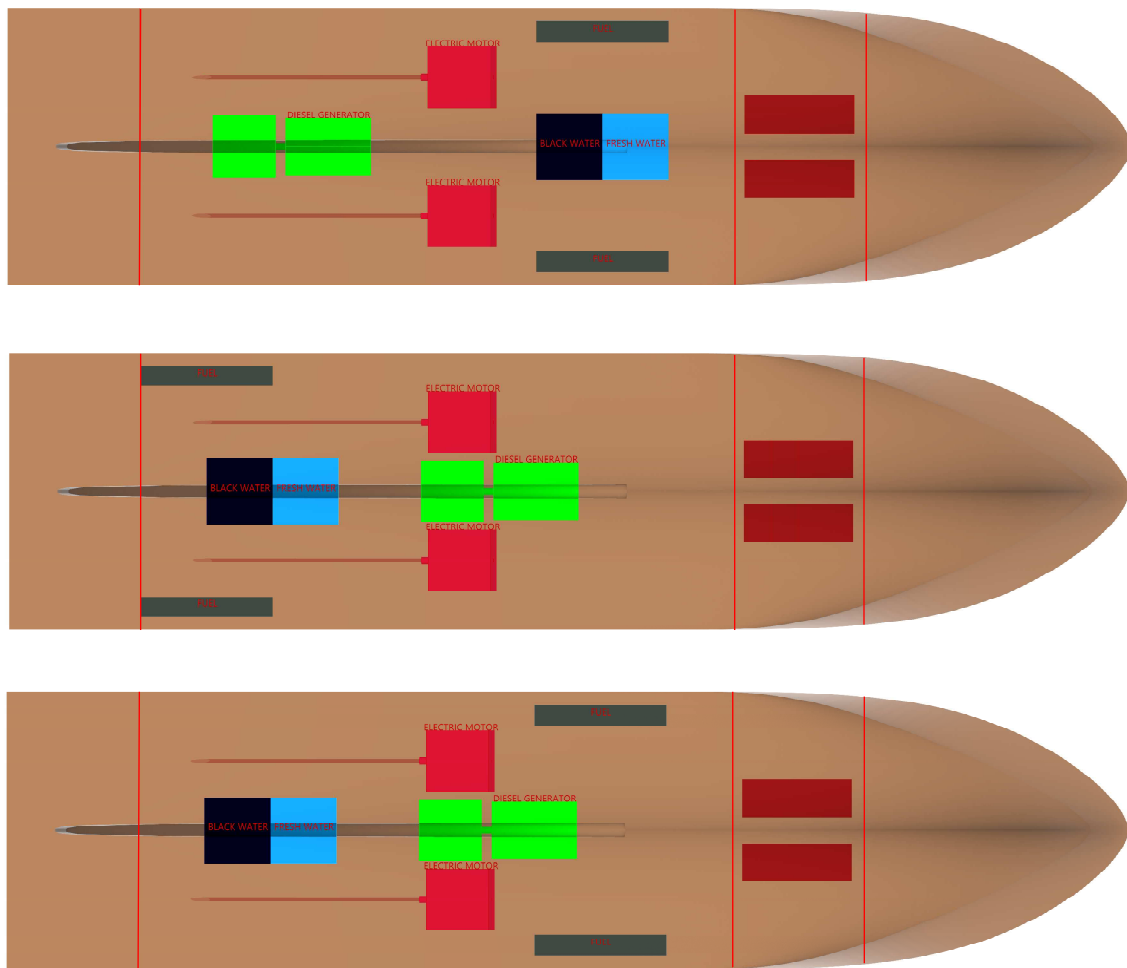


Figure 48 Feasible alternative configurations of the engine room adopted in the parametric design model

### 4.3. 3D General Arrangement Plan and Structures

The generation of three-dimensional general arrangement plans enables the exploration of a wide design domain, while ensuring compliance with the constraints imposed by the RINA Rules, by the Italian national regulatory framework governing passenger vessels engaged in coastal navigation—specifically Presidential Decree DPR 435/91 [90], which defines safety, accommodation, and operational requirements for ships—and by the operational requirements associated with the coastal navigation service in the Gulf of Trieste.

The vessel is configured as a passenger ship with a single operational deck (main deck), positioned at a fixed height of 1 m above the design waterline. This value is treated as a non-parametric input and is defined in accordance with safety, accessibility, and wheelhouse visibility requirements. The main deck therefore represents the geometric reference plane around which the entire functional layout is developed. Passenger spaces, embarkation and

disembarkation areas, the wheelhouse, and the technical volumes compatible with the vessel typology are all arranged on this deck.

#### *4.3.1. Integration of the Primary Structure and Dimensional Constraints*

In accordance with the methodology previously defined, the modelling of the primary structure adopts a longitudinal structural scheme. The elements of the structural grid are generated algorithmically based on the following criteria derived from Chapter 4:

- constant spacing of transverse frames equal to 500 mm;
- definition of reinforced frames at every 2 frame spacings;
- spacing of ordinary longitudinal stiffeners equal to 350 mm;
- definition of reinforced longitudinal girders at every 2 longitudinal stiffener spacings;
- placement of bulkheads exclusively at reinforced frame locations, ensuring structural continuity.

The only bulkhead subject to non-modifiable regulatory constraints is the collision bulkhead, whose position is parameterised but limited to the interval prescribed by the RINA Rules for passenger vessels of the same category [91]. All remaining bulkheads are treated as discrete variables and may translate longitudinally, since the vessel—designed for national coastal navigation and with a capacity of fewer than 150 passengers—is not subject to damaged stability verification requirements under DPR 435/91 [90]. The parametric freedom in bulkhead arrangement allows the evaluation of multiple compartmentation solutions, while consistently preserving coherence with the structural hierarchy defined in the methodology.

It is worth noting that, in accordance with the adopted methodology and with the RINA Rules for ships with aluminium alloy hulls [84], the structural scantlings and the sizing of primary and secondary structural members are defined once and kept constant throughout all the design alternatives generated within the DoE framework. This choice is motivated by the fact that the main dimensions of the vessel,  $L_{OA}$ ,  $B_{OA}$  and  $T$  are kept unchanged across all configurations. Consequently, the parametric variations explored in the case study exclusively affect the arrangement and longitudinal positioning of bulkheads, without

altering the structural dimensioning, which remains compliant with the applicable classification requirements for aluminium hulls.

It is important to clarify that, within the scope of the present methodology, the structural model is not intended to pursue a strict minimisation of structural weight. For passenger vessels operating in coastal liner services, current design practice often favours structurally conservative solutions, deliberately prioritising durability, robustness and damage tolerance over extreme lightweight optimisation. Oversizing is commonly accepted in order to mitigate long-term issues related to corrosion, local impacts, berthing damage and intensive operational cycles, thereby extending the service life of the vessel and reducing maintenance demands.

In this context, the adoption of rule-based scantlings does not represent a limitation of the method, but rather a deliberate normalisation strategy. By applying the same regulatory assumptions and safety margins consistently across all generated configurations, the parametric model enables a coherent comparison between alternative layouts and structural arrangements at the preliminary design stage. While different configurations may appear structurally equivalent within this framework, potential divergences in weight or local optimisation would only emerge through detailed structural refinement, which lies beyond the scope of the present phase.

The proposed methodology therefore focuses on the comparative assessment of design alternatives under a homogeneous, regulation-compliant structural baseline, while detailed weight optimisation is intentionally deferred to subsequent design stages, once a reduced set of promising configurations has been identified.

#### *4.3.2. Parametric Determination of Passenger Capacity*

Passenger capacity is determined by applying the density coefficient prescribed by DPR 435/91 [90] and recalled in the technical document of the Ministry of Infrastructure and Transport (Determinazione del numero di passeggeri sulle unità da passeggeri - R.D. 20.5.1897, n. 178) [101], equal to 0.65 m<sup>2</sup> per passenger for vessels operating in national coastal navigation.

The usable area of the main deck is calculated by subtracting:

- technical and service volumes;

- the toilet compartment;
- areas excluded due to the absence of passenger circulation paths (e.g. the fore area in certain configurations);
- the wheelhouse volumes.

The resulting maximum theoretical number of passengers is therefore given by:

$$N_{pax} = \frac{A_{usable} (m^2)}{0.65 (m^2/n)} (n)$$

Furthermore, since the voyage duration is shorter than three hours, DPR 435/91 requires that at least 50% of passengers be provided with a seat. Seating arrangements are parameterised according to two alternative configurations, as in Figure 49:

- a linear, bus-type layout;
- an island-based layout, more oriented towards comfort and social interaction.

The ULHS sampling explores both typologies, modifying the spatial distribution and automatically evaluating, for each generated configuration, the corresponding impact on weight, centre of gravity, and stability.

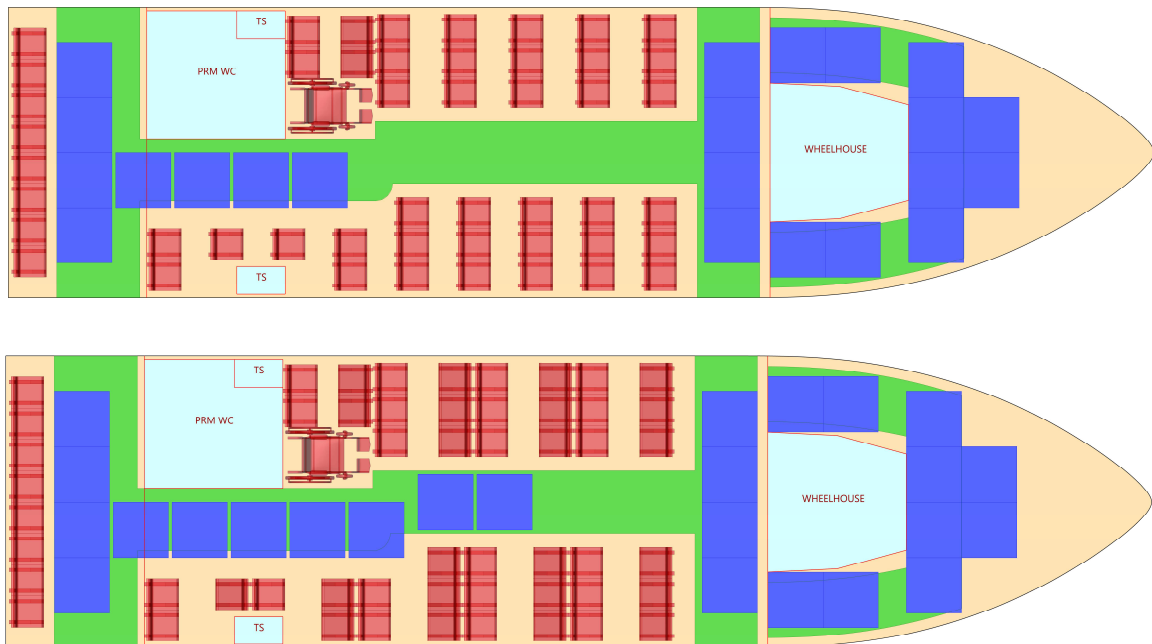


Figure 49 Alternative parametric seating configurations adopted in the case study. Seating in red, standing areas in blue, circulation corridors in green, technical/service spaces in light blue

#### 4.3.3. Parametric Definition of the Main-Deck General Arrangement

The main deck features two principal transverse boundaries. The forward and aft bulkheads of the passenger area are modelled as parametric surfaces that can translate longitudinally (Figure 50). Their position defines the relationship between:

- enclosed internal volume,
- usable external areas located at the bow and stern.

The wheelhouse, parameterised in both shape and volume, is positioned in a raised central location. Its longitudinal extension is constrained by the position of the forward boundary surface, in order to guarantee the prescribed 360° visibility.

The forward external area is intended exclusively for standing passengers; however, if the position of the forward boundary prevents the provision of a compliant circulation path, this area is automatically excluded from the calculation of usable passenger area. The aft external area, by contrast, is modelled to accommodate seated passengers, standing passengers, or a combination of both, depending on the configurations explored.

The internal layout includes a toilet compartment compliant with the requirements for passengers with reduced mobility (PMR), fully parameterised in its dimensions and longitudinal position. Its location, either forward or aft of the enclosed passenger space, also affects the placement of the designated PMR seating position, whose proximity to the toilet represents a design requirement validated by previous ergonomic studies (Figure 51).

The embarkation and disembarkation area, with a regulatory width of 1.20 m, is treated as a discrete variable and may be located either at the bow or at the stern (Figure 52). Its position directly affects the distribution of seating and standing areas on board, with a significant influence on the longitudinal centre of gravity and on the overall usability of the internal spaces.

*At the end of this section, two summary tables are provided to clarify the parametric structure of the model. Table 34 lists the parameters treated as fixed inputs in the case study, while*

Table 35 reports the design variables explored within the parametric framework, together with their respective type of variability.

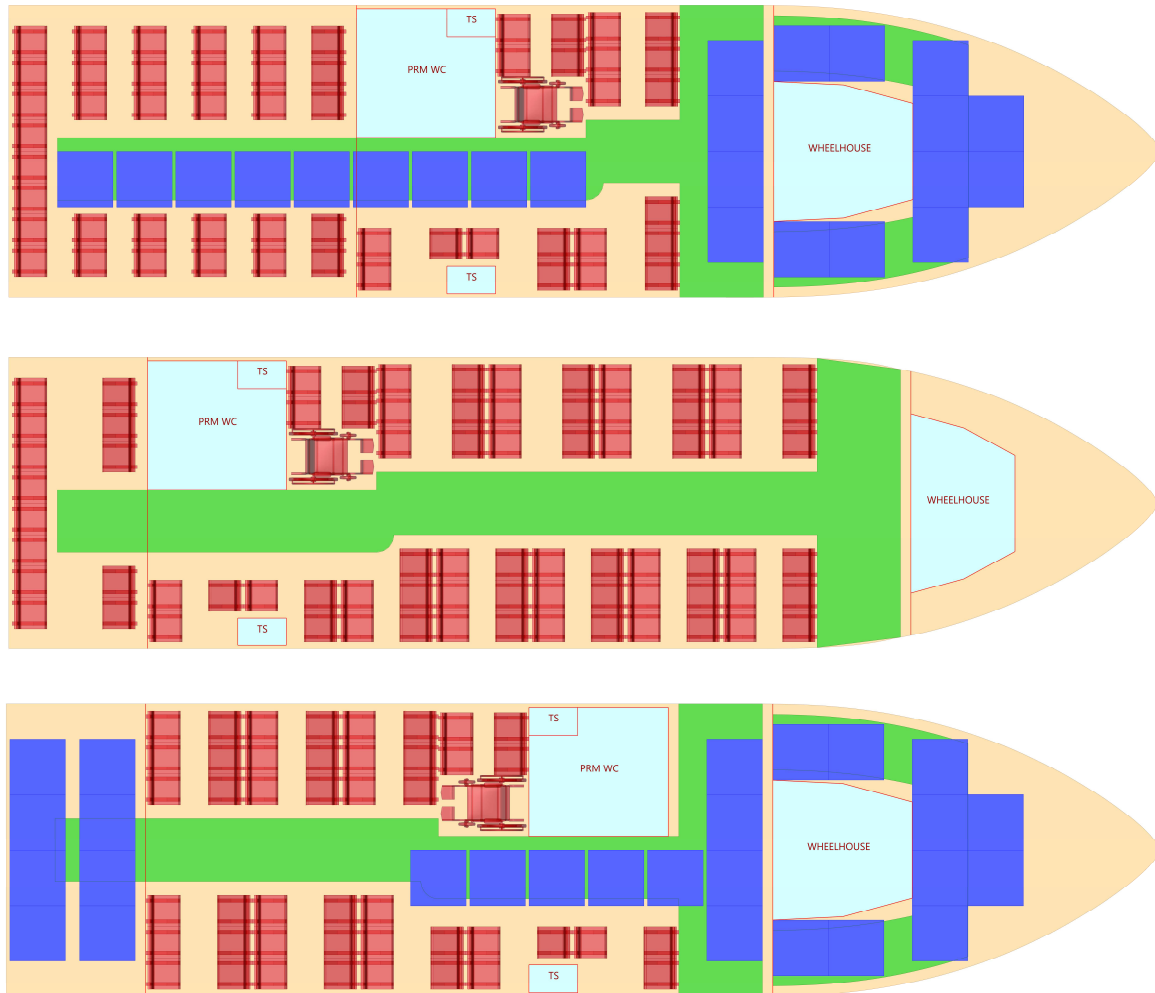


*Figure 50 Effect of the longitudinal positioning of the forward and aft passenger-area bulkheads on the distribution of enclosed internal volume and usable external deck areas. Seating in red, standing areas in blue, circulation corridors in green, technical/service spaces in light blue*



Figure 51 Influence of the longitudinal position of the PMR-compliant toilet compartment on the placement of the associated reserved seating within the passenger area. Seating in red, standing areas in blue, circulation corridors in green, technical/service spaces in light blue

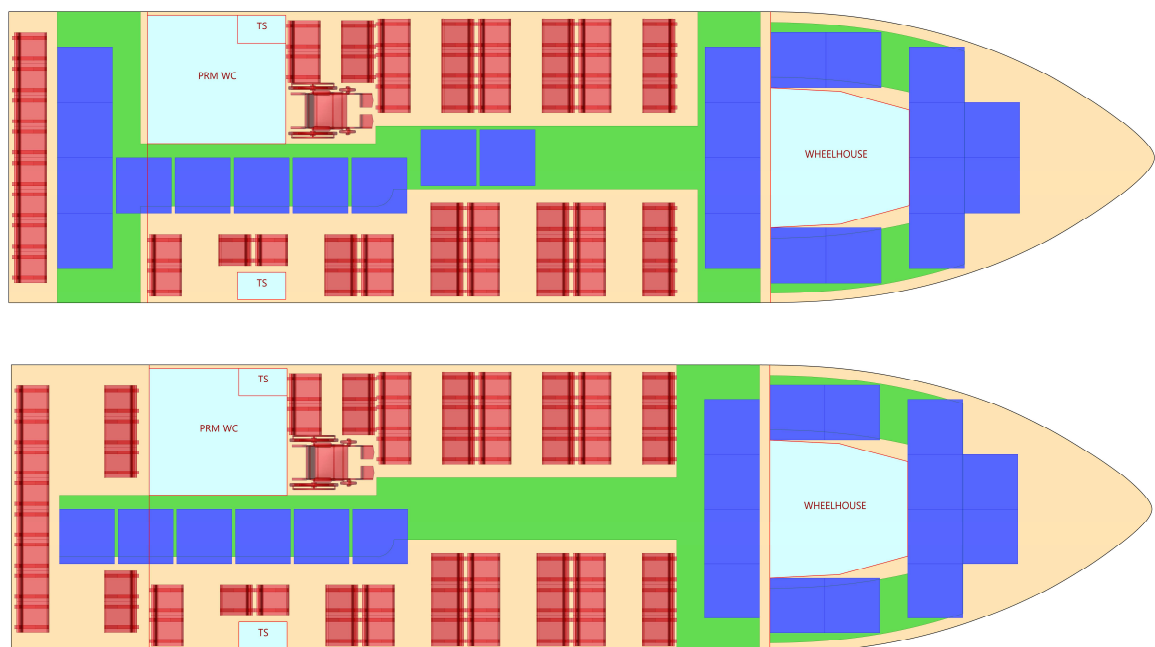


Figure 52 Discrete bow and stern positioning of the embarkation area. Seating in red, standing areas in blue, circulation corridors in green, technical/service spaces in light blue

Table 34 Fixed input parameters adopted in the case study for the definition of the 3D GA

Parameter		Units	Value	Notes
Main Deck Height above DWL	$(D - T)$	m	1	
Number of decks		\	1	
Structural Scheme		\	Longitudinal	
Transverse Frame Spacing	$s$	mm	500	
Passenger Density Coefficient		m <sup>2</sup> /pax	0.65	
Number of Toilets		\	1	
Number of PMR Toilet		\	1	
Area of PMR Toilet		m <sup>2</sup>	3.2	Unobstructed wheelchair turning diameter $\geq 1.50$ m
Number of PMR Reserved Seats		\	1	
Embarkation Width		m	1.2	

Table 35 Design variables considered in the case study

Variable	Value	Step
Longitudinal Position of Bulkheads	Parametric	Discrete
Seating Layout	Linear bus–type / Island configuration	Discrete
PMR Toilet Position	Bow / Stern	Discrete
PMR Reserved Seat Position	Linked to toilet location	Geometry-dependent
Embarkation Area Position	Bow / Stern	Discrete
Longitudinal Position of Forward / Aft Sidewalls	Parametric	Discrete
Wheelhouse Position	Parametric	Linked to forward sidewall position

#### **4.4. Configuration of the base model and description of the outputs**

At the outset of the case-study application, a reference configuration (hereafter referred to as the base model) is defined in order to ensure traceability and coherence throughout the entire design-space exploration process. The base model is generated by assigning initial numerical values to the geometric and functional variables derived from the operational requirements previously described (Table 36), while preserving the parametric structure, constraints, and relationships established in the methodological phase (Table 37).

The base model is geometrically coherent by construction; however, it is not required to satisfy all the feasibility criteria implemented within the integrated verification modules. It therefore does not represent a pre-validated or optimised solution, but rather a consistent and traceable starting point from which the DoE–based exploration of the parametric domain is initiated.

Table 36 Baseline values of the design variables adopted for the reference configuration

Variable		Default Value	Units
<i>Chine Fullness Factor</i>	<i>CFF</i>	0.35	\
<i>Chine Tangent Factor</i>	<i>TFC</i>	0.15	\
<i>Max Chine Position</i>	<i>MAXCP</i>	0.63	\
<i>Deadrise Angle at stern</i>	$\vartheta_T$	20	deg
<i>Deadrise Angle</i>	$\vartheta$	22	deg
<i>Bow Angle</i>	<i>BA</i>	26	deg
<i>Coefficient for positioning point P5 of Centre Line</i>	<i>CI</i>	0.60	\
<i>Coefficient</i>	<i>CTPR</i>	0.25	\
<i>Coefficient</i>	<i>CTPP</i>	0.80	\
<i>Max Beam Position</i>	<i>PB<sub>MAX</sub></i>	0.62	\
<i>Bow Fullness Factor</i>	<i>BFF</i>	0.70	\
<i>Longitudinal Position of Collision Bulkheads</i>		13	m
<i>Longitudinal position of the aft bulkhead of the engine room</i>		2	m
<i>Longitudinal position of the fwd bulkhead of the engine room</i>		11	m
<i>Seating Layout</i>		Island configuration	\
<i>PMR Toilet Position</i>		Stern	\
<i>Embarkation Area Position</i>		Stern	\
<i>Longitudinal Position of Aft Sidewalls</i>		2	m
<i>Longitudinal Position of Forward Sidewalls</i>		11	m

Table 37 Fixed input parameters defining the parametric design domain for the case study

Parameter		Value	Units
<i>Hull Type</i>		Single Chine	\
<i>Presence of Skeg</i>		Yes	\
<i>Length Overall</i>	$L_{OA}$	17	m
<i>Beam Overall</i>	$B_{OA}$	4.2	m
<i>Design Draft</i>	$T$	0.9	m
<i>Design Speed</i>	$V_D$	10	kn
<i>Max ZEM Speed</i>	$V_{ZEM}$	8	kn
<i>Autonomy Requirement in ZEM</i>		3	h
<i>Number of propellers</i>	$n_P$	2	\
<i>Number of Blades</i>	$Z$	4	\
<i>Expanded Area Ratio</i>	$EAR$	0.75	\
<i>Fuel Tank Capacity</i>		2 x 400	l
<i>Fresh Water Tank Capacity</i>		1 x 200	l
<i>Black Water Tank Capacity</i>		1 x 300	l
<i>Main Deck Height above DWL</i>	$(D - T)$	1	m
<i>Number of decks</i>		1	\
<i>Transverse Frame Spacing</i>	$s$	500	mm
<i>Passenger Density Coefficient</i>		0.65	m <sup>2</sup> /pax
<i>Number of Toilets</i>		1	\
<i>Number of PMR Toilet</i>		1	\
<i>Area of PMR Toilet</i>		3.2	m <sup>2</sup>
<i>Number of PMR Reserved Seats</i>		1	\
<i>Embarkation Width</i>		1.2	m

The baseline model provides a complete set of outputs organised according to the main design domains considered in the case study. The geometric definition includes the three-dimensional model of the entire design (Figure 53) and the automatic extraction of the construction drawings (Figure 54). The hydrostatic results are reported in Table 38.

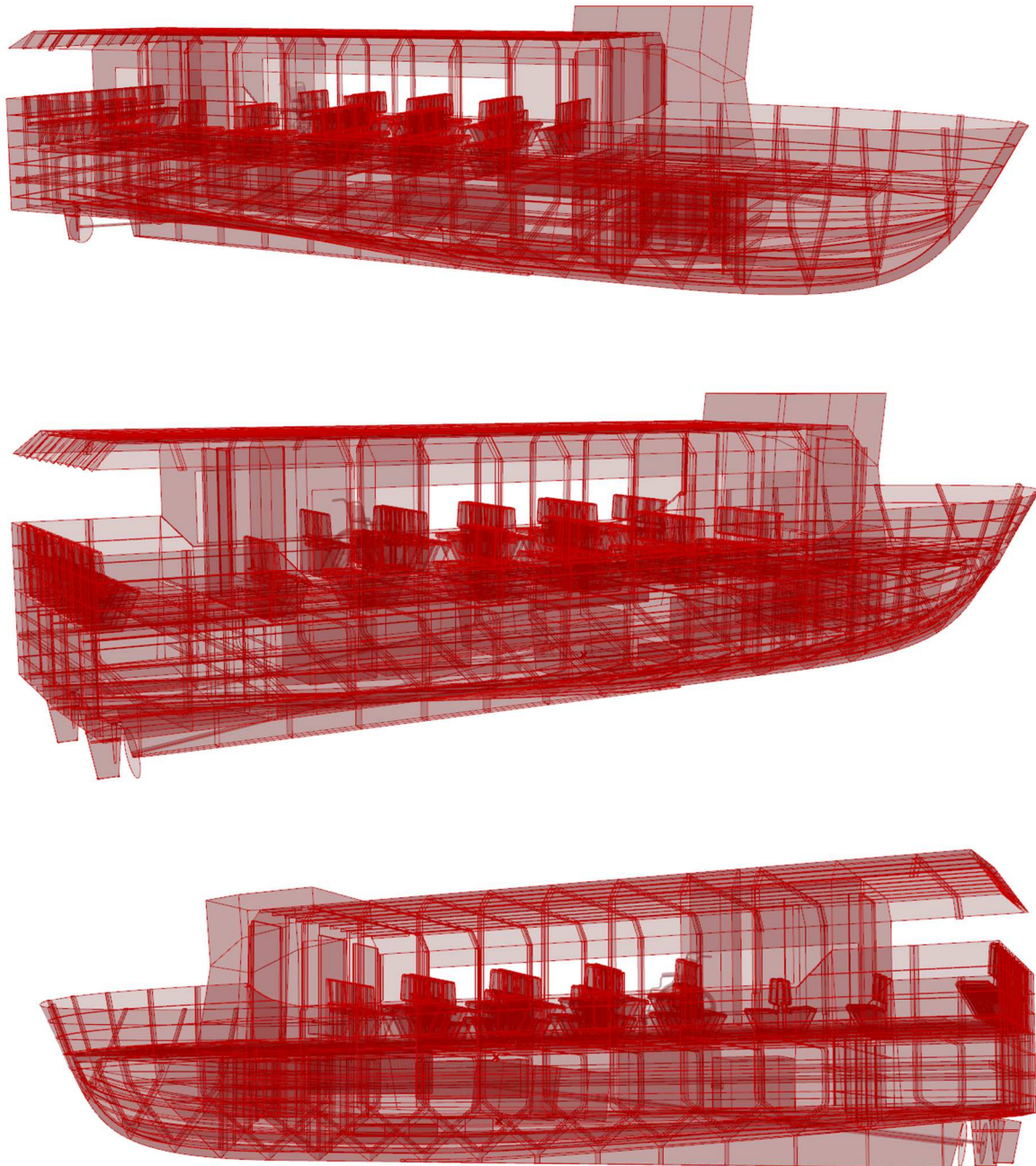


*Figure 53 3D model of the entire design*

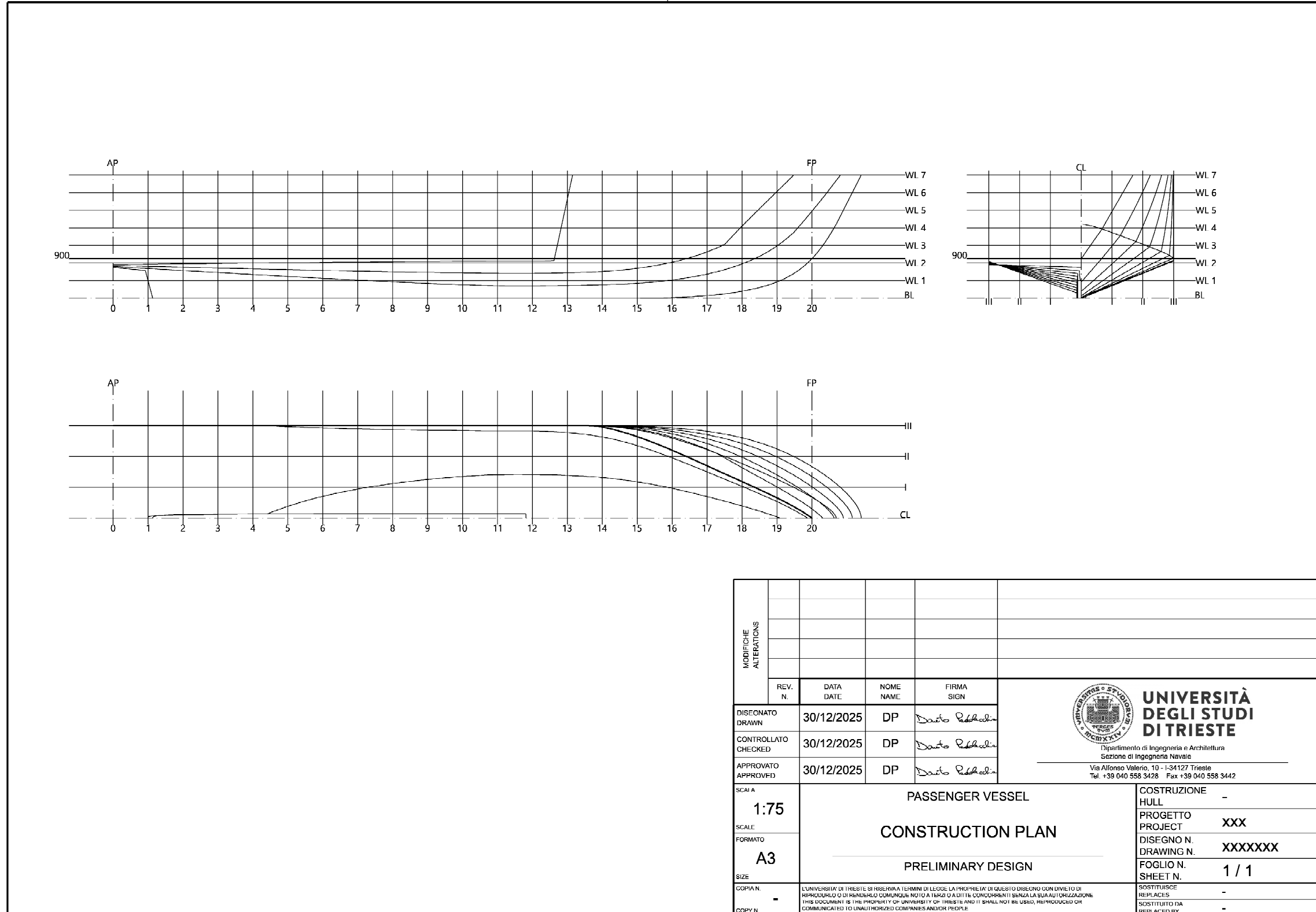


Figure 54 Construction Plan of the base model

Table 38 Summary of the main hydrostatic characteristics computed for the base model

<b>Parameter</b>	<b>Symbol</b>	<b>Unit</b>	<b>Value</b>
<i>Draft</i>	<i>T</i>	(m)	0,90
<i>Volume</i>	$\nabla$	(m <sup>3</sup> )	22,07
<i>Displacement</i>	$\Delta$	(t)	22,62
<i>Length Overall</i>	<i>L<sub>OA</sub></i>	(m)	17,00
<i>Beam Overall</i>	<i>B<sub>OA</sub></i>	(m)	4,20
<i>Waterline Length</i>	<i>L<sub>WL</sub></i>	(m)	15,88
<i>Waterline Beam</i>	<i>B<sub>WL</sub></i>	(m)	4,20
<i>Wetted Surface Area</i>	<i>WSA</i>	(m <sup>2</sup> )	127,12
<i>Waterplane Area</i>	<i>WPA</i>	(m <sup>2</sup> )	57,69
<i>Block Coefficient</i>	<i>C<sub>B</sub></i>	(\)	0,37
<i>Waterplane Area Coefficient</i>	<i>C<sub>WP</sub></i>	(\)	0,87
<i>Longitudinal Centre of Buoyancy</i>	<i>LCB</i>	(m)	7,65
<i>Vertical Centre of Buoyancy</i>	<i>KB</i>	(m)	0,64
<i>Longitudinal Centre of Flotation</i>	<i>LCF</i>	(m)	6,94
<i>LCB as Percentage of L<sub>WL</sub></i>	<i>LCB %</i>	(%)	48,21
<i>LCF as Percentage of L<sub>WL</sub></i>	<i>LCF %</i>	(%)	43,69
<i>Transverse Metacentric Radius</i>	<i>BM<sub>t</sub></i>	(m)	3,51
<i>Longitudinal Metacentric Radius</i>	<i>BM<sub>l</sub></i>	(m)	43,50
<i>Full-load displacement</i>	<i>W</i>	(t)	22.61
<i>Longitudinal centre of gravity</i>	<i>LCG</i>	(m)	7.58
<i>Vertical centre of gravity</i>	<i>KG</i>	(m)	1.96
<i>Transverse centre of gravity</i>	<i>TCG</i>	(m)	0.01
<i>Transverse metacentric radius</i>	<i>GM<sub>t</sub></i>	(m)	2.19
<i>Longitudinal metacentric radius</i>	<i>GM<sub>l</sub></i>	(m)	42.18

<i>Aft draught</i>	$T_A$	(m)	0.91
<i>Forward draught</i>	$T_F$	(m)	0.89

With regard to propulsive performance, the model provides the resistance curve (Figure 55) over the entire operational speed range (Table 39), an estimate of the design power (Figure 56), and a preliminary configuration of the adopted propulsion system (Figure 57). In particular, the main characteristics of the propeller and the operating parameters of the series-hybrid propulsion system are defined, together with an initial sizing of its components consistent with the assumed operational profile (Table 40, Table 41, Table 42, Table 43 and Table 44).

Table 39 Variation of resistance, effective power, and brake power with vessel speed; ZEM operating speed in green, Design speed in yellow

V (kn)	V (m/s)	$F_n$ (t)	$F_{nV}$ (t)	$R_T$ (kN)	$R_T$ with SM (10%) (kN)	$P_E$ (kW)	$P_B$ (kW)
6	3.09	0.25	0.59	2.75	3.02	8.48	19.36
7	3.60	0.29	0.69	6.49	7.14	23.38	53.39
8	4.12	0.33	0.78	9.91	10.91	40.80	93.18
9	4.63	0.37	0.88	13.03	14.33	60.32	137.76
10	5.14	0.41	0.98	15.85	17.44	81.55	186.25
11	5.66	0.45	1.08	18.40	20.24	104.14	237.82
12	6.17	0.49	1.18	20.69	22.76	127.75	291.74
13	6.69	0.54	1.27	22.74	25.02	152.10	347.36
14	7.20	0.58	1.37	24.57	27.02	176.94	404.09

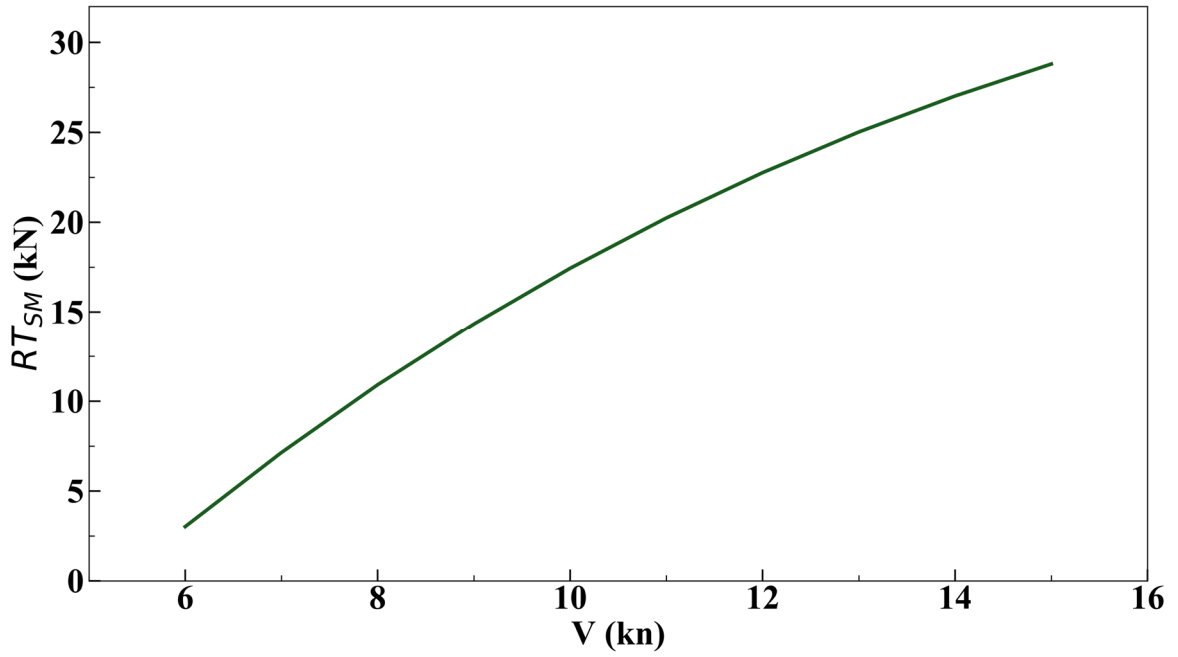


Figure 55 Speed–resistance curve

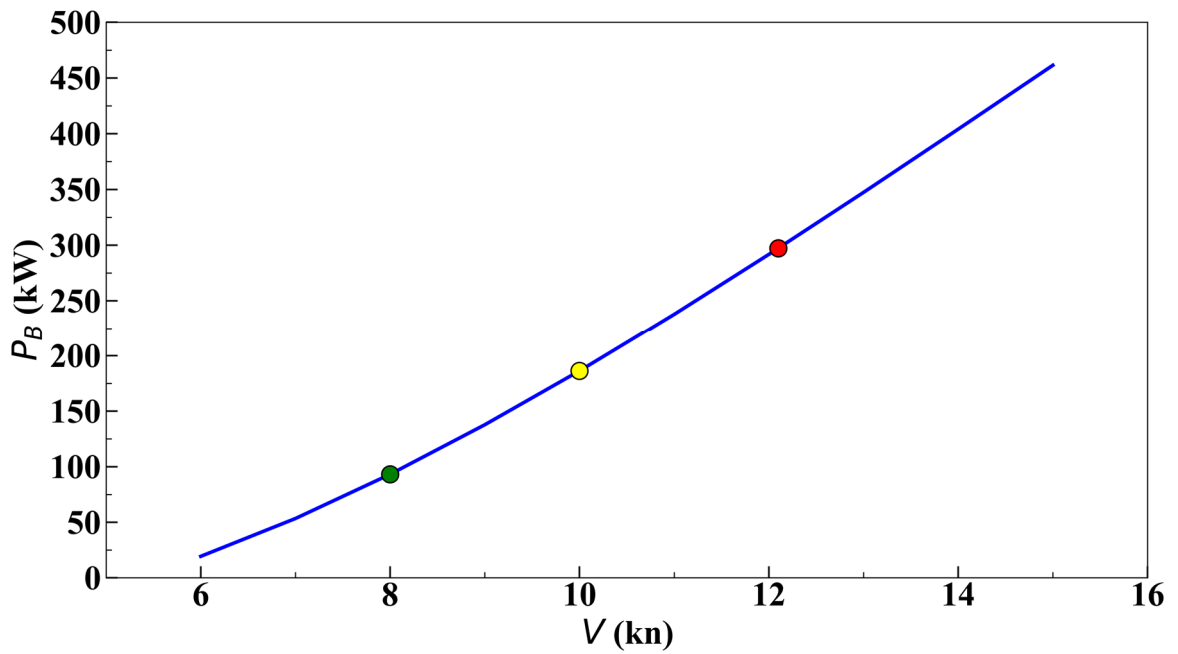


Figure 56 Speed–power relationship, with markers indicating ZEM speed (green), design speed (yellow), maximum speed limited by the installed electric propulsion power (red)

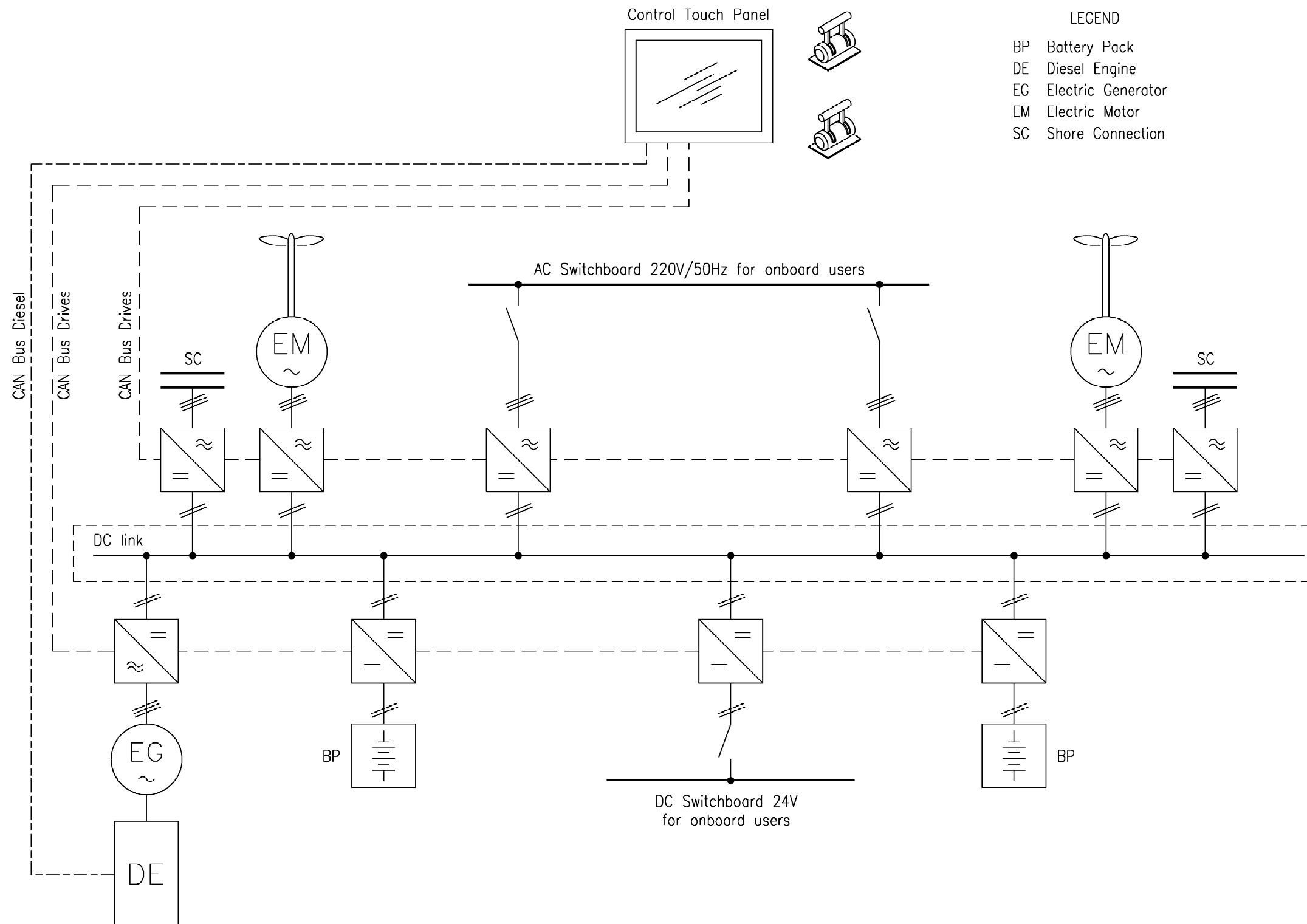


Figure 57 Integrated Power System (IPS)

Table 40 Main characteristics of the selected propulsion motors

Manufacturer and model	Quantity	Rated power (kW)	Total power (kW)
<i>Tema SLPM</i>	2	150	300

Table 41 Main characteristics of the selected diesel-generator

Manufacturer and model	Quantity	Rated power (kW)	Total power (kW)
<i>FPT Cursor 450 kW - Tema</i>	1	450	450

Table 42 Main characteristics of the selected battery Energy Storage System (ESS)

Manufacturer and model	Quantity	Single module energy capacity (kWh)	Total energy capacity (kWh)
<i>Lehman Marine</i>	32	12,5	400

Table 43 Propeller Configuration

Parameter	Symbol	Units	Value
<i>Propeller diameter</i>	$D_{PROP}$	(m)	0.59
<i>Rotational speed</i>	$n$	(rpm)	1122
<i>Number of blades</i>	$Z$	(\)	4
<i>Expanded area ratio</i>	$EAR$	(\)	0.75
<i>Open-water efficiency</i>	$\eta_0$	(\)	0.502

Table 44 Power demand and endurance in Zero Emission Mode at the reference operating condition

Parameter	Units	Value
Battery power demand at 8 kn in ZEM	(kW)	97.06
Hotel and auxiliary loads	(kW)	3.88
Total power demand	(kW)	100.94
Endurance at 8 kn in ZEM	h	03:57:45

In parallel, the GA is generated automatically (Figure 58), returning the functional layout of the main deck and the distribution of technical volumes and the principal onboard spaces (Table 45 and Table 46). In parallel, the anchoring arrangement is defined in Table 47.

Within this context, the baseline model serves as the control configuration of the case study, demonstrating the capability of the applied process to generate a complete, coherent and technically verified solution, suitable for representing in a meaningful manner the vessel under investigation.

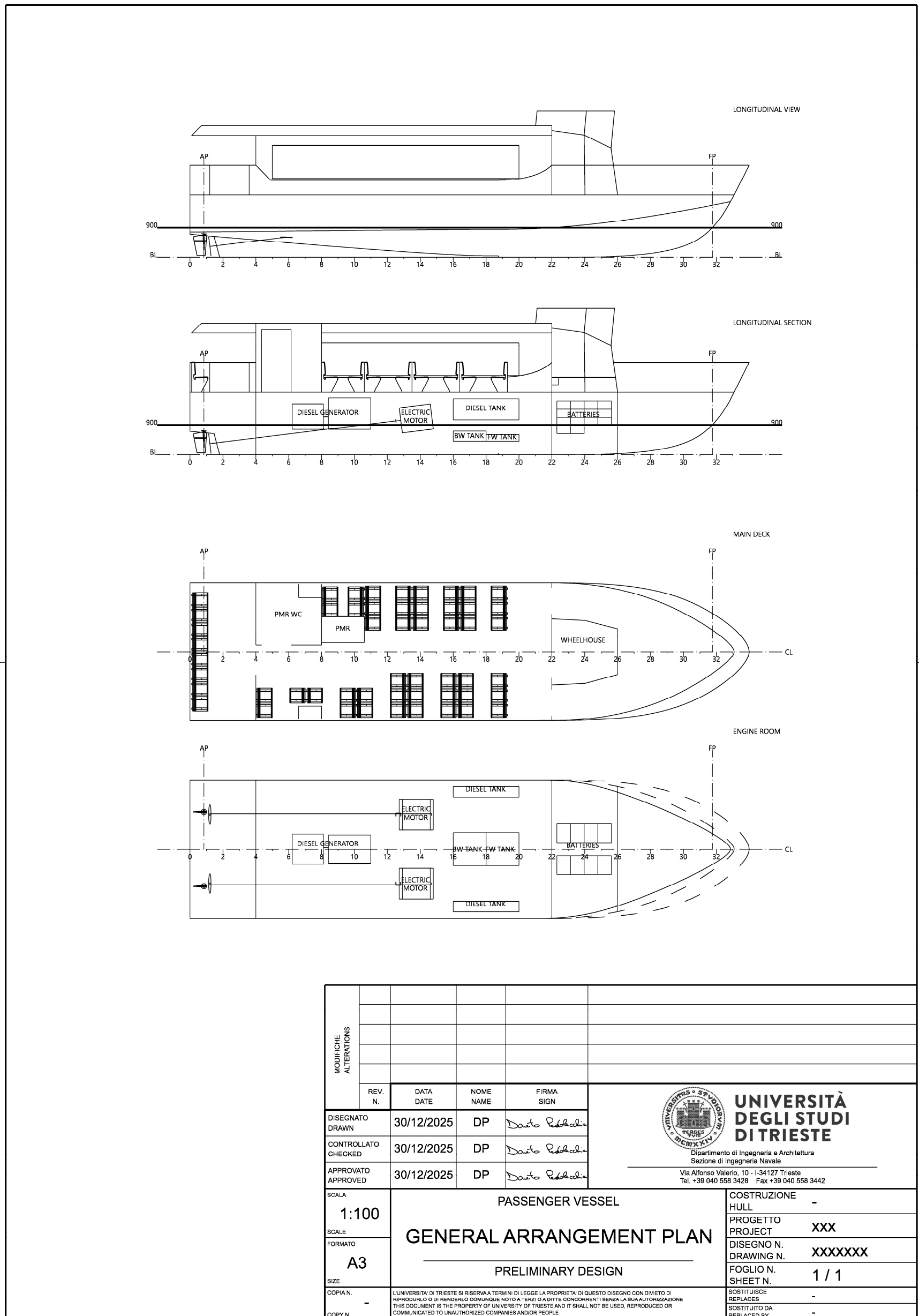


Figure 58 2D GA plans

Table 45 Lightship weight estimate and centres of gravity adopted within the parametric design model

<b>Item</b>	<b>Weight W (t)</b>	<b>LCG (m)</b>	<b>TCG (m)</b>	<b>KG (m)</b>
<i>Structures</i>	7.04	7.21	0.01	1.94
<i>Superstructures</i>				
<i>Outfit</i>	0.27	5.64	0.01	3.70
<i>Glasses</i>	0.67	7.81	0	3.21
<i>Anchor and Chains</i>	0.37	16.55	0	1.90
<i>Main Deck Floor</i>	0.09	7.54	0	1.90
<i>Seats</i>	0.55	5.69	-0.01	2.21
<i>Tanks (Structure)</i>	0.57	8.99	0	1.03
<i>Rudders</i>	0.08	0.30	0	0.39
<i>Propellers</i>	0.10	0.60	0	0.33
<i>WC</i>	0.33	3.00	1.125	1.90
<i>Wheelhouse</i>	0.43	11.98	0	2.35
<i>Safety equipment</i>	0.22	0	0	1.90
<i>Propulsion</i>	4.99	9.42	0	1.22
<b><i>Lightship Total</i></b>	<b>15.80</b>	<b>8.00</b>	<b>0.03</b>	<b>1.76</b>

Table 46 Full-load weight breakdown and centres of gravity

Item	Quantity	Unit Weight (t) / Equivalent Value (l)	Total Weight W (t)	LCG (m)	TCG (m)	KG (m)
<i>Passengers</i>	79	75	5.93	6.53	-0.04	2.63
<i>Port Fuel Tank</i>	1	400	0.34	9.00	1.74	1.38
<i>Starboard Fuel Tank</i>	1	400	0.34	9.00	-1.74	1.38
<i>Fresh Water Tank</i>	1	200	0.20	9.50	0	0.50
<i>Black Water Tank</i>	1	30.612	0.03	8.50	0	0.41
<i>Lightship Total</i>	\	\	15.80	8.00	0.03	1.76
<i>Departure Full-Load Total</i>	\	\	22.61	7.66	0.01	1.96

Table 47 Equipment number and anchoring arrangement parameters

Parameter	Symbol	Units	Value
<i>Equipment number</i>	<i>EN</i>	\	45.50
<i>Number of anchors</i>		\	1
<i>Anchor mass</i>		(kg)	64
<i>Minimum chain length</i>		(m)	82.5
<i>Chain length</i>		(m)	100

#### 4.5. Generation of design variants through Design of Experiments

At the conclusion of the case study, the baseline model and the set of design variables were systematically varied through the integration of the parametric model with the exploration and optimisation software modeFRONTIER. The experimental plan (Figure 59) was configured to produce 10,001 design variants, each of which activated the entire chain of generation, verification and evaluation described in this chapter.

Each configuration was then automatically subjected to checks of geometric feasibility, trim, stability and regulatory compliance, enabling an initial selection of technically admissible solutions.

The following chapter will be devoted to the analysis of the results obtained, to the quantification of the configurations found to be feasible, and to a critical discussion of the emerging trends, with the aim of drawing final considerations on the behaviour of the parametric system and on the effectiveness of the proposed methodology.

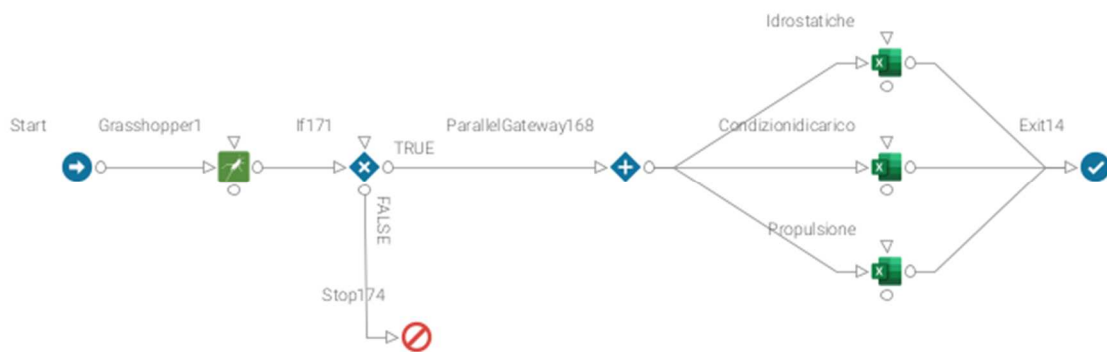


Figure 59 modeFRONTIER workflow and experimental plan

#### 4.6. Feasibility Checks and Regulatory Compliance

In the present case study, each automatically generated configuration was subjected to a set of feasibility checks aimed at ensuring compliance with the main technical and regulatory requirements applicable to passenger vessels operating in national coastal navigation. These checks were employed as preliminary filters to retain only technically admissible solutions within the set of explored configurations.

The first check concerns passenger carrying capacity, requiring that the number of available seats be at least equal to 50% of the total number of embarked passengers, in accordance with the provisions of DPR 435/91 for vessels with voyage durations shorter than three hours. Configurations that do not satisfy this requirement are automatically excluded.

Subsequently, the hydrostatic equilibrium condition is verified by requiring that the total weight of the vessel lies within the admissible interval between 98% of the available buoyancy and the buoyancy itself. This lower margin was introduced to ensure a displacement reserve for subsequent design stages, during which structural and outfit

weights will be defined with greater accuracy. Conversely, configurations that already exhibit a total weight exceeding the available buoyancy at this preliminary stage are discarded, as they lack sufficient development margins.

The longitudinal position of the centre of gravity (*LCG*) is then evaluated with respect to the longitudinal centre of buoyancy (*LCB*), by defining admissible ranges depending on the induced trim condition. For configurations resulting in stern trim, the allowable range limits the trim angle to values below 1°. For configurations leading to bow trim, a more restrictive criterion is applied, limiting the trim angle to approximately 0.5°, or to lower values when the relative shift between *LCG* and *LCB* could result in propeller emergence under any loading condition. These criteria ensure an acceptable attitude already at the preliminary design stage and preserve adequate safety margins for subsequent phases of development.

Once the trim condition has been verified, each configuration is assessed for intact stability in accordance with the criteria set out in the RINA Rules for Passenger Ships [91], [95]. In addition, a passenger crowding heel check is applied, requiring that the heel angle does not exceed the value corresponding to a residual freeboard of 0.10 m prior to deck immersion, or 12°, whichever is more restrictive. The assessment assumes a passenger weight of 75 kg, a centre of gravity located 1 m above deck level for standing passengers and 0.3 m above the seat for seated passengers, as well as a maximum density of 4 persons/m<sup>2</sup> in accessible areas.

Only configurations that simultaneously satisfy the requirements related to passenger capacity, hydrostatic equilibrium, intact stability and crowding heel are considered admissible and retained as technically suitable solutions for subsequent analyses within the case study.

## Chapter 5

### Results and Discussion

This chapter is devoted to the analysis and discussion of the results obtained from the application of the developed parametric methodology described in the preceding chapters to the selected case study. In particular, the outcomes of the design space exploration carried out through the integration of the parametric model with the software modeFRONTIER are examined, with the aim of assessing the combined impact of geometric, hydrostatic, propulsive, and regulatory variables on the overall feasibility of the generated configurations.

The exploration of the solution space was performed through a Uniform Latin Hypercube Sampling (ULHS), configured to generate 10,001 design configurations. Each configuration activated the entire computational chain implemented within the pipeline, including hull geometry generation, hydrostatic evaluation, trim and stability checks, compliance with regulatory requirements, and a preliminary assessment of propulsive performance. The DoE was executed in batch mode, allowing both feasible and unfeasible configurations to be evaluated and enabling a comprehensive mapping of the explored design domain.

At the end of the computational process, which required approximately 85 hours of total computation time, the set of generated configurations was classified according to the outcome of the feasibility checks. Out of the 10,001 designs evaluated, 531 configurations were found to be technically admissible (Appendix II), while the remaining ones failed to satisfy one or more of the constraints imposed by the tool as discussed in greater detail in Chapter 3. This distribution, summarised in Table 48 and Figure 60, highlights that only a limited fraction of the explored design space is compatible with the adopted set of geometric, functional, and regulatory constraints.

Table 48 Overview of feasible and unfeasible configurations within the explored design space

<b>Design Category</b>	<b>Number of Designs</b>	<b>Percentage (%)</b>
<i>Evaluated Designs</i>	10,001	100%
<i>Feasible Designs</i>	531	5.3%
<i>Unfeasible Designs</i>	9470	94.7%

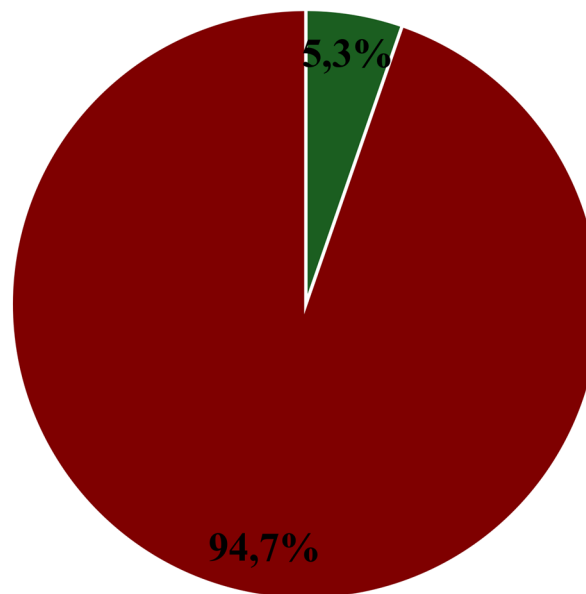


Figure 60 Overview of feasible and unfeasible configurations within the explored design space

Although only 531 configurations (5.31% of the total sample) were found to be technically admissible, this outcome should be interpreted as a meaningful result of the adopted exploratory strategy rather than as an indication of inefficiency. The low acceptance rate reflects the intentionally broad definition of the parametric space and the stringent set of geometric, functional and regulatory constraints embedded in the tool.

From a methodological perspective, the generation and subsequent rejection of a large number of configurations represents a form of aggressive early-stage screening, through which non-realistic or non-compliant solutions are rapidly identified and discarded. This process allows the explored design space to be effectively reduced to a compact and engineering-consistent subset of configurations, which can be directly considered for subsequent decision-making phases.

Within a computation time of approximately 85 hours, the pipeline was therefore able to transform a very large and weakly constrained design domain into a limited set of fully verified and feasible solutions, highlighting the effectiveness of the proposed workflow as a decision-support and filtering tool in the preliminary design context, ready for subsequent multi-criteria evaluations (Multi-Attribute Decision Making, MADM).

In the following sections, the results are analysed in a systematic manner in order to identify the main causes of infeasibility, determine the most influential variables in the selection process, and discuss the recurring features of the admissible configurations. This analysis primarily allows methodological considerations to be drawn regarding the effectiveness of the proposed pipeline and the role of parametric design and DoE techniques as decision-support tools in the preliminary design phases.

These results should also be interpreted in light of the overall time required to develop the parametric model. The learning phase associated with the Grasshopper environment and the development of the computational pipeline, estimated to be on the order of approximately two months, is fully compatible with the timeframes typically associated with preliminary design conducted using traditional approaches, such as the design spiral, provided that a sufficiently structured database is available. This initial time investment may even prove advantageous when approaching the design of this class of vessels for the first time, as it enables a much more rapid exploration of design alternatives in subsequent phases. Once this initial phase has been completed, the methodology can be regarded as reproducible, highly automated, and competitive with respect to currently available tools, particularly in view of the fact that the entire workflow is based exclusively on a Rhinoceros licence, without requiring additional proprietary software.

In light of the above, the contribution of the present research can be interpreted as the definition of an integrated and fully parametric methodology for the preliminary design of passenger vessels. A design office may therefore follow two alternative paths: either independently replicate and adapt the methodology described in this work, or directly employ the developed model by providing the specific design requirements as input. In the latter case, within a matter of hours, it is possible to obtain an extensive set of technically feasible design configurations, which can then be subjected solely to multi-criteria decision-making processes in order to identify the most suitable solution.

### 5.1. Analysis of infeasibility causes and constraint violations

Although the discussion presented in the previous sections focused primarily on the subset of technically feasible configurations, the analysis of the 9,470 inadmissible designs generated during the DoE provides valuable insights into the structure of the explored design space and the effectiveness of the adopted constraints. Rather than being interpreted merely as rejected solutions, these configurations represent an important source of information for identifying the most restrictive criteria and refining the parametric ranges for future design explorations.

A detailed examination of the causes of infeasibility revealed that only a limited portion of the discarded configurations failed due to regulatory or owner-imposed operational requirements, while the majority were filtered out by global equilibrium conditions linking geometry, displacement, and propulsion performance.

A first category of constraint violations concerns passenger arrangement rules derived from the selected operational profile. A very limited number of the inadmissible configurations failed to satisfy the requirement imposing a minimum proportion of seated passengers with respect to standing passengers. According to the adopted regulatory framework for short-range littoral navigation, characterised by travel times below three hours, the number of seated passengers must be at least equal to 50% of the standing passenger capacity. The relatively low percentage associated with this constraint confirms that the parametric model already embeds a reasonably consistent representation of passenger layout requirements.

Another category of failures, comprising a minor fraction of the inadmissible configurations, relates to owner-driven operational requirements, in particular the minimum electric autonomy threshold. The design brief imposed a minimum autonomy in fully electric mode of three hours, and configurations unable to achieve this target were excluded. The analysis indicates that this limitation is primarily linked to the amount of battery capacity that can be physically installed on board, which in turn depends on the available volume within the dedicated compartment. The most influential parameters in this respect include the longitudinal position of the collision bulkhead and the forward boundary of the engine room, as these variables directly affect the volume available for energy storage systems. At the same time, electric autonomy is strongly coupled with the required propulsive power, which is itself a function of vessel displacement and overall geometric configuration.

Consequently, the autonomy constraint emerges not as an isolated requirement but as the result of a complex interaction between geometric layout, weight distribution, and propulsion demand.

By contrast, the most restrictive class of constraints is associated with global equilibrium conditions. All inadmissible configurations were found to violate, either directly or indirectly, the requirements related to weight–displacement balance and longitudinal equilibrium between LCG and LCB. These constraints act as a global consistency filter, ensuring that the generated configurations remain physically realistic from both hydrostatic and propulsive perspectives. Their dominant role in determining feasibility highlights the strong coupling between geometric parameters, displacement, and propulsion system sizing within the explored design space.

Interestingly, no configurations were rejected due to stability or structural criteria. With regard to structural verification, this outcome should be interpreted in light of the adopted modelling assumptions rather than as an indication of particularly conservative geometric ranges. As discussed in the case study description, and in accordance with the RINA Rules for ships with aluminium alloy hulls, the structural scantlings and the sizing of primary and secondary structural members were defined and verified for the base model and kept constant throughout all the design alternatives generated within the DoE framework. Consequently, the parametric variations explored in the case study exclusively affect the arrangement and longitudinal positioning of bulkheads, without altering the structural dimensioning, which remains compliant with the applicable classification requirements.

From a stability perspective, the absence of rejected configurations can instead be interpreted as a direct consequence of specific design choices adopted for the reference vessel. In particular, the decision to develop a single–main-deck configuration represents a conservative approach, resulting in a relatively low KG and therefore providing inherently favourable stability characteristics. This condition is further reinforced by the relatively large BOA of the vessel, equal to 4.2 m for a LOA of 17 m, corresponding to an LOA / BOA ratio of approximately 4.05. The combination of a low vertical centre of gravity and a comparatively wide hull contributes to maintaining adequate transverse stability across the entire range of generated configurations.

Overall, the analysis of infeasibility causes confirms that the adopted parametric ranges are broadly appropriate but could be further refined by narrowing the combinations of geometric parameters that systematically lead to violations of global equilibrium or insufficient battery capacity. From a methodological perspective, these findings demonstrate that the exploration of unfeasible configurations is not merely a by-product of the DoE, but a key component of the decision-support process, enabling a more informed calibration of the design space for subsequent optimisation and design synthesis phases.

## 5.2. Key Outputs and Statistical Distributions

The following analysis focuses on the subset of 531 configurations that were found to be technically feasible after the application of the automatic feasibility checks described in Chapter 3; all remaining generated configurations were discarded because they violated one or more feasibility criteria. In particular, attention is directed towards three indicators considered to be representative of the overall performance of the vessel and relevant for decision-making purposes:

- passenger transport capacity;
- power required ( $P_B$ ) at the operating speed of 8 kn in Zero Emission Mode (ZEM);
- operational autonomy in fully electric mode.

The decision to concentrate the analysis on these three outputs is motivated by both technical and operational considerations. From the perspective of a potential shipowner,  $n_{\text{pax}}$  represents a direct indicator of the vessel's economic viability: for a given set of principal hull dimensions, the ability to accommodate a larger number of passengers constitutes a significant competitive advantage. In parallel,  $P_B$  and electric autonomy play a central role when issues of environmental sustainability and compliance with increasingly stringent regulatory constraints in coastal and port environments are taken into account. Indeed, the design objective pursued in this thesis is to develop vessels capable of operating in ZEM for the largest possible fraction of their mission profile, a requirement that, for comparable dimensions and passenger capacity, entails a reduction in the required power and an increase in the available electric autonomy.

The distribution of passenger capacity, shown in Figure 61, exhibits a relatively limited variability, with values ranging between 69 and 82 passengers. This behaviour reflects the

combined effect of the dimensional, regulatory, and layout-related constraints imposed by the parametric model, which restrict design freedom once feasibility requirements are satisfied.

By contrast, the distribution of the power required at 8 kn (Figure 62) displays a markedly wider dispersion, with values approximately spanning from 85 to 126 kW.

Similarly, the electric autonomy (Figure 63) is characterised by a substantial range of variation, indicating that, even within the feasible design domain, considerable margins for improvement in terms of energy efficiency remain.

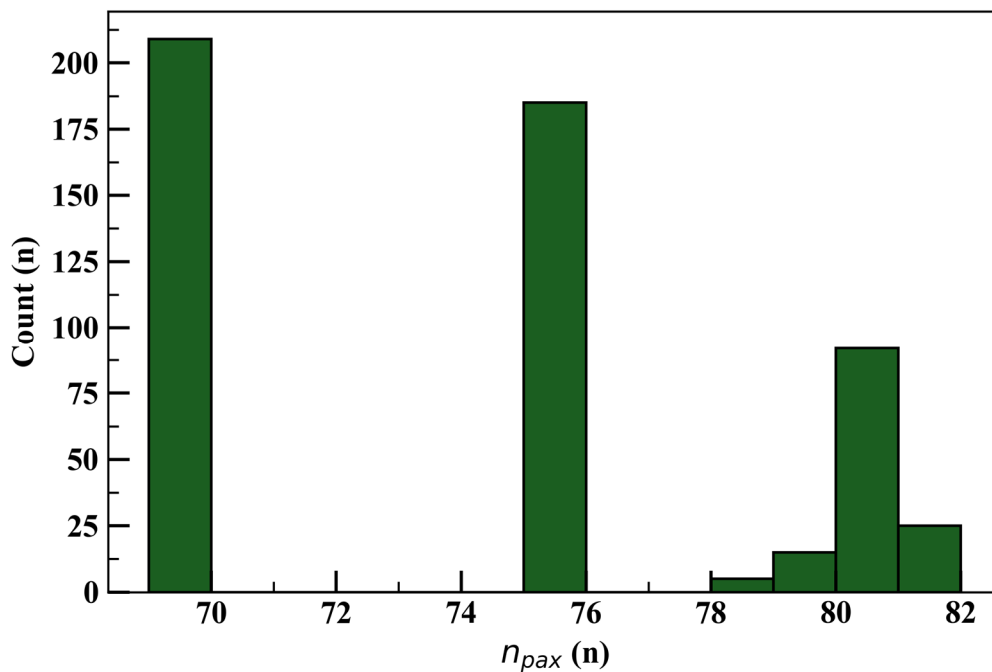


Figure 61 Statistical distribution of passenger capacity across the feasible design configurations

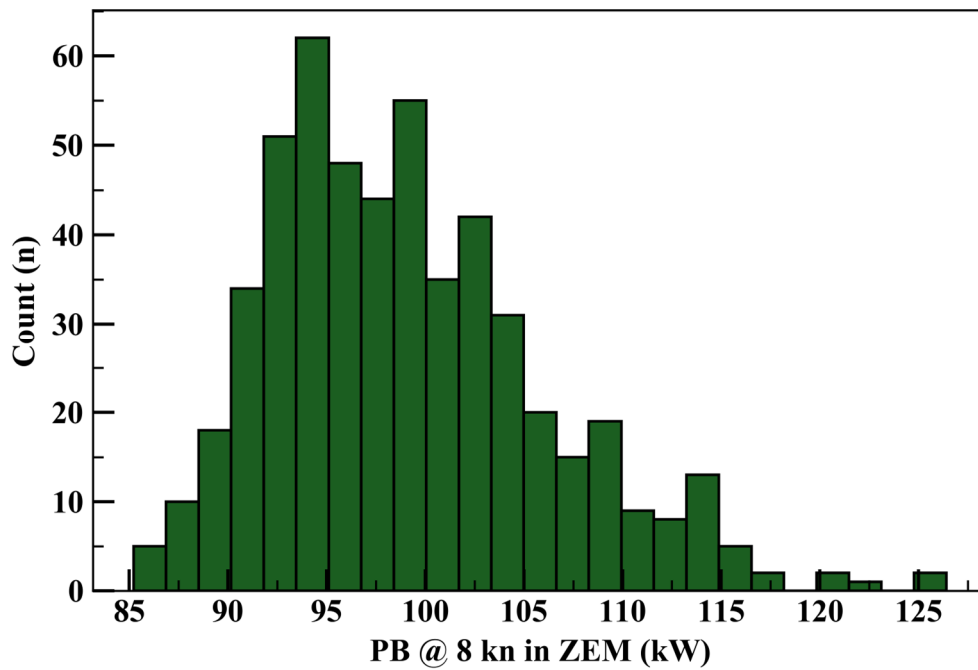


Figure 62 Statistical distribution of the power demand at 8 kn in ZEM for the feasible configurations

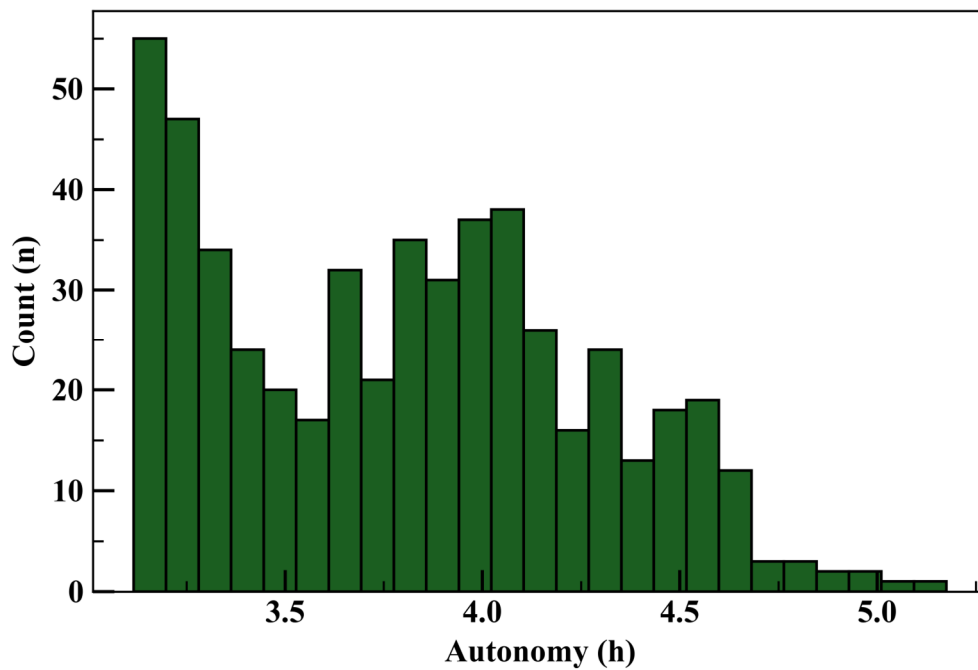


Figure 63 Distribution of operational autonomy in fully electric mode for the feasible design configurations

### 5.3. Relationships and Trade-offs among the Outputs

The joint analysis of the outputs makes it possible to highlight the main design trade-offs within the feasible domain.

Figure 64 illustrates the relationship between passenger capacity and the required power at the reference operating speed. The data points reveal an overall weak correlation between the two indicators: for comparable passenger capacities, significant differences in the required power can be observed.

This result is of particular interest from a design perspective, as it indicates that an increase in  $n_{\text{pax}}$  does not necessarily entail a proportional increase in energy demand. The existence of configurations characterised by high passenger capacity combined with relatively low values of  $P_B$  justifies the adoption of multi-objective criteria in the selection of design solutions.

The relationship between  $n_{\text{pax}}$  and electric autonomy, shown in Figure 65, exhibits a similar degree of dispersion: configurations with comparable transport capacity may provide markedly different levels of electric autonomy. This behaviour confirms that autonomy is not solely a function of passenger capacity, but depends to a significant extent on geometric and plant-related design choices.

Finally, the relationship between  $P_B$  and electric autonomy (Figure 66) shows a clear inverse correlation: a reduction in the required power corresponds to an increase in the operational autonomy in fully electric mode. This outcome, which is consistent with physical expectations, confirms that  $P_B$  represents a particularly effective synthetic indicator for assessing the suitability of a given configuration to operate in ZEM.

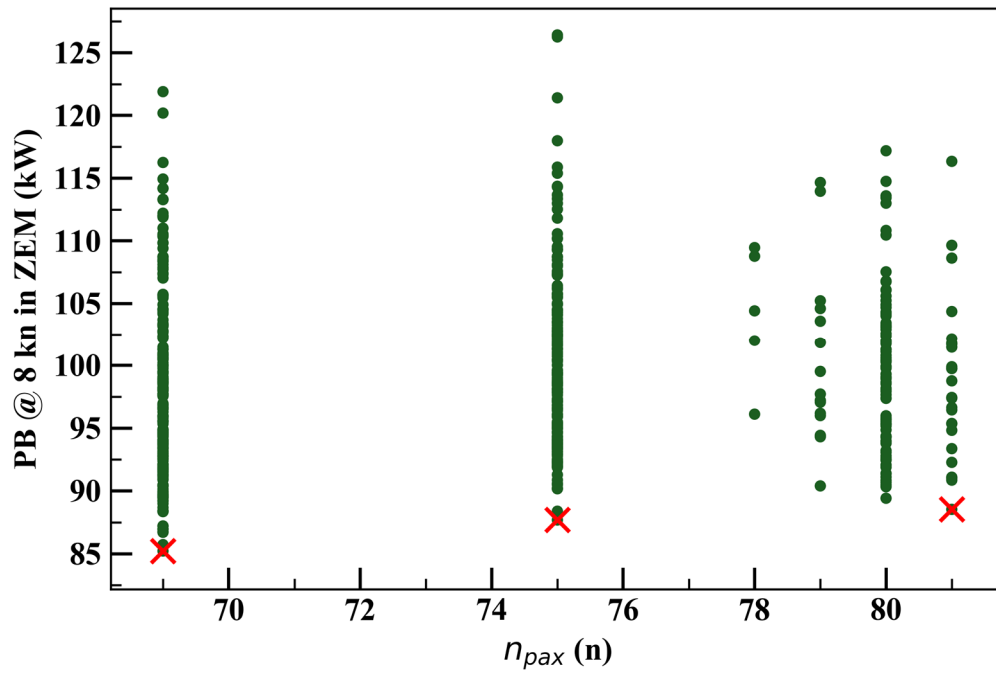


Figure 64 Relationship between passenger capacity and power demand at 8 kn in ZEM, with highlighted bi-objective Pareto-optimal solutions

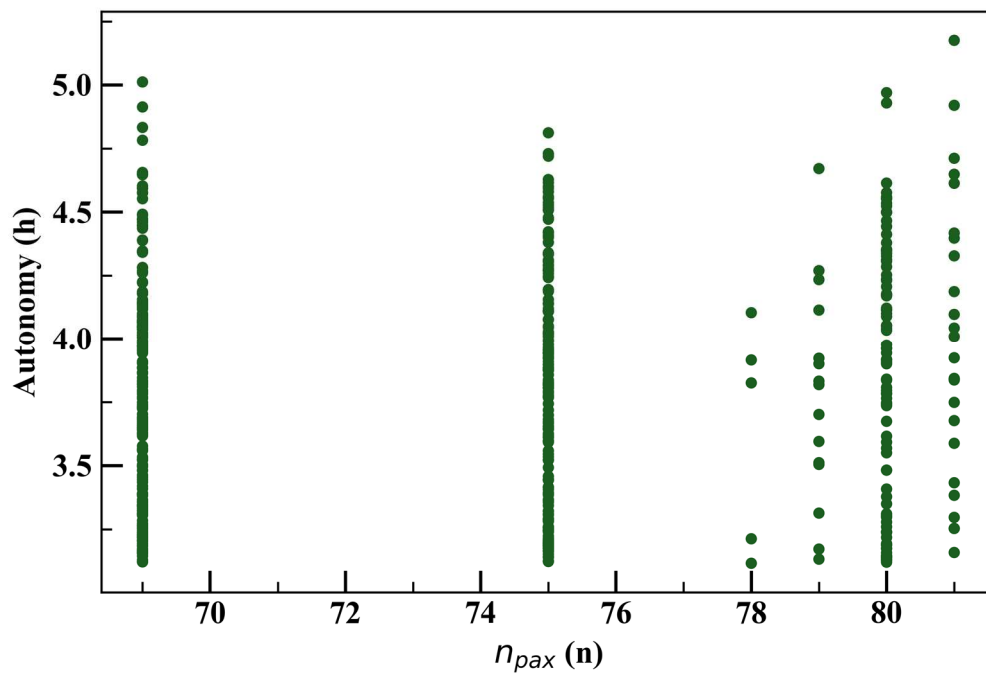


Figure 65 Relationship between passenger capacity and electric operational autonomy

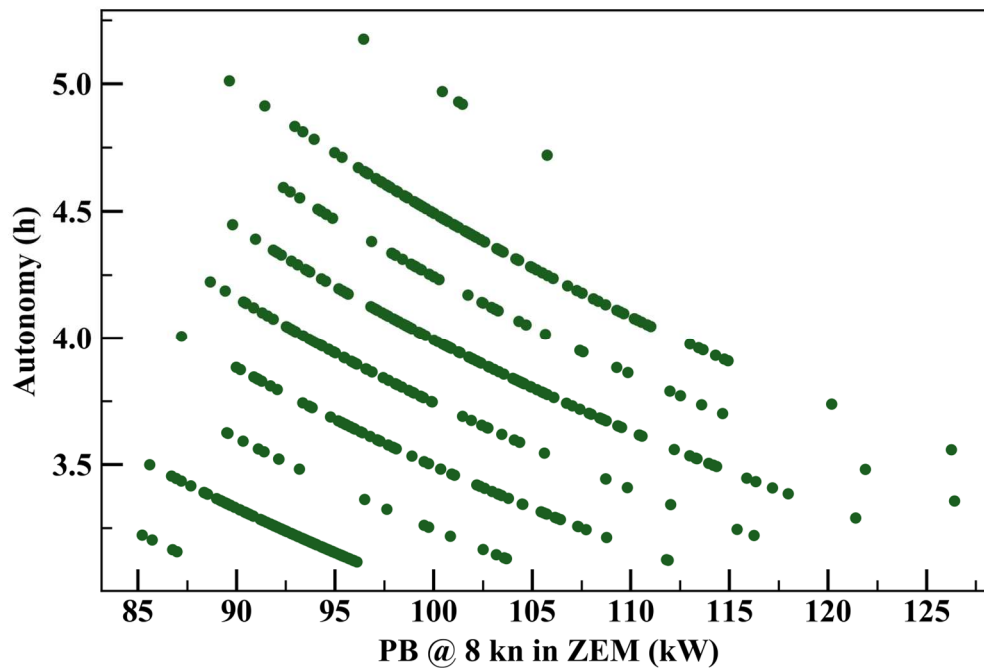


Figure 66 Relationship between power demand at 8 kn in ZEM and operational electric autonomy

#### 5.4. Sensitivity Analysis of Input Variables

To identify the input variables that most strongly influence the behaviour of the key outputs within the feasible set, a sensitivity analysis based on the Spearman rank [102] correlation coefficient was conducted. This approach allows the identification of monotonic relationships, even in the presence of non-linear dependencies.

With regard to the required power  $P_B$ , the results show that the geometric variables associated with the bow region and the transom deadrise configuration are dominant (Figure 67). In particular, the bow angle and transom deadrise exhibit the highest absolute correlation values, consistent with the influence of these parameters on the hydrodynamic mechanisms governing resistance and longitudinal trim at low speeds.

The sensitivity analysis related to passenger capacity, presented in Figure 68, reveals that the most influential variable is the longitudinal position of the maximum beam (*Max Beam Position*). This finding suggests that transport capacity within the feasible domain is primarily governed by the longitudinal distribution of the usable beam, and consequently by the surfaces available for passenger space allocation.

For completeness, Figure 69 presents the analysis of the main correlations concerning electric autonomy, which reflects the interaction between energy demand and storage capacity. Notably, electric autonomy is found to be primarily dependent on the same two geometric variables that govern the required power, namely the bow angle and the transom deadrise. This result is not unexpected, as autonomy is directly linked to the power demand at the reference operating condition; however, it provides a clear and quantitative confirmation that both energetic performance indicators are driven by a common and limited set of geometric parameters. From a design perspective, this outcome is particularly relevant, as it indicates that targeted modifications of a small number of geometric variables can simultaneously improve both power demand and electric autonomy, thereby enhancing the vessel's suitability for extended operation in ZEM.

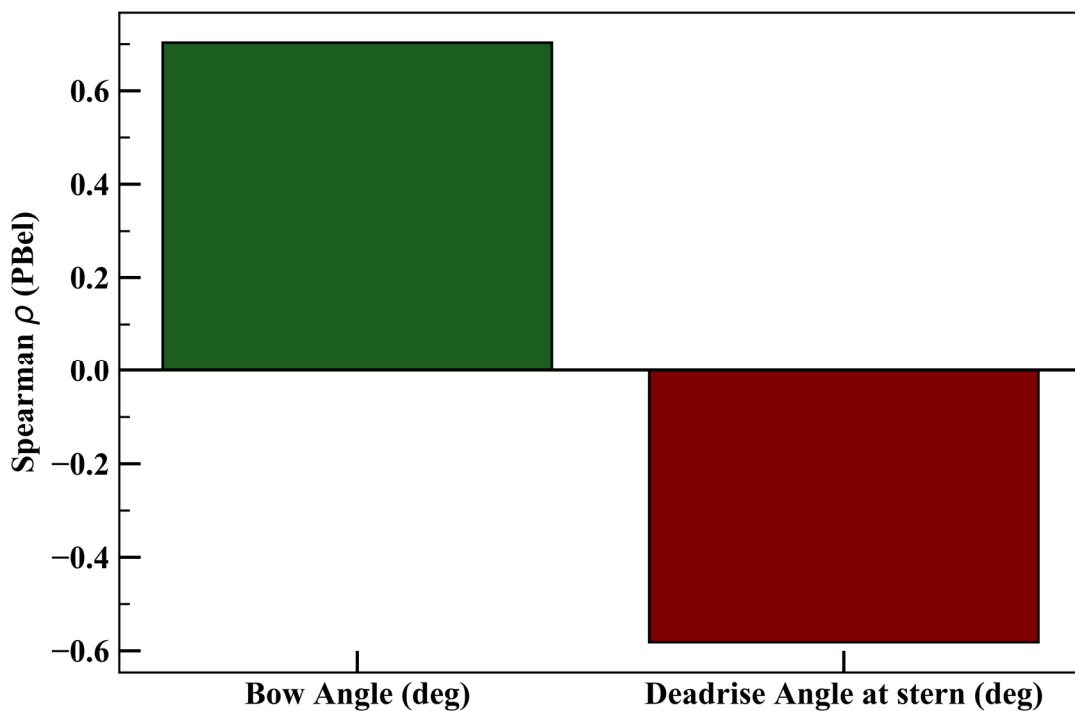


Figure 67 Spearman rank correlations between key input variables and power demand at 8 kn in ZEM

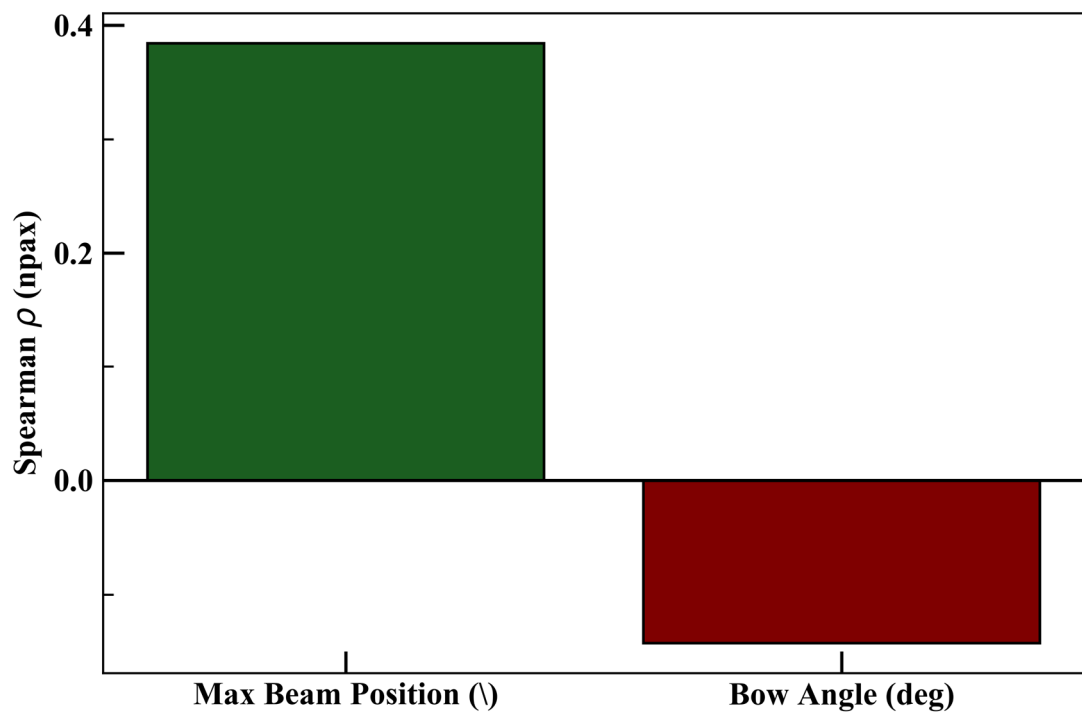


Figure 68 Spearman rank correlations between key input variables and passenger capacity

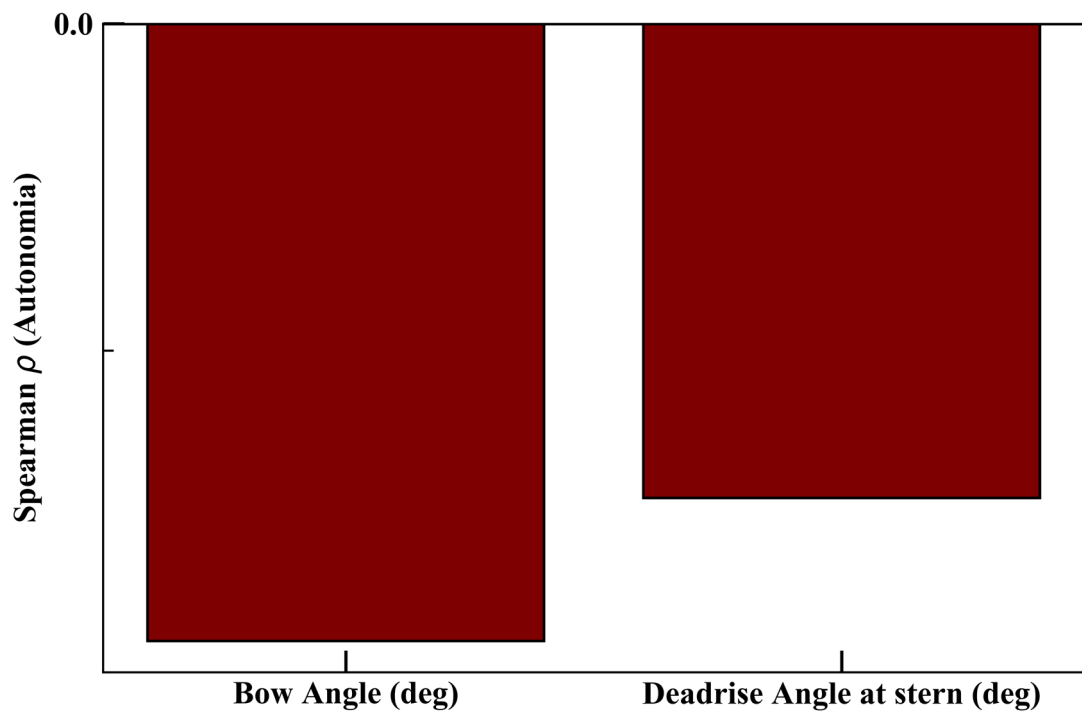


Figure 69 Spearman rank correlations between key input variables and electric autonomy

### 5.5. Design implications and discussion

The combined interpretation of the statistical distributions, trade-off analyses, and sensitivity results provides a number of relevant conclusions regarding both the characteristics of the feasible design space and the effectiveness of the proposed parametric methodology. The results demonstrate that, within the admissible domain identified by the feasibility analysis, it is indeed possible to obtain vessel configurations that combine relatively high passenger transport capacity with favourable energetic performance in Zero Emission Mode. In particular, the weak correlation observed between passenger capacity and required power indicates that an increase in transport capacity does not necessarily entail a proportional penalty in terms of power demand or electric autonomy, provided that appropriate geometric and layout-related choices are adopted.

This outcome is of particular relevance from a design and decision-making perspective. Rather than converging towards a single optimal configuration, the design-space exploration reveals the existence of a Pareto-optimal region populated by multiple admissible solutions that balance economic viability—expressed through passenger capacity—and environmental performance—expressed through power demand and operational autonomy in ZEM. The availability of such a solution set confirms the suitability of a multi-objective approach to preliminary design, in which trade-offs are explicitly exposed and can be consciously managed in accordance with stakeholder priorities.

The sensitivity analysis further strengthens these conclusions by clarifying the nature of the variables that govern the most relevant performance indicators. The parameters exerting the strongest influence on both power demand and electric autonomy—namely the bow angle and the transom deadrise—are geometric shaping variables that remain largely unconstrained by regulatory prescriptions and are not fixed by the principal dimensions of the vessel. As such, they retain a high degree of design freedom during the preliminary design phase. This implies that meaningful improvements in ZEM-related performance can be achieved through targeted geometric refinement, without requiring changes to length, beam, draught, or imposed passenger capacity limits.

Passenger capacity, in turn, is found to be primarily influenced by the longitudinal position of the maximum beam, a parameter that directly affects the distribution of usable deck area. While this variable is indirectly constrained by functional layout requirements and

circulation criteria, it is not imposed by external regulatory limits and therefore retains a significant degree of flexibility within the feasible domain. Its influence highlights the importance of longitudinal volume distribution as a design lever for balancing transport capacity against other functional or operational priorities.

Overall, these results indicate that the most influential variables identified by the analysis correspond to parameters that are effectively controllable by the designer, rather than to rigid or externally imposed constraints. This aspect is particularly significant, as it confirms that the proposed parametric methodology does not merely identify feasibility boundaries, but actively reveals the design levers through which trade-offs between capacity, energy demand, and operational autonomy can be navigated. The methodology therefore provides a robust and transparent decision-support framework for the preliminary design of coastal passenger vessels, forming a solid basis for subsequent design synthesis and selection phases based on Multi-Attribute Decision Making (MADM) approaches aligned with client-specific objectives and operational requirements.

### **5.6. State-of-the-art benchmarking**

In order to properly contextualise the results obtained with respect to the current state of the art, a comparison was conducted between a representative subset of the configurations generated by the proposed methodology and a selection of existing passenger vessels operating in comparable application contexts.

As discussed in the previous sections, the analysis of the results was initially carried out by referring to a bi-objective Pareto front, constructed by considering the maximisation of passenger transport capacity and the minimisation of the power required at the operating speed in Zero Emission Mode. This analysis led to the identification of a limited number of non-dominated configurations, namely three, which represent the most favourable compromises between energetic performance and transport capacity within the admissible design domain.

However, in order to extend the analysis beyond an internal comparison among the generated solutions and to enable a meaningful benchmarking against existing passenger vessels, it was deemed necessary to explicitly introduce the operational autonomy in fully electric mode as an additional design objective. Electric autonomy represents a key parameter for

assessing the actual capability of a vessel to perform a significant portion of its mission profile in Zero Emission Mode and constitutes a metric of immediate relevance when comparing novel design solutions with units already in service.

The extension of the analysis to a tri-objective Pareto framework—defined by the maximisation of passenger capacity and electric autonomy and the minimisation of the required electric power—therefore led to the identification of a broader set of non-dominated configurations, consisting of 17 solutions. This set does not represent a contradiction with the previous bi-objective results, but rather their natural and methodologically consistent completion, made necessary by the introduction of an additional performance criterion that is fundamental for benchmarking purposes and for a comprehensive assessment of the competitiveness of the generated solutions.

The comparison was thus extended to a sample of real passenger vessels of similar size, including both units currently operating in the Italian context and two foreign vessels equipped with series-hybrid propulsion architectures, originating respectively from France and Sweden. This selection makes it possible to analyse the positioning of the generated configurations with respect to different levels of technological maturity and different regulatory and operational frameworks.

A first relevant outcome emerging from the comparison concerns the national context. Within the analysed sample, no passenger vessels currently operating in Italy, with dimensions and mission profiles comparable to those considered in the present research, are equipped with a series-hybrid propulsion architecture. The Italian vessels included in the comparison adopt exclusively conventional diesel propulsion systems, typically designed to maximise transport capacity or service speed, without providing the capability to operate in Zero Emission Mode for a significant portion of the mission profile.

This observation highlights the existence of a technological gap between the national context and some more advanced foreign experiences, and further reinforces the relevance of the present research in addressing this gap by proposing a methodology specifically oriented towards the preliminary design of passenger vessels compatible with future decarbonisation scenarios and increasingly stringent environmental constraints in coastal and port areas.

The comparison with the two foreign passenger vessels equipped with series-hybrid propulsion allows the results obtained in this work to be placed within a more advanced technological framework (Table 49). For comparable orders of magnitude of the principal dimensions, the configurations selected from the tri-objective Pareto front exhibit electric-mode operational performances that are fully competitive, and in some cases superior, to those of the existing solutions.

In particular, the 17 Pareto-optimal configurations identified in this study achieve fully electric operational autonomies, at the reference operating speed of 8 kn, ranging approximately between 28 and 44 equivalent nautical miles. This metric, computed as the product of the electric operating speed and the corresponding evaluated autonomy, shows a significant variability within the admissible design domain and clearly indicates the possibility of covering a substantial portion of the mission profile in Zero Emission Mode, which represents a central design objective of the present thesis.

The foreign vessels considered, despite adopting series-hybrid architectures, are characterised by more limited electric autonomies, often associated with lower operating speeds and significantly smaller installed energy storage capacities. This aspect suggests that the configurations generated by the proposed methodology are deliberately oriented towards maximising the extent of Zero Emission Mode operation, even at the expense of a higher installed energy capacity, reflecting a different set of design priorities.

From the perspective of passenger transport capacity, the comparison highlights that some foreign vessels are able to accommodate a slightly higher number of passengers than the configurations developed in this study, despite having principal dimensions of the same order of magnitude. As discussed in the previous sections, the Pareto-optimal configurations exhibit a relatively narrow range of passenger capacity values, reflecting the combined effect of geometric, regulatory, and layout-related constraints imposed within the parametric model.

Such differences should not be interpreted solely as an intrinsic limitation of the generated solutions, but rather in light of the differences in regulatory and normative frameworks applicable in the various national contexts. Requirements related to maximum passenger density, minimum space per passenger, accessibility criteria, compartmentation, and functional layout can significantly affect the achievable transport capacity for a given set of

geometric dimensions. The results therefore suggest that passenger capacity is strongly dependent on the regulatory context of reference, in addition to layout and spatial distribution choices.

Overall, the comparison carried out allows the generated configurations to be positioned coherently and competitively with respect to the current state of the art, particularly in terms of their capability to operate in Zero Emission Mode and the flexibility of their mission profile. Although in some cases the passenger capacity is lower than that of certain foreign units, the developed solutions offer an advanced balance between vessel size, energetic performance, and environmental sustainability, and are fully aligned with the objectives of decarbonising coastal passenger transport.

In this sense, the proposed methodology does not merely enable the identification of technically feasible configurations, but also supports a conscious exploration of the design positioning with respect to existing solutions, making explicit the trade-offs between transport capacity, electric autonomy, and plant complexity. This confirms the value of the adopted parametric and multi-objective approach as a robust decision-support tool for the preliminary design of low- and zero-emission passenger vessels.

*Table 49 Comparative overview of Pareto-optimal configurations and existing passenger vessels of similar size*

<b>Parameter</b>		<b>Units</b>	<b>Present research</b>	<b>France</b>	<b>Sweden</b>
<i>Length Overall</i>	<i>L<sub>OA</sub></i>	m	17	16	15
<i>Beam Overall</i>	<i>B<sub>OA</sub></i>	m	4.2	5.1	5.1
<i>Passenger capacity</i>	<i>n<sub>PAX</sub></i>	\	69 - 81	94	50
<i>ZEM Speed</i>	<i>V<sub>ZEM</sub></i>	kn	8	6	\
<i>Autonomy Requirement in ZEM</i>	\	h	3.5 – 5.5	3.0	\
<i>Installed battery capacity</i>	\	kWh	300 - 500	103	96

## Conclusions

The present research has addressed in an organic and integrated manner the problem of the preliminary design of passenger vessels intended for sustainable coastal navigation, with the aim of overcoming the structural and conceptual limitations inherent in traditional design processes. The research is situated within a disciplinary context in which naval architecture is increasingly required to confront growing regulatory, technological and operational complexity, further intensified by decarbonisation objectives, integration with land-based mobility systems, and a progressively stronger focus on the vessel life cycle. Within this framework, conceptual design assumes a strategic role, as decisions taken at this stage exert a decisive influence on the performance, costs and environmental impact of the ship as a whole.

The critical analysis of the traditional design spiral paradigm constituted the starting point of the research. While acknowledging its historical and educational value, it has emerged that a rigidly sequential application of this model is inadequate to manage the interdependencies that characterise contemporary passenger vessel design. In particular, the limited ability to systematically explore design alternatives, the slow pace of iteration cycles and the risk of early fixation on specific solutions constrain the designer's capacity to identify truly optimal configurations. The thesis therefore proposes an evolution of the traditional paradigm, in which the spiral retains its role as a structure for verification and validation, while being driven by a parametric process capable of generating filtering, and evaluating a broad set of solutions from the earliest design stages.

Within this context, the adoption of Parametric Design Thinking is introduced as the reference paradigm. The research demonstrates that parametric design represents not merely a collection of geometric tools, but a genuine shift in perspective within design practice. The designer is no longer confined to defining a single configuration, but instead constructs a system of relationships, constraints and variables that describes a design space amenable to systematic exploration. This shift transforms preliminary design from a solution-oriented activity into a space-oriented process, improving traceability, reducing subjective bias, and transforming preliminary design into a structured, repeatable and verifiable process, in which

assumptions and design decisions can be systematically tested against technical and regulatory constraints.

One of the central elements emerging from the research concerns the role of the General Arrangement in the design of passenger vessels for coastal liner services. Contrary to many traditional approaches, the GA cannot be regarded as a simple consequence of hull definition, but rather as a generative element that directly interacts with operational requirements, accessibility, safety, weight distribution and system integration. By embedding the GA within the parametric workflow, layout feasibility is automatically verified across a large number of alternative configurations, highlighting how layout decisions substantially affect the overall feasibility of a configuration and its performance, thereby reducing the risk of late-stage redesign and project inconsistencies.

The coherence between the adopted methodological paradigm and the technological choices represents a further significant outcome of the thesis. The comparative analysis of propulsion architectures led to the selection of the series-hybrid system as the most suitable solution for the vessels under consideration, not only due to its benefits in terms of energy efficiency and emission reduction, but above all because of its compatibility with an integrated parametric design process. The modularity of the series-hybrid system, combined with its algorithmic integration within the workflow, allows propulsion performance to be evaluated consistently across the entire design space, enabling more effective control over weight distribution, internal layout and stability, thus rendering propulsion an active design variable rather than a constraint imposed at later stages.

Similarly, the selection of a hard-chine hull form and aluminium alloy as the structural material was guided by a systemic perspective that takes into account not only hydrodynamic and structural performance, but also producibility, regulatory compliance and environmental implications over the entire life cycle. In particular, the comparison between GRP, aluminium and thermoplastic materials has shown that aluminium currently represents the most balanced solution for coastal passenger vessels, owing to its recyclability, regulatory maturity and effective integration within a parametric workflow.

The most significant original contribution of the research lies in the development of an integrated parametric workflow, implemented within the Grasshopper environment and based on Design of Experiments techniques. Through the use of Uniform Latin Hypercube

sampling, the model enables the systematic exploration of a multidimensional design space, automatically generating a set of complete configurations and subjecting them to geometric, functional and technical feasibility checks. As demonstrated by the case study, this automatic filtering process reduces an initially vast design space to a compact and engineering-consistent subset of admissible solutions, focusing the analysis on configurations of genuine practical relevance.

The results obtained must also be interpreted in light of the overall time required to develop and operate the parametric model. The initial learning and implementation phase, estimated to be on the order of approximately two months, is fully compatible with the timeframes typically associated with preliminary design conducted using traditional approaches, provided that a sufficiently structured database is available. Once this initial investment has been completed, the methodology enables the exploration, verification and comparison of a large number of design alternatives within a matter of hours, a task that would be impractical within comparable timeframes using conventional workflows.

The automated generation of three-dimensional models, two-dimensional drawings, technical tables and performance indicators further enhances the efficiency and operational relevance of the process, allowing the designer to focus on decision-making rather than on repetitive modelling tasks.

From an operational perspective, the developed tool offers a concrete and immediately applicable decision-support capability. A design office may either replicate and adapt the methodology to its own standards or directly employ the implemented model by providing the relevant design requirements as input. Within this framework, the tool enables the systematic screening of design alternatives based on parameters and priority criteria defined by the shipowner, automatically filtering the generated configurations and retaining only those proposals that are consistent with the intended operational profile and strategic objectives. In the latter case, the tool allows the rapid generation and controlled filtering of a large set of technically feasible configurations, effectively decoupling feasibility assessment from the subsequent multi-criteria decision-making phase, which can then be assessed exclusively through multi-criteria decision-making processes to identify the most suitable solution in relation to client priorities and operational objectives.

From a sustainability perspective, the thesis highlights that objectives related to environmental impact reduction cannot be achieved through isolated interventions, but require a systemic integration of hull geometry, propulsion architecture, internal layout and material selection. The developed parametric tool makes these interdependencies explicit and allows the effects of design decisions to be assessed already at the preliminary stage, thereby laying the foundations for a design approach genuinely oriented towards life-cycle thinking and the energy transition of coastal transport.

Despite the results achieved, the research presents certain limitations. The model operates primarily at the preliminary design level and relies on simplified performance evaluation models, which are appropriate for comparative analysis but cannot replace the detailed assessments required in subsequent design stages.

With regard to the operational context, it should be noted that the workflow has been developed and demonstrated through a specific case study, namely a passenger vessel intended for sustainable coastal navigation in the Gulf of Trieste. This choice was deliberately made in order to ground the methodology in a realistic and well-defined operational scenario, characterised by stringent regulatory requirements, frequent port operations and strong constraints on emissions, accessibility and integration with land-based transport systems.

However, the specificity of the case study should not be interpreted as a limitation of the methodological framework itself. The proposed workflow is inherently modular and parametric in nature, and its structure is independent of the particular operational context to which it is applied. Different navigation regimes, mission profiles or geographical areas can be addressed by redefining the relevant input parameters, regulatory constraints and performance criteria, without altering the underlying logic of the design process.

In this sense, the case study represents a concrete instantiation of a more general design framework. The extension of the methodology to other contexts, such as vessels operating in offshore or deep-sea conditions, would require the adoption of different regulatory references, environmental loads and mission requirements, but would follow the same staged approach to design space exploration, feasibility filtering and decision support developed in this research.

With specific reference to the structural aspects, the model operates at a preliminary design level and adopts rule-based, intentionally conservative assumptions. This choice reflects both the regulatory framework and common design practice for coastal passenger vessels, where structural robustness, durability and damage tolerance are often prioritised over aggressive weight minimisation. As a consequence, configurations that appear structurally equivalent within the proposed framework may exhibit different weight outcomes when subjected to detailed structural optimisation at later design stages. However, this limitation is intrinsic to the selected design phase and is coherent with the objectives of the research. The methodology is conceived to enable a consistent and computationally efficient comparison of alternative configurations, all evaluated under the same structural assumptions. Introducing advanced structural optimisation at this stage would significantly increase modelling and computational effort, potentially offsetting the benefits of rapid design-space exploration in an already demanding preliminary design process. Future developments may therefore include the integration of more refined structural analyses and optimisation procedures, applied selectively to a reduced set of promising solutions identified through the parametric screening process, thereby combining early-stage exploration with late-stage optimisation.

With reference to the design space exploration strategy, the relatively low percentage of admissible configurations obtained through the initial ULHS sampling should be interpreted in relation to the objectives of the concept design phase. The methodology deliberately prioritises an extensive and unbiased exploration of a wide parametric domain, allowing infeasible regions of the design space to be identified and excluded through automatic screening.

In practical design applications, the results of this first exploration would naturally be used to progressively refine the parametric ranges and constraints, thereby increasing sampling efficiency in subsequent iterations. In this sense, the generation of a large number of unfeasible configurations is not an end in itself, but a necessary step to inform the controlled reduction of the design space.

In light of these considerations, future development prospects appear both broad and articulated. A first line of development concerns the evolution of the design space exploration strategy itself. The introduction of convergence analyses, adaptive sampling

techniques or surrogate modelling approaches could be employed to optimise the number of required samples once the most relevant regions of the design space have been identified through an initial exploratory phase. Such enhancements would allow the proposed methodology to progressively evolve from a predominantly exploratory framework towards a more targeted and computationally efficient process, while preserving its effectiveness as a decision-support tool in the early stages of ship design.

A second line of development involves the progressive enrichment of the underlying physical and performance models. The integration of more advanced CFD and structural analyses, the adoption of multi-objective optimisation techniques, and the inclusion of economic and life-cycle assessments represent natural extensions of the present work. In the longer term, the combination of refined sampling strategies with higher-fidelity models could enable the proposed framework to evolve into a comprehensive decision-support environment for the design of new passenger vessels, as well as for the retrofit and renewal of existing fleets.

In conclusion, the thesis demonstrates how the adoption of an integrated parametric approach can substantially transform the preliminary design of passenger vessels for coastal navigation, rendering it more informed, transparent and sustainability-oriented. By enabling the rapid generation, automatic verification and structured comparison of a large number of alternatives within a controlled and traceable framework, the proposed methodology enhances design capability by enabling the rapid generation, verification and comparison of alternatives within a controlled and traceable framework. In this sense, the research is intended as a methodological and applied contribution towards a new generation of design processes in the field of naval architecture, consistent with the challenges of sustainable coastal mobility in the twenty-first century.

## Appendix I

### Nomenclature

OPEX	Operating Expenditure
GA	General Arrangement
CAD	Computer Aided Design
2D	Two Dimensional
3D	Three Dimensional
NURBS	Non-Uniform B-Splines
FFD	Free Form Deformation
GDT	Generative Design Techniques
DoE	Design of Experiments
EET	Energy Efficiency Technology
CO <sub>2</sub>	Carbon dioxide
NO <sub>x</sub>	Nitrogen oxides
SO <sub>x</sub>	Sulphur oxides
PDT	Parametric Design Thinking
FPA	Fully Parametric Approach
$L_{OA}$	Length Overall (m)
$B_{OA}$	Beam Overall (m)
$C_P$	Prismatic Coefficient (\\)
$LCB$	Longitudinal Centre of Buoyancy (m)
ROM	Reduced Order Modelling
CFD	Computational Fluid Dynamics
FEM	Finite Element Method
$P_i$	Control Points of a NURBS Curve
$w_i$	Weight of Control Points of a NURBS Curve
$N_{i,p}(u)$	B-spline basis functions of degree $p$

---

$p$	Degree of a NURBS Curve
$u$	Non-dimensional curve parameter
$U$	Knot Vector
$S(u, v)$	NURBS Surface
CAPSD	Computer-Aided Preliminary Ship Design
GRP	Glass-Reinforced Plastic
HDPE	High-Density Polyethylene
ICE	Internal Combustion Engine
GS	Generator - Set
AC	Alternating Current
DC	Direct Current
EM	Electric Motor
ESS	Energy Storage System
$LCG$	Longitudinal Centre of Gravity (m)
$KG$	Vertical Centre of Gravity (m)
PMS	Power Management Systems
OPPT	Optimal Operating Point
BSFC	Brake Specific Fuel Consumption
ZEM	Zero Emission Mode
$Fn_v$	Volumetric Froude Number
LCA	Life Cycle Assessment
ULHS	Uniform Latin Hypercube Sampling
$SH$	Sheer Height (m)
$BA$	Bow Angle (deg)
$C2$	Control coefficient for point P2 (\)
$C1$	Coefficient for positioning point P5 (\)
$CTPR$	Coefficient for the control of bow tangency (\)
$CTPP$	Coefficient for the control of stern tangency (\)
$RA$	Rocker Angle (deg)

---

$T$	Design draft (m)
$BTC$	Beam Transom Coefficient (\)
$BP_{MAX}$	Max Beam Position (\)
$BFF$	Bow Fullness Factor (\)
$CTPP$	Coefficient for the control of stern tangency (\)
$TF$	Bow Tangent Factor (\)
$CHF$	Chine Height Factor Bow (\)
$MAXCP$	Max Chine Position (\)
$MAXCC$	Max Chine Coefficient (\)
$TFC$	Chine Tangent Factor (\)
$CFF$	Chine Fullness Factor (\)
$CTC$	Chine Transom Coefficient (\)
$CTPP$	Coefficient for stern tangency control (\)
$\theta_T$	Deadrise Angle at stern (deg)
$\theta$	Deadrise Angle (deg)
$SRW$	Spray rail width (m)
$\nabla$	Volume (m <sup>3</sup> )
$\Delta$	Displacement (t)
$L_{WL}$	Waterline Length (m)
$B_{WL}$	Waterline Beam (m)
$WSA$	Wetted Surface Area (m <sup>2</sup> )
$WPA$	Waterplane Area (m <sup>2</sup> )
$C_B$	Block Coefficient (\)
$C_{WP}$	Waterplane Area Coefficient (\)
$KB$	Vertical Centre of Buoyancy (m)
$LCF$	Longitudinal Centre of Flotation (m)
$LCB \%$	$LCB$ as Percentage of $L_{WL}$ (%)
$LCF \%$	$LCF$ as Percentage of $L_{WL}$ (%)
$BM_t$	Transverse Metacentric Radius (m)

---

$BM_l$	Longitudinal Metacentric Radius (m)
$EAR$	Expanded Area Ratio (\)
$V_D$	Design Speed (kn)
$V_{ZEM}$	Max ZEM Speed (kn)
$n_P$	Number of propellers (\)
$Z$	Number of Blades (\)
PMR	Passenger with Reduced Mobility
$s$	Transverse Frame Spacing
$D$	Moulded Depth
$W$	Full-load displacement (t)
$TCG$	Transverse centre of gravity (m)
$GM_t$	Transverse metacentric radius (m)
$GM_l$	Longitudinal metacentric radius (m)
$T_A$	Aft draught (m)
$T_F$	Forward draught (m)
$Fn$	Froude number (\)
$R_T$	Total Resistance (kN)
$SM$	Sea Margin
$P_E$	Effective Power (kW)
$P_B$	Brake Power (kW)
$D_{PROP}$	Propeller Diameter (m)
$W$	Weight (t)
$TCG$	Transversal Centre of Gravity (m)

---

## Appendix II

### modeFrontier report

#### Project Info

---

Project Name	V7.prj
modeFRONTIER Version	modeFRONTIER 2024R3
modeFRONTIER Version number	15.7.2 b20241009
modeFRONTIER Home	D:\Padolecchia\modeFRONTIER2024R3- win64\modeFRONTIER2024R3-win64
Date	Mon Nov 24 15:20:47 CET 2025
Project PWD	D:\Padolecchia\FILE DEFINITIVI\V7_00000

#### Host Info

---

Host Name	SRV-ISDLAB02
Host IP Address	140.105.50.98
Operating System	Windows Server 2019 10.0 amd64
Java (SDK/JRE) Version	21.0.2

---

Java Home D:\Padolecchia\modeFRONTIER2024R3-  
 win64\modeFRONTIER2024R3-win64\jre  
 User Name 40234  
 User Home C:\Users\40234  
 Working Directory D:\Padolecchia\FILE DEFINITIVI\V7\_00000  
 Java VM -Xmx1024m --add-opens=java.base/java.lang=ALL-UNNAMED -  
 Arguments Djava.net.preferIPv4Stack=true -Djava.net.useSystemProxies=true

### Run Info

---

Log Level	FINE
Num. Concurrent Des.	1
Clear Des. Dir on Exit	never
Eval Repeated Designs	true
Save Repeated Designs	false
Save Error Designs	true
Eval Unfeasible Designs	true
Force Error Designs to NaN	true
RSM Percentage	0%

Date & Time	Event	Argument
-------------	-------	----------

Mon, 24 November 2025

---

15:20:47:889 ENGINE STARTING [Logs, Dir](#)

15:20:52:376 PROJECT SAVED D:\Padolecchia\FILE  
DEFINITIVI\V7\_00000\V7.prj

15:20:53:393 LICENSE CHECKOUT FEATURE = mf\_batch[1]

15:20:53:408 LICENSE CHECKOUT FEATURE = features[6]

15:20:53:484 LICENSE CHECKOUT FEATURE =  
mf\_integration\_grasshopper[1]

15:20:53:522 LICENSE CHECKOUT FEATURE = features[3]

15:20:53:559 LICENSE CHECKOUT FEATURE = mf\_integration\_excel[1]

15:20:53:572 LICENSE CHECKOUT FEATURE = features[1]

15:20:53:590 LICENSE CHECKOUT FEATURE = mf\_integration\_logic[1]

15:20:53:600 LICENSE CHECKOUT FEATURE = features[2]

15:20:53:609 LICENSE CHECKOUT FEATURE = mf\_batch\_npe[1]

15:20:57:144 PLAN [DOE Plan-0](#)

15:20:57:647 DESIGNS DB [V7.des](#)

15:20:59:175 SCHEDULING STARTED

15:20:59:259 PLUG-IN START [DOE Sequence](#)

15:20:59:632 DESIGNS GROUP STARTED [00000-00999](#)

Tue, 25 November 2025

00:02:52:212 **DESIGNS GROUP COMPLETED** [00000-00999](#) (COMPLETED=58,  
**FAILED=942**) ELAPSED TIME = 8h:41m:52.584s

00:02:52:214 DESIGNS GROUP STARTED [01000-01999](#)

08:41:00:097 **DESIGNS GROUP COMPLETED** [01000-01999](#) (COMPLETED=56,  
**FAILED=944**) ELAPSED TIME = 8h:38m:7.884s

08:41:00:098 DESIGNS GROUP STARTED [02000-02999](#)

---

---

17:04:34:400 **DESIGNS GROUP COMPLETED** [02000-02999](#) (COMPLETED=54, **FAILED=946**) ELAPSED TIME = 8h:23m:34.303s

17:04:34:401 **DESIGNS GROUP STARTED** [03000-03999](#)

Wed, 26 November 2025

01:38:38:829 **DESIGNS GROUP COMPLETED** [03000-03999](#) (COMPLETED=49, **FAILED=951**) ELAPSED TIME = 8h:34m:4.429s

01:38:38:831 **DESIGNS GROUP STARTED** [04000-04999](#)

10:10:27:135 **DESIGNS GROUP COMPLETED** [04000-04999](#) (COMPLETED=46, **FAILED=954**) ELAPSED TIME = 8h:31m:48.305s

10:10:27:137 **DESIGNS GROUP STARTED** [05000-05999](#)

18:37:50:308 **DESIGNS GROUP COMPLETED** [05000-05999](#) (COMPLETED=33, **FAILED=967**) ELAPSED TIME = 8h:27m:23.172s

18:37:50:310 **DESIGNS GROUP STARTED** [06000-06999](#)

Thu, 27 November 2025

03:09:29:671 **DESIGNS GROUP COMPLETED** [06000-06999](#) (COMPLETED=65, **FAILED=935**) ELAPSED TIME = 8h:31m:39.362s

03:09:29:673 **DESIGNS GROUP STARTED** [07000-07999](#)

11:39:58:706 **DESIGNS GROUP COMPLETED** [07000-07999](#) (COMPLETED=57, **FAILED=943**) ELAPSED TIME = 8h:30m:29.034s

11:39:58:708 **DESIGNS GROUP STARTED** [08000-08999](#)

20:07:52:671 **DESIGNS GROUP COMPLETED** [08000-08999](#) (COMPLETED=59, **FAILED=941**) ELAPSED TIME = 8h:27m:53.964s

20:07:52:672 **DESIGNS GROUP STARTED** [09000-09999](#)

Fri, 28 November 2025

04:40:42:890 **DESIGNS GROUP COMPLETED** [09000-09999](#) (COMPLETED=54, **FAILED=946**) ELAPSED TIME = 8h:32m:50.219s

04:40:42:892    DESIGNS GROUP STARTED    [10000-10999](#)

04:41:39:874    PLUG-IN EXITED    [DOE Sequence](#) ELAPSED TIME =  
85h:20m:40.689s

04:41:39:878    **DESIGNS GROUP COMPLETED**    [10000-10999](#) (COMPLETED=0,  
**FAILED=1**) ELAPSED TIME = 0h:0m:56.987s

04:41:54:717    SCHEDULING COMPLETED    [Logs, Dir](#), (COMPLETED=531,  
**FAILED=9470**) ELAPSED TIME = 85h:20m:55.424s

04:41:55:803    PROJECT SAVED    D:\Padolecchia\FILE  
DEFINITIVI\V7\_00000\V7.prj

04:41:55:813    LICENSE CHECKIN    FEATURE = mf\_integration\_logic[1]

04:41:55:837    LICENSE CHECKIN    FEATURE = mf\_integration\_grasshopper[1]

04:41:55:837    LICENSE CHECKIN    FEATURE = mf\_batch\_npe[1]

04:41:55:837    LICENSE CHECKIN    FEATURE = mf\_integration\_excel[1]

04:41:55:837    LICENSE CHECKIN    FEATURE = mf\_batch[1]

---

## Bibliography

- [1] A. Papanikolaou, *Ship design: methodologies of preliminary design*. Springer, 2014.
- [2] B. Jeong, H. Wang, E. Oguz, e P. Zhou, «An effective framework for life cycle and cost assessment for marine vessels aiming to select optimal propulsion systems», *J. Clean. Prod.*, vol. 187, pp. 111–130, 2018.
- [3] J. H. Evans, «Basic design concepts», *J. Am. Soc. Nav. Eng.*, vol. 71, fasc. 4, pp. 671–678, 1959.
- [4] C. Vossen, R. Kleppe, e S. R. Hjørungnes, «Ship design and system integration», presentato al DMK Conference, 2013.
- [5] K. L. Rødseth, K. Fagerholt, e S. Proost, «Optimal planning of an urban ferry service operated with zero emission technology», *Marit. Transp. Res.*, vol. 5, p. 100100, 2023.
- [6] D. Padolecchia, N. T. Marchesi, S. Bertagna, e V. Bucci, «3D Parametric Modeling for Ship Concept Design: A Flexible Approach to General Arrangement Plan».
- [7] M. G. Parsons, H. Chung, E. Nick, A. Daniels, S. Liu, e J. Patel, «Intelligent ship arrangements: a new approach to general arrangement», *Nav. Eng. J.*, vol. 120, fasc. 3, pp. 51–65, 2008.
- [8] K.-S. Kim e M.-I. Roh, «Review of ship arrangement design using optimization methods», *J. Comput. Des. Eng.*, vol. 12, fasc. 1, pp. 100–121, 2025.
- [9] S. Khan, E. Gunpinar, e B. Sener, «GenYacht: An interactive generative design system for computer-aided yacht hull design», *Ocean Eng.*, vol. 191, p. 106462, nov. 2019, doi: 10.1016/j.oceaneng.2019.106462.
- [10] D. R. Elvekrok, «Concurrent engineering in ship design», *J. Ship Prod.*, vol. 13, fasc. 04, pp. 258–269, 1997.
- [11] R. I. Winner, J. P. Pennell, H. E. Bertrand, e M. M. Slusarczyk, «The role of concurrent engineering in weapons system acquisition», 1988.
- [12] P. Zhang, «Parametric approach to design of hull forms», *J. Hydrodyn. Ser B*, vol. 20, fasc. 6, pp. 804–810, 2008.
- [13] F. L. Pérez-Arribas e E. Peter-Cosma, «Parametric generation of planing hulls with NURBS surfaces», *J. Ship Res.*, vol. 57, fasc. 04, pp. 241–261, 2013.
- [14] N. Demo, G. Ortali, G. Gustin, G. Rozza, e G. Lavini, «An efficient computational framework for naval shape design and optimization problems by means of data-driven reduced order modeling techniques», *Boll. DellUnione Mat. Ital.*, vol. 14, fasc. 1, pp. 211–230, 2021.
- [15] S. Khan, K. Goucher-Lambert, K. Kostas, e P. Kaklis, «ShipHullGAN: A generic parametric modeller for ship hull design using deep convolutional generative model», *Comput. Methods Appl. Mech. Eng.*, vol. 411, p. 116051, 2023.
- [16] N. J. Bagazinski e F. Ahmed, «Shipgen: A diffusion model for parametric ship hull generation with multiple objectives and constraints», *J. Mar. Sci. Eng.*, vol. 11, fasc. 12, p. 2215, 2023.
- [17] D. Padolecchia, S. Bertagna, L. Braidotti, V. Bucci, e A. Marino, «Evaluating Virtual Prototyping Approaches in Integrated Ship Design: A Case-Based Analysis», *Int. J. Interact. Des. Manuf. IJIDeM*, pp. 1–18, 2025.
- [18] A. F. Molland, S. R. Turnock, e D. A. Hudson, *Ship resistance and propulsion*. Cambridge university press, 2017.

- 
- [19] D. Padolecchia, S. Utzeri, A. Marinò, e V. Bucci, «Feasibility Study for the Fuel Switch of a Fast Ferry», *Prog. Mar. Sci. Technol.*, vol. 7, pp. 101–108, 2023.
- [20] E. A. Bouman, E. Lindstad, A. I. Riolland, e A. H. Strømman, «State-of-the-art technologies, measures, and potential for reducing GHG emissions from shipping—A review», *Transp. Res. Part Transp. Environ.*, vol. 52, pp. 408–421, 2017.
- [21] L. A. Díaz-Secades, «Enhancement of maritime sector decarbonization through the integration of fishing vessels into IMO energy efficiency measures», *J. Mar. Sci. Eng.*, vol. 12, fasc. 4, p. 663, 2024.
- [22] Y. Tahara, D. Peri, E. F. Campana, e F. Stern, «Computational fluid dynamics-based multiobjective optimization of a surface combatant using a global optimization method», *J. Mar. Sci. Technol.*, vol. 13, fasc. 2, pp. 95–116, 2008.
- [23] S. Bertagna, L. Braidotti, D. Padolecchia, e V. Bucci, «Feasibility Study of a Hybrid-electric Taxi Boat for the Venice Lagoon», presentato al 2022 International Symposium on Power Electronics, Electrical Drives, Automation and Motion (SPEEDAM), IEEE, 2022, pp. 701–706.
- [24] A. Ziakas e M. Boile, «Toward zero-emission ferries: integrating systematic review and bibliometric analysis insights on alternative fuels and policies», *J. Shipp. Trade*, vol. 10, fasc. 1, p. 27, 2025.
- [25] P. T. Pedersen, «Marine structures: future trends and the role of universities», *Engineering*, vol. 1, fasc. 1, pp. 131–138, 2015.
- [26] D. Watson, «Practical Ship Design, vol. 1, no», 1998.
- [27] D. Padolecchia e V. Bucci, «An Application of Smart-Microgrid in Slow-Speed Tourism», in *Nautical and Maritime Culture, from the Past to the Future*, IOS Press, 2024, pp. 172–181.
- [28] J. Abedin, F. Franklin, e S. I. Mahmud, «A Two-Stage Optimisation of Ship Hull Structure Combining Fractional Factorial Design Technique and NSGA-II Algorithm», *J. Mar. Sci. Eng.*, vol. 12, fasc. 3, p. 411, 2024.
- [29] N. Demo, M. Tezzele, A. Mola, e G. Rozza, «Hull shape design optimization with parameter space and model reductions, and self-learning mesh morphing», *J. Mar. Sci. Eng.*, vol. 9, fasc. 2, p. 185, 2021.
- [30] M. J. Roth, «Analysis of general arrangements created by the TU Delft packing approach», 2017.
- [31] D. J. Andrews, «Art and science in the design of physically large and complex systems», *Proc. R. Soc. Math. Phys. Eng. Sci.*, vol. 468, fasc. 2139, pp. 891–912, 2012.
- [32] L. Piegl e W. Tiller, *The NURBS book*. Springer Science & Business Media, 2012.
- [33] H. Lackenby, «On the systematic variation of ship forms», *Trans. RINA*, vol. 92, pp. 289–316, 1950.
- [34] R. Oxman, «Thinking difference: Theories and models of parametric design thinking», *Des. Stud.*, vol. 52, pp. 4–39, 2017.
- [35] A. Eltaweel e S. Yuehong, «Parametric design and daylighting: A literature review», *Renew. Sustain. Energy Rev.*, vol. 73, pp. 1086–1103, 2017.
- [36] B. Martens, G. Wurzer, T. Grasl, W. Lorenz, e R. Schaffranek, «Real Time-Proceedings of the 33rd International Conference on Education and Research in Computer Aided Architectural Design in Europe-Volume 2», eCAADe, 2015.
- [37] S. Han, Y.-S. Lee, e Y. B. Choi, «Hydrodynamic hull form optimization using parametric models», *J. Mar. Sci. Technol.*, vol. 17, fasc. 1, pp. 1–17, 2012.
- [38] B. Singh, «Top 5 Benefits of Parametric Design in Architecture». 23 maggio 2024.

- 
- [39] S. Brizzolara, G. Vernengo, C. Pasquinucci, e S. Harries, «Significance of parametric hull form definition on hydrodynamic performance optimization», presentato al MARINE VI: proceedings of the VI International Conference on Computational Methods in Marine Engineering, CIMNE, 2015, pp. 254–265.
- [40] F. Pérez-Arribas, «Parametric generation of small ship hulls with CAD software», *J. Mar. Sci. Eng.*, vol. 11, fasc. 5, p. 976, 2023.
- [41] J. Chen, Y. Ou, G. Xiang, Q. Ye, e W. Wang, «A Parametric Design Method for Unstepped Planing Hulls Using Longitudinal Functions and Shape Coefficients.», *Appl. Sci.* 2076-3417, vol. 15, fasc. 5, 2025.
- [42] I. Biliotti *et al.*, «Automatic parametric hull form optimization of fast naval vessels», presentato al 11th international conference on fast sea transportation (FAST), Honolulu, Hawaii, USA, 2011.
- [43] F. Pérez-Arribas, «Parametric generation of planing hulls», *Ocean Eng.*, vol. 81, pp. 89–104, 2014.
- [44] T. W. Sederberg e S. R. Parry, «Free-form deformation of solid geometric models», presentato al Proceedings of the 13th annual conference on Computer graphics and interactive techniques, 1986, pp. 151–160.
- [45] D. Villa, S. Gaggero, A. Coppede, e G. Vernengo, «Parametric hull shape variations by Reduced Order Model based geometric transformation», *Ocean Eng.*, vol. 216, p. 107826, 2020.
- [46] S. Menzel, M. Olhofer, e B. Sendhoff, «Application of free form deformation techniques in evolutionary design optimisation», presentato al Proceedings of 6th World Congress on Structural and Multidisciplinary Optimization, Rio de Janeiro, Brazil, 2005.
- [47] F. Pérez, J. Clemente, J. Suárez, e J. González, «Parametric generation, modeling, and fairing of simple hull lines with the use of nonuniform rational B-spline surfaces», *J. Ship Res.*, vol. 52, fasc. 01, pp. 1–15, 2008.
- [48] H. Zhou, B. Feng, Z. Liu, H. Chang, e X. Cheng, «NURBS-based parametric design for ship hull form», *J. Mar. Sci. Eng.*, vol. 10, fasc. 5, p. 686, 2022.
- [49] J. Wu, X. Liu, M. Zhao, e D. Wan, «Neumann-Michell theory-based multi-objective optimization of hull form for a naval surface combatant», *Appl. Ocean Res.*, vol. 63, pp. 129–141, 2017.
- [50] M. R. Hasan, «Automating the Creation of Ship Hull & Lines Plan from Offset Table Using Grasshopper», 2024.
- [51] R. MEPC, «2023 IMO strategy on reduction of GHG emissions from ships», 2023.
- [52] U. la Monaca, S. Bertagna, A. Marinò, e V. Bucci, «Integrated ship design: An innovative methodological approach enabled by new generation computer tools», *Int. J. Interact. Des. Manuf. IJIDeM*, vol. 14, fasc. 1, pp. 59–76, 2020.
- [53] D. Padolecchia, S. Bertagna, V. Bucci, e A. Marinò, «The Role of Virtual Prototyping in a New Approach to Integrated Ship Design», presentato al International Conference of the Italian Association of Design Methods and Tools for Industrial Engineering, Springer, 2024, pp. 525–533.
- [54] D. Padolecchia, S. Savarese, A. Marino, e V. Bucci, «Electrification of a large catamaran water bus for everyday commuting in the Venice Lagoon», presentato al 2023 AEIT International Annual Conference (AEIT), IEEE, 2023, pp. 1–6.
- [55] H. Yi, «Optimal operation strategy of a large fuel-cell hybrid ship», *J. Adv. Mar. Eng. Technol. JAMET*, vol. 45, fasc. 4, pp. 167–173, 2021.
-

- 
- [56] X. Sun, F. Xin, e K. Gao, «Energy efficiency research of propulsion system for series-parallel hybridization of amphibious vehicles», *Heliyon*, vol. 10, fasc. 15, 2024.
- [57] C. Tsoumpris e G. Theotokatos, «Energy management and health monitoring for hybrid ship power plants», *J. Mar. Eng. Technol.*, vol. 24, fasc. 4, pp. 320–337, 2025.
- [58] D. Padolecchia, S. Utzeri, L. Braidotti, e A. Marino, «A Hybrid-Electric Passenger Vessel for Inland Waterway», presentato al 2023 IEEE International Conference on Electrical Systems for Aircraft, Railway, Ship Propulsion and Road Vehicles & International Transportation Electrification Conference (ESARS-ITEC), IEEE, 2023, pp. 1–6.
- [59] Q. Yang *et al.*, «A two-stage energy management strategy for hybrid ship power systems considering the dynamic output characteristics of batteries», *Appl. Energy*, vol. 396, p. 126232, 2025.
- [60] V. Bucci, F. Mauro, A. Vicenzutti, D. Bosich, e G. Sulligoi, «Hybrid-electric solutions for the propulsion of a luxury sailing yacht», presentato al 2020 2nd IEEE International Conference on Industrial Electronics for Sustainable Energy Systems (IESES), IEEE, 2020, pp. 280–286.
- [61] M. Asli *et al.*, «Thermal management challenges in hybrid-electric propulsion aircraft», *Prog. Aerosp. Sci.*, vol. 144, p. 100967, 2024.
- [62] E. Kurt, A. Y. Arabul, F. K. Arabul, e I. Senol, «Parallel hybrid propulsion system with integration of designed electric machine for medium altitude long endurance UAV», *Heliyon*, vol. 11, fasc. 4, 2025.
- [63] D. Bailey, *The NPL High Speed Round Bilge: Displacement Hull Series; Resistance, Propulsion, Manoeuvring and Seakeeping Data*. in Maritime technology monograph. Royal Inst. of Naval Architects, 1976. [Online]. Disponibile su: <https://books.google.it/books?id=VWbatwEACAAJ>
- [64] E. P. Clement e D. L. Blount, «Resistance tests of a systematic series of planing hull forms», *Trans Sname*, vol. 71, fasc. 3, pp. 491–579, 1963.
- [65] J. Gerritsma, J. A. Keuning, e R. Onnink, *The Delft systematic yacht hull series II experiments*. Delft University of Technology, Ship Hydromechanics Laboratory, 1991.
- [66] L. Keuning e W. Hillege, «The results of the delft systematic deadrise series», presentato al Proceedings of 14th International Conference on Fast Sea Transportation (FAST 2017), 2017, pp. 97–106.
- [67] R. H. Compton, «Resistance of a systematic series of semiplaning transom-stern hulls», *Mar. Technol. SNAME News*, vol. 23, fasc. 04, pp. 345–370, 1986.
- [68] M. P. Wheeler, K. I. Matveev, e T. Xing, «Numerical study of hydrodynamics of heavily loaded hard-chine hulls in calm water», *J. Mar. Sci. Eng.*, vol. 9, fasc. 2, p. 184, 2021.
- [69] D. Savitsky e P. W. Brown, «Procedures for hydrodynamic evaluation of planing hulls in smooth and rough water», *Mar. Technol. SNAME News*, vol. 13, fasc. 04, pp. 381–400, 1976.
- [70] D. L. Blount e D. L. Fox, «Small-craft power prediction», *Mar. Technol. SNAME News*, vol. 13, fasc. 01, pp. 14–45, 1976.
- [71] C. Nasso *et al.*, «Integrated design of an eco-friendly wooden passenger craft for inland navigation», *Int. Shipbuild. Prog.*, vol. 66, fasc. 1, pp. 35–55, 2019.
- [72] ANSA, «Cominciamo a parlarne: che fine fanno le barche abbandonate? INCHIESTA: LA ROTTAMAZIONE DELLE BARCHE IN VTR». 2023.
- [73] F. Rubino, A. Nisticò, F. Tucci, e P. Carlone, «Marine application of fiber reinforced composites: a review», *J. Mar. Sci. Eng.*, vol. 8, fasc. 1, p. 26, 2020.
-

- 
- [74] A. Ziemińska-Stolarska, M. Sobulska, M. Pietrzak, e I. Zbiciński, «Application of life cycle assessment to analysis of fibre composite manufacturing technologies in shipyards industry», *Processes*, vol. 12, fasc. 3, p. 461, 2024.
- [75] S. Bertagna, N. Taucer Marchesi, V. Bucci, e A. Marino', «On the Structural Response of Innovative Plastic Materials for Boatbuilding Applications», in *Progress in Marine Science and Technology*, N. Degiuli, M. Valčić, V. Bucci, e L. Braidotti, A c. di, IOS Press, 2024. doi: 10.3233/PMST240024.
- [76] J. Li, H. Yi, e Y. F. Zhang, «Research on green shipbuilding and concurrent green ship design», *Appl. Mech. Mater.*, vol. 44, pp. 614–618, 2011.
- [77] A. Rahman e M. M. Karim, «Green shipbuilding and recycling: Issues and challenges», *Int. J. Environ. Sci. Dev.*, vol. 6, fasc. 11, p. 838, 2015.
- [78] H. L. Xu *et al.*, «Discuss on green shipbuilding technology: Design and material», *Adv. Mater. Res.*, vol. 490, pp. 3296–3300, 2012.
- [79] N. T. Marchesi, S. Bertagna, D. Padolecchia, V. Bucci, e A. Marino', «Parametric Design of HDPE Testing Specimens for Boatbuilding Applications».
- [80] F. Cucinotta, E. Guglielmino, e F. Sfravara, «Life cycle assessment in yacht industry: A case study of comparison between hand lay-up and vacuum infusion», *J. Clean. Prod.*, vol. 142, pp. 3822–3833, 2017.
- [81] M. Önal e G. Neşer, «End-of-life alternatives of glass reinforced polyester boat hulls compared by LCA», *Adv. Compos. Lett.*, vol. 27, fasc. 4, p. 096369351802700402, 2018.
- [82] M. Burman, J. Kutteneuler, I. Stenius, K. Garne, e A. Rosén, «Comparative Life Cycle Assessment of the hull of a high-speed craft», *Proc. Inst. Mech. Eng. Part M J. Eng. Marit. Environ.*, vol. 230, fasc. 2, pp. 378–387, 2016.
- [83] J. Gerber, *Global aluminium recycling: a cornerstone of sustainable development*. International Aluminium Institute, 2006.
- [84] «RES22 Rules for Ships with Plastic, Aluminium Alloy or Wooden Hull EIF 1.5.2023 Corr1».
- [85] S. Bertagna, N. T. Marchesi, V. Bucci, F. Distefano, V. Crupi, e A. Marino', «Investigation on the tensile properties of virgin and recycled HDPE for boatbuilding applications through experimental tests».
- [86] «RES27\_Rules for the Classification of Workboats EIF 1.5.2023».
- [87] D. Savitsky, «Hydrodynamic design of planing hulls», *Mar. Technol. SNAME News*, vol. 1, fasc. 04, pp. 71–95, 1964.
- [88] D. Radojčić, A. Zgradic, M. Kalajdzic, e A. Simic, «Resistance prediction for hard chine hulls in the pre-planing regime», *Pol. Marit. Res.*, 2014.
- [89] A. P. Keller, «Cavitation scale effects-empirically found relations and the correlation of cavitation number and hydrodynamic coefficients», *Httpresolver Caltech Educ. Lect. 001*, 2001.
- [90] «dpr435\_1991».
- [91] «REP2 Rules for Ships - Part B Vol.2 1.1.2024».
- [92] B. Tang, «Orthogonal array-based Latin hypercubes», *J. Am. Stat. Assoc.*, vol. 88, fasc. 424, pp. 1392–1397, 1993.
- [93] M. D. McKay, R. J. Beckman, e W. J. Conover, «A comparison of three methods for selecting values of input variables in the analysis of output from a computer code», *Technometrics*, vol. 42, fasc. 1, pp. 55–61, 2000.
- [94] H. Røstum, S. Gros, e K. Aas-Jakobsen, «Constrained Bayesian optimization for engineering bridge design», *Struct. Multidiscip. Optim.*, vol. 68, fasc. 1, p. 20, 2025.
-

- [95] «REP5 Rules for Ships Part E Vol.2 1.1.2024».
- [96] A. Trobec *et al.*, «Thickness of marine Holocene sediment in the Gulf of Trieste (northern Adriatic Sea)», *Earth Syst. Sci. Data*, vol. 10, fasc. 2, pp. 1077–1092, giu. 2018, doi: 10.5194/essd-10-1077-2018.
- [97] Rai News FVG, «I numeri da record del Delfino verde», 19 ottobre 2023.
- [98] «Ord-n-27-del-06052025-Ordinanza-di-Sicurezza\_250508\_112738».
- [99] D. L. Blount e R. J. Bartee, «Design of propulsion systems for high-speed craft», *Mar. Technol. SNAME News*, vol. 34, fasc. 04, pp. 276–292, 1997.
- [100] M. W. C. Oosterveld e P. van Oossanen, «Further computer-analyzed data of the Wageningen B-screw series», *Int. Shipbuild. Prog.*, vol. 22, fasc. 251, pp. 251–262, 1975.
- [101] Ministro delle Infrastrutture e dei Trasporti, «Determinazione del numero di passeggeri sulle unità da passeggeri - R.D. 20.5.1897, n. 178». 14 marzo 2002.
- [102] C. Spearman, «The proof and measurement of association between two things.», 1961.

---

## List of Figures

Figure 1 The traditional Evans' spiral illustrating the iterative nature of early-stage ship design (Evans, 1959) [4].....	2
Figure 2 Comparison between conventional, linearly organised design and a concurrent-engineering-based design paradigm [11].....	4
Figure 3 Comparison of parametric and conventional design workflows.....	10
Figure 4 Schematic representation of Parametric Design Thinking.....	11
Figure 5 Example of the FPA [41] .....	12
Figure 6 Example of the FFD [46] .....	14
Figure 7 Methodological comparison of hull form generation using the FPA and FFD [39] .....	14
Figure 8 Integration of Grasshopper and Rhinoceros for parametric modelling.....	18
Figure 9 Series Hybrid architecture [58] .....	22
Figure 10 Parallel Hybrid architecture [58].....	24
Figure 11 Body-plan of NPL High-Speed Round-Bilge Series (Bailey, 1976) .....	27
Figure 12 Body-plan of the Series 62 systematic set (Clement & Blount, 1962) .....	27
Figure 13 Body-plan of the Semiplaning Systematic Series (Compton, 1986).....	28
Figure 14 MAMBO prototype: an experimental GRP hull [https://alumni.polimi.it/2020/10/14/la-prima-barca-al-mondo-in-fibra-di-vetro-stampata-in-3d-e-made-in-polimi/] .....	33
Figure 15 Typical example of an ageing GRP coastal passenger vessel.....	34
Figure 16 Example of an HDPE workboat [https://tidemanboats.com/].....	37
Figure 17 Information flow within the integrated parametric design model.....	44
Figure 18 High-level schematic of the parametric design workflow .....	45
Figure 19 Logical framework of the parametric hull definition.....	47
Figure 20 Generating curves of the parametric hull geometry .....	48
Figure 21 Geometric definition of the hull generating curves.....	49
Figure 22 Logical framework of the parametric hull - Centre Line Module.....	50
Figure 23 Longitudinal layout of the control points defining the Centre Line .....	50
Figure 24 Aft view of the hard-chine hull featuring a parametrically modelled skeg.....	52
Figure 25 Logical framework of the parametric hull - Sheer Line Module .....	53

---

Figure 26 Plan view of the control-point layout defining the Sheer Line .....	53
Figure 27 Logical framework of the parametric hull - Chine Line Module.....	56
Figure 28 Plan view of the control-point layout defining the Chine Line.....	57
Figure 29 Longitudinal layout of the control points defining the Chine Line.....	57
Figure 30 Plan view of Spray Rail NURBS .....	58
Figure 31 Spray rail geometry obtained through parametric offset of the chine line.....	58
Figure 32 Logical framework of the Hydrostatic output.....	63
Figure 33 Geometric output.....	63
Figure 34 Construction Plan .....	65
Figure 35 Logical framework of the Resistance, Propulsive selection and System Integration .....	67
Figure 36 Integrated Power System (IPS).....	70
Figure 37 3D model of the propulsion system and engine room.....	73
Figure 38 Speed–resistance curve .....	75
Figure 39 Logical framework of the 3D General Arrangement Plan and Structures .....	78
Figure 40 View 1 of the complete 3D model .....	84
Figure 41 View 2 of the complete 3D model .....	84
Figure 42 2D GA plans.....	85
Figure 43 Uniform Latin hypercube sampling with two variables and six points [94].....	89
Figure 44 Logical framework of the Feasibility Analysis.....	91
Figure 45 Linear coastal study area with the main settlements distributed along a short maritime axis .....	94
Figure 46 Annual passenger volumes for selected maritime services in Friuli Venezia Giulia and for Bus Line 6 .....	96
Figure 47 Speed–resistance curve of the reference hull configuration obtained through the Simple Mathematical Model [87].....	102
Figure 48 Feasible alternative configurations of the engine room adopted in the parametric design model.....	105
Figure 49 Alternative parametric seating configurations adopted in the case study. Seating in red, standing areas in blue, circulation corridors in green, technical/service spaces in light blue .....	108

---

Figure 50 Effect of the longitudinal positioning of the forward and aft passenger-area bulkheads on the distribution of enclosed internal volume and usable external deck areas. Seating in red, standing areas in blue, circulation corridors in green, technical/service spaces in light blue.....	110
Figure 51 Influence of the longitudinal position of the PMR-compliant toilet compartment on the placement of the associated reserved seating within the passenger area. Seating in red, standing areas in blue, circulation corridors in green, technical/service spaces in light blue .....	111
Figure 52 Discrete bow and stern positioning of the embarkation area. Seating in red, standing areas in blue, circulation corridors in green, technical/service spaces in light blue .....	111
Figure 53 3D model of the entire design .....	116
Figure 54 Construction Plan of the base model.....	117
Figure 55 Speed–resistance curve .....	120
Figure 56 Speed–power relationship, with markers indicating ZEM speed (green), design speed (yellow), maximum speed limited by the installed electric propulsion power (red).....	120
Figure 57 Integrated Power System (IPS).....	121
Figure 58 2D GA plans.....	124
Figure 59 modeFRONTIER workflow and experimental plan .....	127
Figure 60 Overview of feasible and unfeasible configurations within the explored design space .....	130
Figure 61 Statistical distribution of passenger capacity across the feasible design configurations .....	135
Figure 62 Statistical distribution of the power demand at 8 kn in ZEM for the feasible configurations .....	136
Figure 63 Distribution of operational autonomy in fully electric mode for the feasible design configurations .....	136
Figure 64 Relationship between passenger capacity and power demand at 8 kn in ZEM, with highlighted bi-objective Pareto-optimal solutions.....	138
Figure 65 Relationship between passenger capacity and electric operational autonomy..	138
Figure 66 Relationship between power demand at 8 kn in ZEM and operational electric autonomy .....	139

---

Figure 67 Spearman rank correlations between key input variables and power demand at 8 kn in ZEM..... 140

Figure 68 Spearman rank correlations between key input variables and passenger capacity ..... 141

Figure 69 Spearman rank correlations between key input variables and electric autonomy ..... 141

---

## List of Tables

Table 1 Typical mechanical properties of GRP laminates .....	32
Table 2 Mechanical properties of marine-grade aluminium alloys.....	36
Table 3 Typical mechanical properties of HDPE.....	39
Table 4 Variables adopted in the parametric formulation of the hull centre line.....	60
Table 5 Variables adopted in the parametric formulation of the hull sheer line .....	60
Table 6 Variables adopted in the parametric formulation of the hull chine line.....	61
Table 7 Summary of the main hydrostatic characteristics computed for the hull geometry	64
Table 8 Structure of the electric motor database .....	71
Table 9 Structure of the batteries database.....	72
Table 10 Structure of the generator-sets database .....	73
Table 11 Shipowner specifications relevant to resistance and propeller selection.....	74
Table 12 Preliminary Design choices relevant to resistance and propeller selection.....	74
Table 13 Parametric variables involved in the propulsion module .....	74
Table 14 Main categories of technical data extracted from the propulsion and energy-system databases.....	75
Table 15 Preliminary Propeller Configuration .....	76
Table 16 Main characteristics of the selected propulsion motors .....	76
Table 17 Main characteristics of the selected diesel-generators .....	76
Table 18 Main characteristics of the selected battery Energy Storage System (ESS) .....	76
Table 19 Power demand and endurance in Zero Emission Mode at the reference operating condition.....	77
Table 20 Alluminium alloy T-beam Catalogue.....	80
Table 21 Alluminium alloy Flat Bar Catalogue .....	81
Table 22 Design variables associated with owner requirements and preferences.....	82
Table 23 Summary of design variables and their implications .....	82
Table 24 Regulatory requirements governing space design and layout .....	83
Table 25 Regulatory-derived parameters for structural design .....	83
Table 26 Lightship condition: weight and centre of gravity summary.....	86
Table 27 Full Load condition: weight and centre of gravity summary .....	87
Table 28 Maritime services and annual passenger volumes .....	95

---

Table 29 Main characteristics of vessels currently operating in the Gulf of Trieste.....	97
Table 30 Principal hull characteristics and dimensions derived from the operational requirements .....	99
Table 31 Definition and bounds of the geometric design variables adopted.....	100
Table 32 Main operational and propulsion system parameters adopted in the study, including shipowner requirements.....	104
Table 33 Discrete propulsion and energy system variables adopted in the parametric model .....	104
Table 34 Fixed input parameters adopted in the case study for the definition of the 3D GA .....	112
Table 35 Design variables considered in the case study .....	112
Table 36 Baseline values of the design variables adopted for the reference configuration .....	114
Table 37 Fixed input parameters defining the parametric design domain for the case study .....	115
Table 38 Summary of the main hydrostatic characteristics computed for the base model	118
Table 39 Variation of resistance, effective power, and brake power with vessel speed; ZEM operating speed in green, Design speed in yellow.....	119
Table 40 Main characteristics of the selected propulsion motors .....	122
Table 41 Main characteristics of the selected diesel-generator.....	122
Table 42 Main characteristics of the selected battery Energy Storage System (ESS) .....	122
Table 43 Propeller Configuration .....	122
Table 44 Power demand and endurance in Zero Emission Mode at the reference operating condition .....	122
Table 45 Lightship weight estimate and centres of gravity adopted within the parametric design model.....	125
Table 46 Full-load weight breakdown and centres of gravity .....	126
Table 47 Equipment number and anchoring arrangement parameters .....	126
Table 48 Overview of feasible and unfeasible configurations within the explored design space .....	130
Table 49 Comparative overview of Pareto-optimal configurations and existing passenger vessels of similar size .....	146

---

## List of Publications

This section lists the publication produced during Ph.D. years. They are subdivided into three categories: Journal Article, Journal Article under review and Conference Publications.

### Journal Article

1. D. Padolecchia, S. Bertagna, L. Braidotti, V. Bucci, A. Marinò, “Evaluating Virtual Prototyping Approaches in Integrated Ship Design: A Case-Based Analysis”  
In: *International Journal on Interactive Design and Manufacturing (IJIDeM)*  
DOI: 10.1007/s12008-025-02370-y

### Journal Article Under Review

1. N. Taucer Marchesi, E. Del Piero, S. Utzeri, D. Padolecchia, S. Bertagna, L. Braidotti, V. Bucci, “Energy Costs Evolution of an Adriatic Cruise: Diesel, LNG and Methanol comparison”  
submitted on 18/11/2025 to: *Transportation Part D*

### Conference Publications

1. D. Padolecchia, S. Bertagna, M. Pinzan, N. Taucer Marchesi, S. Utzeri, V. Bucci, “Bim-Based Approach for Smart HVAC Design in Cruise Shipbuilding: Automation and Simulation Insights”  
In press
2. S. Bertagna, L. Braidotti, D. Padolecchia, C. Trombini, S. Benvegna, V. Bucci, A. Marinò, “Bridging Design Domains in Digital Shipbuilding: Virtual Prototypes and Immersive Workflows for System Integration”  
In press
3. D. Padolecchia, N. Taucer Marchesi, S. Bertagna, V. Bucci, “3D Parametric Modeling for Ship Concept Design: a Flexible Approach to General Arrangement Plan”  
In: *Technology and Science for the Ships of the Future. Vol. 10, P. 1028-1037, Amsterdam: IOS PRESS*  
DOI: 10.3233/PMST250121

- 
4. N. Taucer Marchesi, S. Bertagna, D. Padolecchia, V. Bucci, A. Marinò, “Parametric Design of HDPE Testing Specimens for Boatbuilding Applications”  
In: *Technology and Science for the Ships of the Future. Vol. 10, P. 1028-1037, Amsterdam: IOS PRESS*  
DOI: 10.3233/PMST250120
  5. S. Utzeri, L. Braidotti, S. Bertagna, D. Padolecchia, N. Taucer Marchesi, E. Del Piero, V. Bucci, A. Marinò, “Optimisation of a hybrid-parallel power train for a Aframax tanker to minimise emissions in every operative condition”  
In: *Technology and Science for the Ships of the Future. Vol. 10, P. 1028-1037, Amsterdam: IOS PRESS*  
DOI: 10.3233/PMST250116
  6. D. Padolecchia, V. Bucci, “An Application of Smart-Microgrid in Slow-Speed Tourism”  
In: *Nautical and Maritime Culture, from the Past to the Future. Progress in Marine Science and Technology, Vol 8, P. 172-181, IOS PRESS, 2024.*  
DOI: 10.1007/978-3-031-76597-1\_55
  7. D. Padolecchia, S. Bertagna, V. Bucci, A. Marinò, “The Role of Virtual Prototyping in a New Approach to Integrated Ship Design”  
In: *Lecture Notes in Mechanical Engineering, P 525-533*  
DOI: 10.1007/978-3-031-76597-1\_55
  8. D. Padolecchia, S. Utzeri, L. Braidotti, A. Marinò, “A Hybrid-Electric Passenger Vessel for Inland Waterway”  
In: *2023 IEEE International Conference on Electrical Systems for Aircraft Railway Ship Propulsion and Road Vehicles and International Transportation Electrification Conference Esars Itec*  
DOI: 10.1109/ESARS-ITEC57127.2023.10114841
  9. D. Padolecchia, S. Utzeri, A. Marinò, V. Bucci, “Feasibility study for the Fuel Switch of a Fast Ferry”  
In: *HSMV 2023 Proceedings of the 13<sup>TH</sup> Symposium on High-Speed Marine Vehicles. Progress in Marine Science and Technology, Vol. 7/2023, P. 101-108, IOS PRESS, ISBN: 9781643684420, ISSN: 2543-0955*  
DOI: 10.3233/PMST230014

10. D. Padolecchia, S. Savarese, A. Marinò, V. Bucci, “Electrification of a Large Catamaran Waterbus for Everyday Commuting in the Venice Lagoon”  
In: *2023 115<sup>TH</sup> AEIT International Annual Conference, AEIT 2023. P. 1-6, Institute of Electrical and Electronics Engineers Inc., ISBN: 978-88-87237-60-3*  
DOI: 10.23919/AEIT60520.2023.10330317
11. L. Braidotti, S. Bertagna, M. Zanin, D. Padolecchia, A. Marinò, V. Bucci, “A Methodology for the Hull Forms Design of a Passenger Catamaran for the Venice Lagoon”  
In: *Technology and Science for the Ships of the Future. VOL. 6, P. 546-554, Amsterdam: IOS PRESS*  
DOI: 10.3233/PMST220065
12. S. Bertagna, L. Braidotti, D. Padolecchia, A. Marinò, V. Bucci, “Feasibility Study of a Hybrid-Electric Taxi Boat for the Venice Lagoon”  
In: *Proceedings of the 2022 International Symposium on Power Electronics, Electrical Drives and Motion*  
DOI: 10.1109/SPEEDAM53979.2022.9842145



# UNIVERSITÀ DEGLI STUDI DI TRIESTE

La borsa di dottorato è cofinanziata con risorse dell'Unione europea, NextGeneration EU - Piano Nazionale di Ripresa e Resilienza, Missione 4 – Componente 1 – Investimento 3.4 – CUP J92B22000870007



Finanziato  
dall'Unione europea  
NextGenerationEU



Ministero  
dell'Università  
e della Ricerca



Italiadomani  
PIANO NAZIONALE  
DI RIPRESA E RESILIENZA



UNIVERSITÀ  
DEGLI STUDI  
DI TRIESTE